university of groningen

University Medical Center Groningen

University of Groningen

Evaluation of tumor therapy by pet : use of 11C-amino acids and 18FDG

Daemen, Bernard Joseph Giovanni

IMPORTANT NOTE: You are advised to consult the publisher's version (publisher's PDF) if you wish to cite from it. Please check the document version below.

Document Version
Publisher's PDF, also known as Version of record

Publication date:
1991

Link to publication in University of Groningen/UMCG research database

Citation for published version (APA):
Daemen, B. J. G. (1991). *Evaluation of tumor therapy by pet : use of 11C-amino acids and 18FDG*. [Thesis fully internal (DIV), University of Groningen]. [S.n.].

Copyright
Other than for strictly personal use, it is not permitted to download or to forward/distribute the text or part of it without the consent of the author(s) and/or copyright holder(s), unless the work is under an open content license (like Creative Commons).

The publication may also be distributed here under the terms of Article 25fa of the Dutch Copyright Act, indicated by the “Taverne” license. More information can be found on the University of Groningen website: https://www.rug.nl/library/open-access/self-archiving-pure/taverne-amendment.

Take-down policy
If you believe that this document breaches copyright please contact us providing details, and we will remove access to the work immediately and investigate your claim.

Downloaded from the University of Groningen/UMCG research database (Pure): http://www.rug.nl/research/portal. For technical reasons the number of authors shown on this cover page is limited to 10 maximum.

Download date: 04-05-2023

EVALUATION OF TUMOR THERAPY BY PET

USE OF ^{11}C-AMINO ACIDS AND ^{18}FDG

B.J.G. DAEMEN

EVALUATION OF TUMOR THERAPY BY PET

USE OF ^{11}C-AMINO ACIDS AND ^{18}FDG

STELLINGEN

1. Positronemissie tomografie, in combinatie met ^{11}C–gemerkte aminozuren en ^{18}FDG, is een potentiële methodiek voor klinische evaluatie van tumortherapie.

Dit Proefschrift

2. De interpretatie van de door Phelps *et al.* (1979) gebruikte methode om met ^{18}FDG het glucoseverbruik van weefsels te bepalen, is van dezelfde moeilijkheidsgraad, als de interpretatie van de schatting van de over de A28 van Groningen naar Zwolle rijdende stroom personenauto's, gebaseerd op tellingen van rode vrachtauto's met een actieradius tot Assen.

Phelps *et al.*, Ann. Neurol. 6,371–388 (1979)

3. De hiaten in de beschrijving van de door Di Chiro gebruikte materialen en methoden bij de bepaling van het tumorstadium van gliomen en astrocytomen met PET en ^{18}FDG geven geen aanleiding tot uitspraken met een hoge betrouwbaarheid.

Di Chiro, Invest. Radiol. 22,360–371 (1986)

4. PET in combinatie met ^{11}C–thymidine lijkt een goede en in de toekomst bruikbare methode om, via het bepalen van de door straling geremde DNA synthese, het effect van radiotherapie na te gaan.

5. De synthese van L–[1–^{11}C]tyrosine, volgens de methode van Bolster *et al.*, dient niet met een natte vinger uitgevoerd te worden.

Bolster *et al.*, Eur. J. Nucl. Med. 12, 321–324 (1986)

6. De verantwoordelijkheid die academici in de huidige samenleving geacht worden te dragen, strookt vaak niet met hun universitaire voorbereiding daarop.

7. Wie een wereld wil met meer rechtvaardigheid zal genoegen moeten nemen met (een buurman met) minder materiële welvaart.

8. Volgens Fromm's definitie van macht, is machtsmisbruik een contradictio in terminis.

Erich Fromm, Escape from freedom

9. Gezien de complexe musculatuur en innervatie, met de daaruitvolgende verfijnde motoriek, van de tromp van de Loxodonta africana en de Elephas maximus, is het bekende Nederlandse gezegde "als een olifant in een porceleinkast" niet geheel terecht.

10. Oliebelangen doen een schonere toekomst in rook opgaan.

11. Het is de hoogste tijd dat het proces van vervanging van het paasmaal door het agapèmaal, van het agapèmaal door de avondmaalviering met enkel brood en wijn, van wijn door druivesap en zelfs algehele weglating van wijn, omgekeerd wordt.

Stellingen behorende bij het proefschrift van B.J.G. Daemen
Evaluation of tumor therapy by PET
Use of ^{11}C–amino acids and ^{18}FDG
Groningen, 5 juni 1991

RIJKSUNIVERSITEIT GRONINGEN

EVALUATION OF TUMOR THERAPY BY PET

USE OF ^{11}C-AMINO ACIDS AND ^{18}FDG

PROEFSCHRIFT

ter verkrijging van het doctoraat in de Geneeskunde
aan de Rijksuniversiteit Groningen
op gezag van de Rector Magnificus Dr. L.J. Engels
in het openbaar te verdedigen op woensdag 5 juni 1991
des namiddags te 2.45 uur precies
door

BERNARD JOSEPH GIOVANNI DAEMEN
geboren 14 april 1958
te Venlo

Promotores: Prof. Dr. W. Vaalburg
Prof. Dr. A.W.T. Konings

Overige leden promotiecommissie:
Prof. Dr. O. Schober (Münster)
Prof. Dr. C. Streffer (Essen)
Prof. Dr. K.G. Go (Groningen)

This work was supported by grant GUKC 86–5 of the Dutch Cancer Society Koningin Wilhelmina Fonds.

Extract from "Prince Caspian" by C.S. Lewis Pte 1951 by kind permission of HarperCollins Publishers Limited.

"You come of the Lord Adam and the Lady Eve," said Aslan. "And that is both honour enough to erect the head of the poorest beggar, and shame enough to bow the shoulders of the greatest emperor on earth. Be content."

From "Prince Caspian" by C.S.Lewis

CONTENTS

CHAPTER 1

INTRODUCTORY CHAPTER

1.1 General introduction

In the last fifteen years, positron emission tomography (PET) has developed from basic research with cyclotron–generated isotopes into a powerful research technique for clinical investigation of physiology and pathophysiology. PET was brought about by the efforts of many scientists in the fields of chemistry, physics, biology and medicine. A non–exhaustive list of early pivotal discoveries and inventions is given in the appendix at the end of this chapter as an illustration of the multidisciplinary foreland of PET and hence of this thesis.

PET is based on the application of tracers labelled with short–lived ($t_{1/2}$ <2 hours) positron–emitting radionuclides, such as ^{11}C, ^{13}N, ^{15}O and ^{18}F. These radionuclides are generated by bombardment of appropriate target materials with cyclotron–accelerated charged particles, e.g. protons. After separation from the target material, the radionuclides produced are incorporated into organic compounds by means of a radiochemical synthesis. These organic compounds are designed to trace the biochemical or physiological functions desired. After purification and sterilization, the radiolabelled compounds are used as radiopharmaceuticals. When injected intravenously into

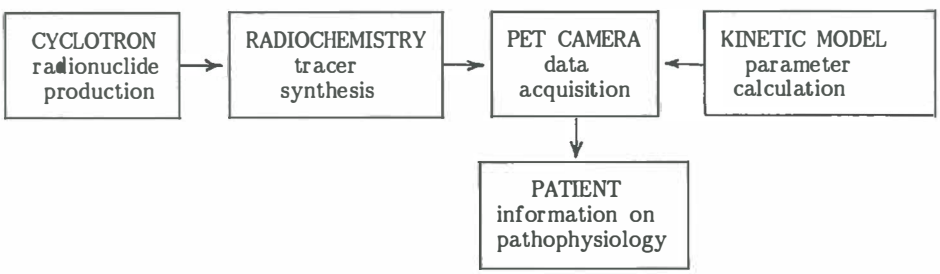

Figure 1. *Basic elements of positron emission tomography, a technique for non–invasive investigation of pathophysiology in patients.*

the organism (man, animal), the radiopharmaceutical distributes into the tissue. In the tissue, electron–positron annihilation produces two 511 keV γ–rays, which are detected by a positron camera, externally positioned to the body. From these acquired data, by use of reconstruction techniques, computer images are generated, representing the quantitative spatial distribution of the radioactivity in the body. This distribution of radioactivity can be obtained in time course. Since rates of biochemical processes are desired, the dynamic PET data together with dynamic plasma data are implemented into mathematical models that describe the kinetics of the radiopharmaceutical and its labelled metabolites in the tissue. From these mathematical models, rates of biochemical process are calculated.

PET offers different information as compared to other imaging modalities such as X–ray computed tomography (CT), ultra sound and magnetic resonance imaging (MRI). These latter techniques offer primarily anatomic information, while PET yields mainly physiological and biochemical information. PET is most often applied in the fields of neurology, cardiology and oncology. In oncology, physiological and biochemical as well as anatomic information are needed. Therefore PET is to be considered complementary to CT, ultra sound and MRI.

On account of their enhanced proliferative activity, tumor cells are associated with altered biochemical and physiological processes, when compared to the cells they originated from. Consequently, it is often possible to discriminate between the concentration of tracer in a volume of tumor cells and in the surrounding tissues. A number of the radiopharmaceuticals for the deviant functions in tumor are listed in table 1. This table shows that PET is able to monitor a variety of physiological functions such as tumor blood flow, tumor–induced disruptions of the blood brain barrier, enhanced energy requirements, and synthesis of macromulecules such as proteins and DNA. In tumors, using suitable ligands, e.g. steroid, dopamine and benzodiazepine receptors can be visualized and quantified by PET. Furthermore, the sensitivity of the tumor for and the pharmacokinetics of antineoplastic drugs can be investigated by the use of their radiolabelled counterparts.

This introductory chapter will mainly focus on radiolabelled amino acids and monosaccharides, and on their possibilities for application in diagnosis and treatment of tumors. The development of PET to monitor amino acid and glucose metabolism in tumors has provided opportunities to obtain answers to questions which are of utmost importance in oncology. For instance, it is now

Table 1. *Some radiopharmaceuticals labelled with positron–emitting radionuclides used by PET for the investigation of various biochemical and physiological functions in tumors.*

Radiopharmaceutical	Function
^{77}Kr, ^{11}C–alcohols, $H_2{}^{15}O$, $C^{15}O_2$, $^{13}NH_3$	Tumor blood flow
^{11}CO, $C^{15}O_2$	Tumor blood volume
^{82}Rb, ^{68}Ga–EDTA	Blood brain barrier
$^{15}O_2$	Oxygen metabolism
^{11}C–DMO, $^{11}CO_2$	Tumor tissue pH
^{18}F–fluoromisonidazole	Hypoxia
^{18}F–2–fluorodeoxyglucose, ^{11}C–2–deoxyglucose,	Glycolysis
^{11}C–3–0–methylglucose, ^{11}C–1–glucose	Monosaccharide uptake
L–[1–^{11}C]met, L–[methyl–^{11}C]met	Methionine metabolism
L–[1–^{11}C]tyr, L–[1–^{11}C]leu, L–[2–^{18}F]fluoro–tyr	Protein synthesis
D,L–[1–^{11}C]phe, D,L–[1–^{11}C]val, L–[1–^{11}C]orn	Amino acid uptake
[1–^{11}C]gly, ^{13}N–glu	
L–[1–^{11}C]AIB, L–[1–^{11}C]ACPC	Amino acid transport
L–[2–^{18}F]fluorodopa, L–[1–^{11}C]dopa	Melanin synthesis
^{11}C–, ^{18}F–fluoro–putrescine	Polyamine formation
^{18}F–fluorodeoxyuridine, ^{11}C–thymidine	Nucleotide uptake
^{18}F–fluorouracil, ^{13}N–, ^{11}C–carmustin,	Pharmacokinetics of
^{55}Co–bleomycine, ^{13}N–cisplatin	antineoplastic drugs
^{18}F–ethyl–norprogesteron, ^{18}F–estradiol	Steroid receptors
^{11}C–flunitrazepam	Benzodiazepine receptors
^{11}C–bromocryptine, ^{11}C–methyl–spiperone	Dopamine receptors

possible to discriminate between treatment–induced necrosis and recurrent tumor tissue. Other questions are still open for investigation. For example, does PET enable an early assessment of the grade of the tumor to facilitate a better choice of tumor treatment? Is PET able to produce better coordinates of the actual tumor extent than other imaging modalities? Is prognosis of success of a treatment already possible at the pretreatment phase or shortly after the initiation of treatment? Is PET useful in the follow–up of tumors after treatment in order to validate the efficacy of treatment protocols and to determine the kinetics of tumor growth after treatment?

1.2 Amino acids for PET in oncology.

1.2.1 Biochemical functions of tumors monitored with amino acids.

Nearly all natural and many unnatural amino acids have been labelled with positron–emitting radionuclides for the investigation of a variety of physiological functions in tumors (Fowler and Wolf 1986).

Radiolabelled methionine, tyrosine and leucine are the amino acids most often postulated for the investigation of protein synthesis rates (PSR) by PET. These three amino acids are discussed in more detail in sections 2.2 and 2.3 of this chapter. Other amino acids, such L–[1–^{11}C]phenylalanine and L–[1–^{11}C]valine, have also been proposed for the measurement of PSR. (Washburn *et al.* 1978, Casey *et al.* 1981, Barrio *et al.* 1983a). For this purpose both amino acids are inappropriate. Phenylalanine is rapidly transported into cells e.g. brain cells (Oldendorf 1971). But in rat and man, phenylalanine is hydroxylated into tyrosine with a figure of 22 and 15%, respectively (Moldaver *et al.* 1983, Clarcke and Bier 1982). It is therefore difficult to correct for the possible error due to phenylalanine hydroxylation on the PSR as determined with L–[1–^{11}C]phenylalanine. D,L–[1–^{11}C]valine was used for the evaluation of pancreatic carcinomas, brain tumors, lymphomas, and lung and breast carcinomas with an overall sensitivity for tumor detection of 85–90% (Hübner 1980 *et al.*). Nevertheless, animal studies with L–[1–^{14}C]valine in brain and tumor revealed a large amount of unmetabolized [1–^{14}C]valine in tissue (Banker and Cotman 1971, Kirikae *et al.* 1989) Therefore, advantages are not to be expected from L–[1–^{14}C]valine for application in PET when compared to L–[1–^{11}C]tyrosine and L–[1–^{11}C]leucine.

Non–natural amino acids such as [1–^{11}C]–α–aminoisobutyric acid (^{11}C–AIB) and [1–^{11}C]aminocyclopentane–1–carboxylic acid (^{11}C–ACPC) have been used for the investigation of the transport mechanisms of amino acids into tumor tissue. After transport into the tumor cell, mediated by the L–(leucine)–preferring carrier for ^{11}C–AIB or the A–(alanine)–preferring carrier for ^{11}C–ACPC, these amino acids are not metabolized further into proteins, but slowly diffuse back into the plasma. In patients, metastatic malignant melanoma and malignant fibrous histiocytomas in bone were clearly visualized with ^{11}C–AIB (Conti *et al.* 1986, Schmall *et al.* 1987). In patients with bronchogenic cancer, liver and breast tumors, Hübner *et al.* (1981) observed active transport of ^{11}C–ACPC. In 28 patients with different tumors,

De Vis *et al.* (1987) found that ^{11}C–ACPC uptake seemed to be independent of blood flow as measured with $^{13}NH_3$.

Amino acids are eligible for the detection of blood–brain barrier disruptions. A comparative PET study with [1–^{11}C]glycine, and L–[methyl–^{11}C]methionine in a astrocytoma revealed that [1–^{11}C]glycine delineated the tumor extent smaller than the actively transported L–[methyl–^{11}C]methionine and is considered eligible for delineation of tumor–induced blood–brain barrier disruptions (Johnström *et al.* 1987).

L–[^{13}N]glutamate has been applied to study amino acid transport and alterations of transamination. In tumor, glutamate provides the NH_2–group for transamination and the carbon hydrogen skeleton for the citrate cycle, only a relatively small amount is incorporated into protein (Nyhan and Busch 1958, Sauer *et al.* 1982). Hence, this amino acid is not suitable to measure PSR with PET. In patients, L–[^{13}N]glutamate was evaluated in osteogenic and primary Ewing sarcomas in bone and in a variety of brain tumors (Reiman *et al.* 1981 1982a,b). The uptake of L–[^{13}N]glutamate into the brain tumors also correlated well with the extent of the disruption of the blood–brain barrier.

Amino acids may also be useful for the determination of activities of specific enzymes in tumors. For example, in Walker 256 carcinosarcoma–bearing rats, Elsinga *et al.* (1990) demonstrated that the difference in tissue uptake between L–[1–^{14}C]ornithine and L–[5–^{14}C]ornithine of tumor and prostate correlated with activity of the enzyme ornithine decarboxylase (ODC). Hence, PET studies with the two ^{11}C–labelled ornithines may be a method to measure ODC activity in tumor and other tissues.

The amino acid dopa is a precursor for melanin synthesis. Since melanin synthesis is enhanced in melanomas, L–[1–^{11}C]dopa, [2–^{18}F]fluorodopa and have been tested for melanoma imaging. In melanomas of B16 melanoma–bearing mice, L–[2–^{18}F]fluorodopa was readily taken up into tumor tissue with uptake values comparable to that of non–melanoma tumors (Ishiwata 1989 *et al.*). These finding tally with the observations of van Langevelde and co–workers (1988), who found active transport of L–[1–^{11}C]dopa into melanotic Greene melanomas of hamsters but low incorporation percentages into melanin. The uptake of radiolabelled dopa into melanomas is mainly determined by amino acid transport and to a lesser extent by melanin synthesis.

1.2.2 Methionine

Methionine, an essential amino acid, is the main source of the active methyl–group. The important metabolic pathways of methionine are depicted in figure 1 (Lombardini and Talalay 1971, Aquilar *et al.* 1974, Finkelstein 1978). In the mammalian cell, the major part of methionine is incorporated into proteins. But, a substantial amount of methionine is converted into S–adenosyl–methionine (SAM). SAM donates its activated methyl–group to a variety of methyl–group acceptors, e.g. taurine, choline and nucleotides. The remaining S–adenosyl–homocysteine is resynthetized via homocysteine. Methionine is also involved in polyamine formation and sulphur metabolism.

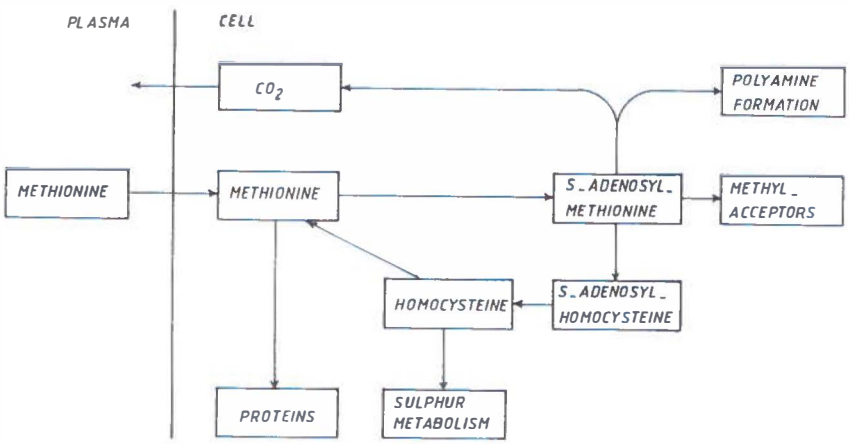

Figure 2. *The metabolic pathways of methionine.*

For use in PET, methionine has been labelled with ^{11}C in the methyl (Comar *et al.* 1976, Langström *et al.*1976) as well as in the carboxyl position (Bolster *et al.* 1986a). L–[methyl–^{11}C]methionine is the amino acid most often used in tumor PET studies. The main reason for this is the convenient radiochemical synthesis method. In the preparation of L–[methyl–^{11}C]methionine, the time of synthesis is short (<30 min), the radiochemical yields are high (>60%) and complex purification procedures are not required.

A number of experimental animal tumors have been investigated with

L–[methyl–^{11}C]methionine. For example, in AH109A tumor bearing rats, Kubota *et al.* (1984) observed for methionine the highest uptake values as compared to leucine and phenylalanine. In this tumor, Abe *et al.* (1988) observed that uptake of L–[methyl–^{11}C]methionine was coupled with tumor blood flow.

In patients, mostly intracranial tumors have been studied with L–[methyl–^{11}C]methionine. Bustany *et al.* (1985, 1986) observed active transport of methionine into gliomas, astrocytomas and normal brain tissues. For the determination of the in vivo PSR with L–[methyl–^{11}C]methionine, Bustany and co–workers (1981) proposed a three–compartment model. This model included compartments for free methionine in plasma and tissue, and a compartment for methionine incorporated into protein. The presence of non–protein metabolites was explicitly excluded. For this, in animals, Jones *et al.* (1985) and Ishiwata *et al.* (1988a) observed substantial amounts of non–protein metabolites, implicating that a fourth compartment is a necessity for the methionine model. Mazoyer *et al.* (1989) tested the compatibility of Bustany's data to several different compartmental models and verified that at least a fourth compartment was necessary for the description of the kinetics of L–[methyl–^{11}C]methionine.

Kinetics of L–[methyl–^{11}C]methionine transport into gliomas were investigated by Bergström *et al.* (1987a), who found a competition between the uptake of methionine and branched chain amino acids. Using phenylalanine as competing amino acid, O'Tuama *et al.* (1990) observed a similar competition in childhood brain tumors. In this study, it was postulated that a dual L–[methyl–^{11}C]methionine PET study procedure including a competition study with phenylalanine might be useful in the discrimination between vital and necrotic tumor tissue.

Attempts to assess the degree of malignancy with L–[methyl–^{11}C]methionine appeared to be fruitful. Several groups of investigators found consistent evidence that the grade of malignancy of gliomas and astrocytomas can be discriminated with L–[methyl–^{11}C]methionine. (Lilja *et al.* 1985, Bustany *et al.* 1986, Schober *et al.* 1986, Derlon *et al.* 1989).

Only few studies report investigations of extracranial tumors with PET using L–[methyl–^{11}C]methionine. Kubota *et al.* (1985, 1989) investigated bronchogenic tumors and was able to discriminate between benign and malignant forms. Also with lung tumors, Fujiwara *et al.* (1989) found a correlation between the methionine uptake values and, respectively the tumor doubling times and the histological type of lung tumors. With L–[methyl–^{11}C]methionine,

differential diagnosis was possible between large cell and squamous cell tumor. PET studies of pancreatic disease showed a depressed uptake of methionine in pancreas carcinomas as compared to pancreas tissue (Syrota *et al.* 1982), but chronic pancreatitis was not distinguishable from cancer.

Methionine has also been labelled in the carboxyl–group (Bolster *et al.* 1986a). A comparative metabolic study with L–[1–^{14}C]methionine and L–[methyl–^{14}C]methionine has been performed in tissues of the Walker 256 carcinosarcoma–bearing rats (Ishiwata *et al.* 1988a). In tumor, fewer non–protein metabolites were found with L–[1–^{14}C]methionine than with L–[methyl–^{14}C]methionine; in brain the reverse situation was observed. These data implicate that further investigations are necessary to elucidate whether L–[1–^{11}C]methionine is less useful for PSR measurements than L–[1–^{11}]tyrosine or L–[1–^{11}C]leucine.

PET studies with L–[methyl–^{11}C]methionine for the determination of treatment effects are discussed in section 4 of this chapter.

1.2.3 Tyrosine and Leucine

In this section, L–[1–^{11}C]tyrosine and L–[1–^{11}C]leucine are evaluated as two outstanding amino acids for PSR measurements in tissue.

^{14}C– and ^{15}N–labelled amino acids for the investigation of in vivo protein synthesis rates, were first used in continuous infusion experiments to determine non–invasively whole–body protein synthesis rates (PSR) and in invasive experiments to measure the PSR of specific organs. From studies in animals (Garlick and Marshall 1971, Simon *et al.* 1978, Lobley *et al.* 1980), in normal volunteers (James *et al.* 1976), and in patients with cancer (Eden *et al.* 1984, Hunter *et al.* 1989) or hepatic disease (Shanbhoque *et al.* 1987) it appears that tyrosine and leucine are the amino acids most suitable to determine PSR in vivo. Both tracers have a rapid incorporation into protein and a small intra–cellular pool of free amino acid. Desai *et al.* (1983) determined comparatively protein synthesis rates as obtained with L–[U–^{14}C]tyrosine and L–[1–^{14}C]leucine in ten patients and observed strong correlations between the PSR as assessed with both amino acids.

Furthermore, Pardridge and Oldendorf (1975) analyzed the kinetics of blood–brain barrier transport of amino acids and found that, except for phenylalanine, tyrosine and leucine had the smallest K_m values for transport into brain, and that both amino acids had the same brain uptake indexes.

In specific cells, both tracers are, besides protein synthesis, involved in other metabolic pathways. In melanocytes, tyrosine is a precursor for melanin synthesis, and in specific exocrin glands it is involved in the biosynthesis of hormones such as adrenalin and thyroxin (Karlson 1977). Leucine yields intermediates e.g. hydrox–methyl–glytaryl–CoA and Acetyl–CoA, which are incorporated into cholesterol (Rosenthal *et al.* 1974) and fat (Meikle and Klain 1972).

Banker and Cotman (1971), and James and co–workers (1974) pointed out that for the measurement of PSR the best position for labeling amino acids is the carboxyl group. The label in this position is decarboxylated, and the radioactivity is rapidly washed from tissue into the plasma bicarbonate pool and hereafter expired from lung into the air. The contribution of non–protein metabolite to the total tissue radioactivity is thus reduced substantially. Therefore, L–[1–^{11}C]tyrosine (Bolster *et al.* 1986b, Halldin *et al.* 1987) and L–[1–^{11}C]leucine (Barrio *et al.* 1983b) have been developed for the non–invasive investigation of PSR in tissue.

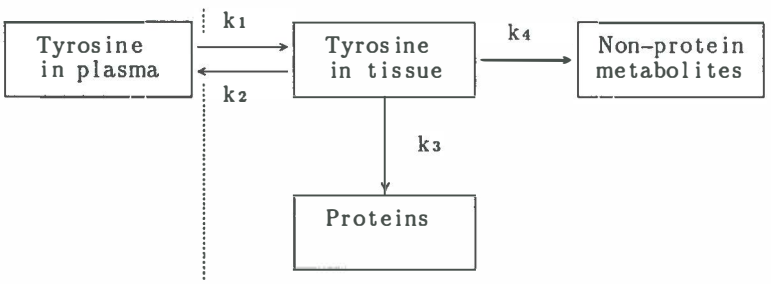

Figure 3. *Kinetic model for L–[1–^{11}C]tyrosine*

In figure 3, the kinetic model for L–[1–^{11}C]tyrosine is shown. For L–[1–^{11}C]leucine the model is basically the same. After an iv injection, tyrosine is transported from plasma into the cell (k_1), and is then converted into protein (k_3) or non–protein metabolite (k_4). With this model it is assumed that during the time required for a PET study (up to 1 hour after injection), no proteins synthetized from L–[1–^{11}C]tyrosine are degraded, resynthesis of L–[1–^{11}C]tyrosine from metabolites does not occur and the specific activity of free L–[1–^{11}C]tyrosine in the tissue is reflected by its specific activity in plasma. During the PET study, the dynamic regional tissue

^{11}C–radioactivity is determined as well as the dynamic L–[1–^{11}C]tyrosine concentration in plasma and the non–radioactive tyrosine level in plasma. The rate constants are obtained with curve–fitting procedures. Without going into details of the mathematical formulas, PSR can be approximated and is expressed as nmol protein/ml tissue/min.

Until now, L–[1–^{11}C]tyrosine has predominantly been used for the investigation of protein synthesis in tumors. In tissues of the Walker 256 carcinosarcoma–bearing rats, compartmental analysis of the above–mentioned model has been performed with L–[1–^{14}C]tyrosine (Ishiwata *et al.* 1988b). It was observed that L–[1–^{14}C]tyrosine had a higher incorporation into proteins and a lower amount of metabolites than L–[methyl–^{14}C]methionine and L–[1–^{14}C]methionine (Ishiwata *et al.* 1988a) in brain and tumor tissue. Hence, L–[1–^{11}C]tyrosine is more adequate than the ^{11}C–labelled methionines for the measurement of the PSR by PET.

In experimental tumor models, a correlation was observed between the growth rate of the tumor and the rate of amino acid incorporation into protein (Wagle *et al.* 1963, Bhargava *et al.* 1976). In studies with L–[1–^{11}C]tyrosine in experimental animal tumors, PSR of 0.8 and 0.4 nmol/ml/min were calculated for the Walker 256 tumor and a rhabdomyosarcoma tumor, respectively. This was expected from the doubling times of the Walker tumor (18 hours) and the rhabdomyosarcoma (4 days).

Tyrosine is also a precursor of melanin synthesis in malignant melanoma (Farishian and Whittaker 1979). In studies with cultured B–16 mouse melanoma cells, tyrosine was preferentially transported into cell as compared to methionine and leucine (Saga and Shimojo 1981). High uptakes of D,L–[1–^{11}C]tyrosine into melanotic Greene melanomas of hamsters were monitored by PET. Incorporation studies with L–[1–^{14}C]tyrosine in the same tumor revealed that 30 minutes after injection, 85% of the tracer was already incorporated into protein (van Langevelde *et al.* 1988). In malignant melanomas, conversion of L–[1–^{11}C]tyrosine into melanin is only a minor metabolic pathway, as compared to protein synthesis

In humans, experience with L–[1–^{11}C]tyrosine is still limited. Liver metastases, primary breast cancer, meningiomas were clearly visualized by PET in patients (Bolster *et al.* 1986b).

The longer physical half–life of ^{18}F (110 min) makes ^{18}F–labelled fluoro amino acids advantageous for the investigation of protein synthesis by PET. For this purpose, most fluorinated amino acids are nevertheless considered

inappropriate, because of the rapid in vivo defluorination (Fowden 1972).

Recently, ^{18}F–labelled fluoro aromatic amino acids have gained a renewed interest because of their relatively high stability in vivo. Out of these developments L–[2–^{18}F]fluorotyrosine has arisen as most promising for monitoring protein synthesis with PET. In mouse brain, 85% of L–[2–^{18}F]fluorotyrosine was incorporated into protein 60 minutes after injection, while no metabolites were detectable (Coenen *et al.* 1989). A three compartmental model has been proposed for the assessment of protein synthesis rates in brain. In tumors, possibly a four compartmental model is desired.

Carboxylic–labelled leucine, unlike tyrosine, has mainly been used for the investigation of protein synthesis in normal brain tissues. Smith and co–workers (1980) proposed a four–compartmental model for L–[1–^{14}C]leucine in order to estimate PSR in brain. Compartmental analyses of L–[1–^{14}C]leucine in rat brain revealed that at 35 min after injection 90% of the tracer was incorporated into protein, the plasma radioactivity of free L–[1–^{14}C]leucine was low (7%) and the amount of the metabolite α–ketoisocaproic acid was almost negligible (Keen *et al.* 1989). For application of L–[1–^{11}C]leucine in PET, this model was adapted by Phelps and co–workers (1984) and refined by Hawkins *et al.* (1989) by introducing a vascular term for the correction of the radioactivity measured in brain tissue.

1.3 ^{18}FDG for PET in oncology

In classical studies with tumor cells, Warburg *et al.* (1924) found enhanced lactate formation. In tumors, glycolysis appeared to be higher under aerobic and anaerobic conditions as compared to most normal tissues. In cancer cells, it was demonstrated that glucose transport and levels of the three key glycolytic enzymes such as hexokinase appeared to be elevated (Hatanaka *et al.* 1970, Weber 1977).

In order to calculate regional metabolic rates for glucose (rMRglu), Sokoloff *et al.* (1977) developed a kinetic three compartment model for ^{14}C–deoxyglucose in rat brain. After 2–[^{18}F]fluoro–2–deoxy–D–glucose (^{18}FDG) has been made available (Ido *et al.* 1977), the Sokoloff model has been adapted for this compound (Phelps *et al.* 1979, Reivich *et al.* 1979).

After transport into the cell (k_1), ^{18}FDG is phosphorylated to ^{18}FDG–6–PO_4 by the enzyme hexokinase (k_3). Because phosphorylated deoxyglucoses, unlike D–glucose, are no substrates for

glucose–6–PO_4–isomerase, ^{18}FDG–PO_4 is not metabolized further along the glycolytic pathway. Consequently, after injection of ^{18}FDG, the ^{18}F–radioactivity in tissue, as measured by PET, is predominantly in the phosphorylated form, although dephosphorylation by the enzyme phosphatase remains possible (k_4).

Figure 4. *Kinetic model for ^{18}FDG.*

The ^{18}FDG model yields regional metabolic rates of glucose found as the net rate of phosphorylation, i.e. (k3xCe)–(k4xCm). A complicating factor in the ^{18}FDG is the so–called lumped constant (LC), an expression that corrects for the differences in affinity for transport and hexokinase as well as the distribution volumes between glucose and FDG. This LC is not constant but varies for each different tissue, especially in heterogeneous and pathophysiological tissues such as tumors. Therefore, to circumvent these complications, ^{18}FDG metabolism is often expressed as an uptake value or a tissue–to–tissue ratio in stead of rMRglu (Di Chiro and Brooks 1988a).

Experiments with tumor–bearing animals, showed high uptake values for ^{18}FDG in a variety of tumors (Som *et al.* 1980, Kearfott *et al.* 1984, Kairento *et al.* 1985, Paul *et al.* 1989). The differences in the uptake values of ^{18}FDG into the different tumors were explained by differences in blood supply, hexokinase activity and growth rate of the tumor.

PET studies with ^{18}FDG are legion in patients with intracranial tumors. In more than 100 patients with gliomas and astrocytomas, rMRglu has been assessed using ^{18}FDG in tumors with varying grades of malignancy (Di Chiro 1986). In these studies, the grade of malignancy correlated with the rMRglu. In another study, Tyler and co–workers (1987) were not able to asses the grade of astrocytomas with PET using ^{18}FDG. The differences were explained by several facts. In the studies of Di Chiro, patients were investigated that had already received treatments, a camera with a low spatial resolution was used (16 mm), giving rise to substantial partial volume effects, the histology was already known before the PET study, and for the calculation of the rMRglu

fixed k and LC values were used (Di Chiro and Brooks 1988b, Tyler *et al.* 1988). Grading of astrocytomas and gliomas with FDG remains controversial.

Besides the many ^{18}FDG–PET studies with intracranial tumors, the number of studies with peripheral tumors is increasing. In head and neck tumors, Minn and co–workers (1988a) compared tumor–to–non–tumor uptake ratios of ^{18}FDG by PET with DNA flow–cytometry. A correlation was found between the percentage of S–phase cells and the uptake of ^{18}FDG, being an eligible indicator of aggressiveness of human cancer growth. Based on a limited number of patients, the metabolic activity of extremity musculoskeletal tumors as measured with ^{18}FDG correlated roughly with grade of malignancy (Kern *et al.* 1988). Nolop and co–workers (1987) observed high tumor–to–normal lung tissue uptake ratios for ^{18}FDG in human pulmonary neoplasms. Despite the excellent visualization, little correlation was observed between the tumor type and the rate of ^{18}FDG uptake. Also in advanced breast cancer, Minn and Soini (1989) were not able to discriminate between grade of malignancy and the uptake of ^{18}FDG.

Table 2. *PET Studies in a variety of tumors evaluating the possible use of ^{18}FDG for assessing the grade of malignancy.*

Investigators	Tumor	Patients	Grading/malignancy
Di Chiro (1986)	Glioma/Astrocytoma	100	+
Tyler *et al.* (1987)	Glioma/Astrocytoma	17	–
Minn *et al.* (1988a)	Head/Neck cancer	13	+
Kern *et al.* (1988)	Musculoskeletal cancer	5	±
Nolop *et al.* (1987)	Lung carcinoma	12	–
Minn *et al.* (1989)	Breast cancer	17	–

Glycolysis in tumors is considered to be a link between PET and magnetic resonance spectroscopy (MRS) (Lear 1990). In human gliomas, Alger *et al.* (1990) acquired images with PET using ^{18}FDG and compared these with H–1 MR signal intensities of acetyl aspartate, choline, lactate and creatine concentrations obtained in tumor volumes of at least 8 cm^3. Elevated lactate intensities were observed in tumors that were hypometabolic as well as hypermetabolic on the ^{18}FDG images. In intracranial tumor, Luyten *et al.* (1990), due to technical improvements, was able to acquire topographic metabolite maps in volumes of 1.5 cm^3 in H–1 spectroscopic images. For the first time, with this better spatial resolution, increased ^{18}FDG uptake could

topographically be related to lactate formation. In intracranial tumors, Heiss and co–workers (1990) compared ^{18}FDG metabolism with ^{31}P–MRS. In all tumors studied, the concentrations of the energy–rich phosphates appeared to be decreased. Because ^{31}P–MRS needs volumes of at least 27 cm^3 for adequate data acquisition, a correlation between type of tumor and the ^{31}P–MRS data was difficult to establish. Heiss *et al.* concluded that PET and ^{31}P–MRS can independently and complementarily contribute to the differential diagnosis of tumor.

The use of ^{18}FDG in tumor therapy is discussed in section 4 of this chapter

1.4 PET to evaluate tumor therapy

1.4.1 Some thermo and radiobiological considerations in oncology

Hyperthermia

Hyperthermia is treatment of tissue with heat applied at temperatures above the normal body temperature. In tumor therapy, hyperthermia is used at temperatures between 41 and about 47 °C. The dose of heat applied is a function of temperature and duration of treatment. Treatment of tumor tissue with heat may cause an arrest of uncontrolled proliferation and a killing of tumor cells. The killing of tumor cells is possibly a result of denaturation of proteins and is not likely caused by direct damage to DNA, as is the case with ionizing radiation (Konings 1987). Furthermore, hyperthermia induces alterations in membrane, nuclear and cytoskeletal structures. Also metabolism and synthesis of macromolecules, such as proteins and DNA, are changed. Tumors are generally more sensitive to hyperthermic treatments than normal cells because of the poorer blood supply (resulting in higher temperatures than normal tissues), the lower pH and the nutrient deficiencies (Field 1983).

Radiotherapy

During a radiotherapeutic treatment, tumors are irradiated with a dose of ionizing radiation, such as γ–rays, β–particles or neutrons. Ionizing radiation has the ability to stop cell divisions and to eliminate cells in tumors (Hall 1987). Two types of radiation–induced cell death may be distinguished: reproductive death and interphase death. During irradiation,

free radicals are generated that induce chemical reactions in the cells. Many compounds, such as DNA, RNA, proteins, lipids and glucose are damaged by ionizing radiation. For dividing cells, intact DNA is essential for mitosis. The loss of a cell's ability to divide is called reproductive death. At biologically relevant doses, ionizing radiation has been shown to cause damage to DNA, which is correlated to induction of chromosomal aberrations in proliferating cells. Interphase death is the impairment of cellular metabolism by disintegration of the cell before entering mitosis. In most cells, interphase death occurs at much higher doses (20–400 Gy) than those necessary to cause reproductive death (0–20 Gy).

Radiation in combination with heat

When a tumor tissue is subjected to a combined treatment of hyperthermia and radiation, synergism with respect to cell killing is observed. Thus, hyperthermia has a sensitizing effect on the efficacy of a radiotherapeutic treatment. It is generally believed that hyperthermia inhibits the repair of radiation damage in a heat dose dependent way. The critical molecular target for this radiation damage is DNA. Hyperthermia seems to cause a decreased accessibility of the repair enzymes to the damaged sites of the DNA molecule.

Effects of treatment on tumor growth

An effective treatment, in vivo, is reflected in inhibition of tumor growth (Overgaard *et al.* 1987). In figure 5, tumor volume is plotted against time. Tumor growth kinetics can be quantified by the tumor doubling time (TD). The TD is the time needed to double a certain tumor volume. The efficacy of a therapeutic treatment can be derived from changes in the TD and is calculated as growth delay (GD):

$$GD = \frac{TD_{\text{untreated tumor}} - TD_{\text{treated tumor}}}{TD_{\text{untreated tumor}}} .$$

Synergism between heat and radiation on tumor growth can be calculated as a thermal enhancement ratio (TER):

$$TER = \frac{\text{GD of the combination of radiation with heat}}{\text{GD of radiation alone + GD of heat alone}} .$$

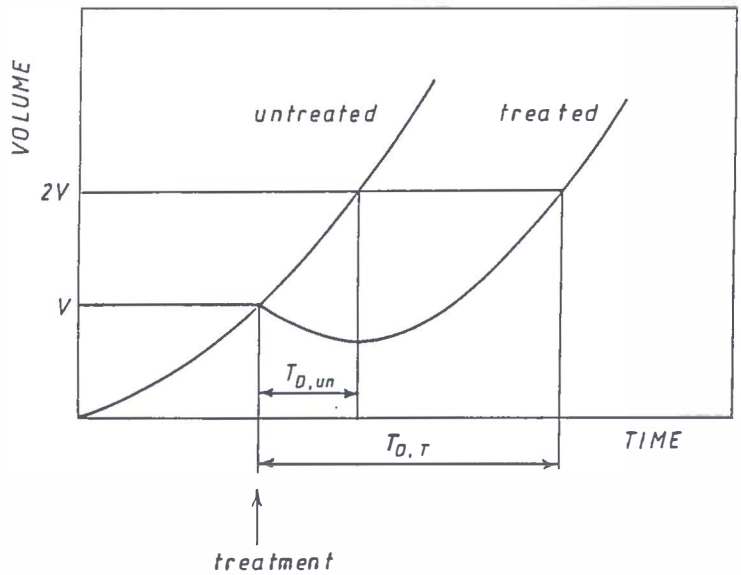

Figure 5. *Schematic representation of growth curves of treated and untreated tumor demonstrating the effect of treatment on tumor doubling time as a delay in growth after treatment.*

PET as a diagnostic tool to monitor growth

In tumor therapy, DNA and protein synthesis as well as glycolysis (monitored with PET) can be evaluated at different phases:

(1) In the pretreatment phase, untreated tumors are diagnosed, which may lead to characterization of the tumor and as such contributes to the treatment plan.

(2) During treatment, acute metabolic changes are monitored which may have value for early prognosis on tumor cell killing. At this phase, it is possible to adjust the treatment plans in case PET shows inadequacy of initial treatment.

(3) In the follow–up phase of treatment. At this phase, insight can be obtained on the achieved extent of cell killing by the treatment or on the possible recurrence of tumors. PET data acquired in this phase may have consequences for possible follow–up treatments of the cancer patient.

In the following parts of section 4, investigations are summarized on the evaluation of radiotherapy, chemotherapy and surgery in tumors using ^{11}C–labelled amino acids and ^{18}FDG. In the majority of these PET studies evaluating therapeutic treatments with ^{11}C–labelled amino acids and ^{18}FDG, PET data are used in the follow–up phase. PET studies in tumors, performed in the pretreatment phase or during treatment, in order to guide planning of treatment are scarce. More PET data should become available to explore these possibilities of PET.

1.4.2 Radiotherapy

PET offers opportunity to determine the radiobiological effects of ionizing radiation on tumor biochemistry in relation to tumor growth.

The applicability of labelled amino acids and glucose analogs for the investigation of radiotherapy with PET has been demonstrated in studies with tumor–bearing animals. In different rodent tumor models, Abe *et al.* (1986) were able to discriminate radiosensitivity and radioresistance of tumors by measuring differences in uptake of ^{18}FDG into tumor tissue between the untreated and the irradiated situation. With a radiosensitive tumor, Kubota *et al.* (1989) found a rapid linear decrease of L–[methyl–^{11}C]methionine uptake after irradiation preceding extension of radiation necrosis and tumor shrinkage. This decline in methionine uptake was ascribed to a radiation–induced damage of the amino acid transport across the cell membrane.

The number of clinical studies using PET to evaluate radiotherapeutic treatment in patients is rapidly increasing, and from these studies, applications are emanating.

Patients with brain tumors that underwent a course of radiotherapeutic treatment often deteriorate after a period of months or years due to radiation necrosis of brain tissue. With MRI and X–ray CT, attempts to discriminate brain necrosis from recurrent tumor appeared to be not successful (Graeb *et al.* 1982, Dooms *et al.* 1986).

With PET and ^{18}FDG, Patronas and co–workers (1982) correctly differentiated between radiation necrosis (low uptake) and recurrent tumor (high uptake) in a number of astrocytomas 24 to 52 months post–irradiation. The PET findings were confirmed by histological analysis of biopsy. These findings are in line with results from Doyle *et al.* (1987), who compared ^{18}FDG with ^{82}Rb images for detection of blood–brain barrier disruptions. Although

the ^{82}Rb images did not provide information on radiation necrosis, they were considered useful for accurate delineation of tumor on the ^{18}FDG images. Valk *et al.* (1988) investigated deteriorating patients with brain tumors treated with external radiotherapy in combination with implanted ^{125}I–sources (brachytherapy). In this study, ^{18}FDG proved to be an eligible indicator for radiation necrosis and recurrent tumor. Histological analysis of biopsy obtained after subsequent surgery revealed presence of viable tumor cells of the brain necrosis lesions. It was suggested that surviving tumor cells remain morphologically intact but have little glycolytic activity.

Short term effects of radiotherapy on metabolic activity of tumor cells are also of interest for PET. Minn *et al.* (1988b) compared ^{18}FDG uptake into a variety of head and neck tumors prior to and directly after a course of 30 Gy radiotherapy. With PET and ^{18}FDG, early distinction between respondent and non–respondent tumors to irradiation was observed, leaving opportunity for early adjustments of possible subsequent treatments. Relative short term effects were studied by Ogawa *et al.* (1988) in patients with glioma one month after radiotherapy in combination with ACNU and FT207 chemotherapy. In this study, the ^{18}FDG utilization of the tumors appeared to be decreased with an average of 40%, whereas O_2 consumptions and tumor blood flow remained unaffected.

Till now ^{11}C–labelled amino acids are seldomly applied in radiotherapeutic studies. In 4 patients with gliomas, Derlon and co–workers (1989) observed decreased L–[methyl–^{11}C]methionine uptake one month after irradiation. Definite conclusions about these effects could not be drawn because the measured metabolic changes did not correlate with the observed therapeutic outcome.

1.4.3 Chemotherapy

Two main avenues are open to explore PET in relation to pharmacotherapy of cancer. Firstly, antineoplastic agents are labelled with positron–emitting radionuclides for the evaluation of pharmacokinetics and for the assessment of therapeutic sensitivity in tumors. Secondly, effects of chemotherapeutics and other drugs acting on tumors can indirectly be monitored by PET in terms of effects on other metabolic functions e.g. glycolysis or protein synthesis.

In patients with glioma, effects of intra–arterial BCNU infusions were studied by PET and ^{18}FDG (Di Chiro *et al.* 1988c). With PET using ^{18}FDG it was

possible to differentiate between tumor necrosis and residual tumor. Furthermore, the neurotoxic side-effects of BCNU due to chemonecrosis of normal brain were found as a suppression of the ^{18}FDG uptake. Similar side effects of metotrexate on normal brain were observed as increased brain capillary permeability and inhibited phosphorylation of ^{18}FDG (Phillips *et al.* 1987).

The results of intra-arterial BCNU therapy of gliomas, as measured by changes in L-[methyl-^{11}C]methionine uptake were not convincing (Derlon *et al.* 1989). Chemotherapy resulted in unpredictable changes of methionine uptake into the glioma. Furthermore, a correlation between the induced changes in methionine uptake and survival rate could not be established.

Bergström *et al.* (1987b) observed a rapid decrease in L-[methyl-^{11}C]methionine uptake into prolactin-secreting pituitary adenomas after treatment. The reduced methionine uptake was accompanied by a reduction of the elevated serum prolactin level and by a shrinkage of the tumor volume.

1.4.4 Surgery

The beneficial value of PET in conjunction with surgical treatment of cancer is demonstrated in the provision of accurate coordinates of extent of brain tumors and to post-operative follow-up to discriminate between scar and recurrent tumor.

MRI, X-ray CT and PET using L-[methyl-^{11}C]methionine or [^{68}Ga]EDTA were compared with histology, as obtained with stereotactic biopsies, in a variety of supratentorial tumor e.g. gliomas and astrocytomas (Lilja *et al.* 1985, Mosskin *et al.* 1987, 1989). From these studies it can be concluded that (1) the MRI signal, on account of edema, overestimated the extent of the tumor (2) X-ray CT and [^{68}Ga]EDTA, although apposite for the detection of disruptions of the blood-brain barrier, gave an underestimation of extent of viable tumor (3) PET using L-[methyl-^{11}C]methionine gave the best correlation with the extent of viable tumor as verified with histological analysis. Accurate coordinates of tumor extent is a valuable contribution of PET in the planning of surgery and other therapeutic modalities.

Recently, PET has been applied in the post-operative follow-up of malignancies. In long-term survivors of brain tumor surgery, Lilja and co-workers (1989) observed that L-[methyl-^{11}C]methionine highly accumulated in recurrent tumor, while hypometabolism was observed in clinically stable

patients. Thus, PET using L-[methyl-^{11}C]methionine discriminated more accurately between postoperative brain lesions and tumor recurrence than X-ray CT.

In 18 post-operative rectal masses, which could not be identified with CT, Schlag *et al.* (1989) differentiated by the use of PET and ^{18}FDG between scar and recurrent tumor. For differentiation, the ^{18}FDG method was more effective than immunoscintigraphy using ^{131}I-labelled $F(ab')_2$ fragments against carcinoembryonic antigen (CEA). Similar findings were reported by Strauss *et al.* (1989) in 29 patients with colorectal tumor. After surgery PET using ^{18}FDG differentiated clearly between recurrent colorectal malignancy and scar in all cases.

1.5 Scope of the thesis.

The scope of this thesis is to evaluate the use of PET during treatment of cancer. For this purpose, protein synthesis was chosen as an important biochemical process in tumor tissue influenced by therapy. In chapter 2, comparative PET studies are described for the selection of an amino acid appropriate for the investigation of protein synthesis in tumors. To obtain answers to clinical questions regarding the use of PET in cancer therapy, PET data obtained from experiments with tumor-bearing animals are a prerequisite. Therefore, in chapter 3, five experimental animal models are evaluated for their applicability in experimental PET. PET experiments for an early prognosis on the efficacy of an hyperthermic treatment are reported in chapter 4. In these animal experiments, acute hyperthermic effects on protein synthesis, as measured by PET, are correlated with later effects on tumor growth. The use of PET in radiotherapy is described in chapter 5. In tumor-bearing animals, acute and indirect effects of radiation or a combination of radiation with heat on protein synthesis and glycolysis are correlated with alterations in tumor growth. In chapter 6, dopamine agonist treatment of prolactinoma patients is evaluated by PET. In these patients, the effects of bromocryptine on amino acid uptake, as monitored by PET, are correlated with effects on the serum prolactin level.

Appendix

Pivotal scientific discoveries and inventions indicating the foreland of PET and hence of this thesis.

1840 First reference of Berzelius's postulate, proteins (Mulder)

1846 Isolation of tyrosine from casein (Liebig)

1895 Generation of X–rays (Röntgen)

1896 Discovery of natural radioactivity (Becquerel)

1901 Construction of Babbage's analytical machine, first computer (Ohdner)

1903 Treatment of cancer with radioactive sources (Bell)

1923 Development of tracer principle (v. Hevesy)

1924 Enhanced lactate formation in tumors (Warburg)

1931 Invention of cyclotron (Lawrence)

1932 Detection of positron as first example of antimatter (Anderson)

1935 Artificially produced positron–emitting radionuclides (Joliot & Curie)

1939 $^{11}CO_2$ used in photosynthesis studies (Kamen)

1958 Presentation of gamma–camera (Anger)

1975 PET–I in operation (Ter–Pogossian)

1977 ^{14}C–Deoxyglucose model (Sokoloff)

References

Abe Y, Matsuzawa M, Fujiwara T, Fukuda H, Itoh M, Yamamada K, Yamaguchi K, Sato T and Ido T, Eur. J. Nucl. Med. 12, 325–328 (1986).

Abe Y, Matsuzawa T, Itoh M, Ishiwata K, Fujiwara T, Sato T, Yamaguchi K and Ido T, Eur. J. Nucl. Med. 14, 388–392 (1988).

Alger JR, Frank JA, Bizzi A, Fulham MJ, DeSouza BX, O'Duhaney MO, Inscoe SW, Black JL, van Zijl PC, Moonen CT and Di Chiro G, Radiology 177, 633–641 (1990).

Aquilar TS, Benevenga NJ and Harper AE, J. Nutr. 104, 761–771 (1974).

Banker G and Cotman CW, Arch. Biochem. Biophys. 142, 565–573 (1971).

Barrio JR, Keen R, Chugani H, Ackerman R, Chugani DC and Phelps ME, J. Nucl. Med. 24, P70 (1983a).

Barrio JR, Keen RE, Ropchan JR, MacDonald NS, Baumgartner FJ, Padgett HC and Phelps MC, J. Nucl. Med. 24, 515–521 (1983b).

Bergström M, Ericson K, Hagenfeldt L, Mosskin M, von Holst H, Norén G, Erikson L, Ehrin E and Johnström P, J. Comp. Ass. Tom. 11, 208–213 (1987).

Bergström M, Muhr C, Lundberg PO, Bengström K, Gee AD, Fasth KJ and Långström B, J. Comp. Ass. Tom. 11, 815–819 (1987).

Bhargava PM, Szafarz D, Bornecque CA and Zajdela F, J. Membrane Biol. 26, 31–41 (1976).

Bolster JM, Vaalburg W, Elsinga PH, Wynberg H and Woldring MG, J. Appl.Radiat. Isot. 37, 1069–1070 (1986a).

Bolster JM, Vaalburg W, Paans A, van Dijk TH, Elsinga PH, Zijlstra JB, Piers DA, Mulder NH, Woldring MG and Wynberg H, Eur. J. Nucl. Med. 12, 321–324 (1986b).

Bustany P, Sargent T, Saudubray JM, Henry JF and Comar D, J. Cereb. Blood Flow Metab. 1, S17–S18 (1981).

Bustany P and Comar D, In: *Positron Emssion Tomography.* Ed. Reivich M, Alan R. Liss, 183–201 (1985).

Bustany P, Chatel M, Derlon JM, Darcel F, Sgouropoulos F, Soussaline F and Syrota A, J. Neuro–Onc. 3, 397–004 (1986).

Casey DL, Digenis GA, Wesner DA, Washburn LC, Chaney JE, Hayes RL and Callahan AP, J. Appl. Radiat. Isot. 32, 325–330 (1981).

Clarke JT and Bier DM, Metabolism 31, 999–1005 (1982).

Coenen H, Kling P and Stöcklin G, J. Nucl. Med. 30, 1367–1372 (1989).

Comar D, Cartron JC, Maziere M and Marazano C, Eur. J. Nucl. Med. 1, 11–14 (1976).

Conti PS, Sordillo PP, Schmall B, Benua RS, Bading JR, Bigler RE and Laughlin JS, Eur. J. Nucl. Med 12, 353–356 (1986).

Derlon JM, Bourdet C, Bustany P, Chatel M, Theron J, Darcel F and Syrota A, Neurosurgery 25, 720–728 (1989).

Desai S, Moldawer LL, Bistrian BR and Blackburn GL, Clin. Sci. 65, 499–505 (1983).

Di Chiro G, Invest. Radiol. 22, 360–371 (1986).

Di Chiro G and Brooks RA, J. Nucl. Med. 29, 1603–1604 (1988a).

Di Chiro G and Brooks RA, J. Nucl. Med. 29, 421–422 (1988b).

Di Chiro G, Oldfield E, Wright DC, De Michele D, Katz DA, Patronas NJ, Doppman JL, Larson SM, Ito M and Kufta CV, Am. J. Radiol. 150, 189–197 (1988c).

Dooms GC, Hecht S, Brant–Zawadski M, Berthiaume Y, Norman D and Newton HT, Radiology 158, 149–155 (1986).

Doyle WK, Budinger TF, Valk PE, Levin VA and Gutin PH, J. Comp. Ass. Tom. 11, 563–570 (1987).

Edén E, Ekman L, Bennegård K, Lindmark L and Lundholm K, Metabolism 33, 1020–1027 (1984).

Elsinga PH, Daemen B, Ishiwata K and Vaalburg W, J. Nucl. Med. Biol. 17, 587–600 (1990).

Farishian RA and Whittaker JR, Arch. Biochem. Biophys. 196, 449–461 (1979).

Field SB, In: *The radiobiological basis of radiotherapy.* Eds. Steel GG, Adams GE and Peckham MJ, Elsevier, 287–303 (1983).

Finkelstein JD, In: *Transmethylation.* Eds. Usdin E, Borchardt RT and Creveling RT, Elsevier, 49–58 (1978).

Fowden L, In: *Ciba Foundation Symposium, carbon–fluorine compounds*, Elsevier, 141–159 (1972).

Fowler JS and Wolf AP, In: *Positron Emission Tomography and Autoradiography: Principles and Applications for the brain and heart.* Eds. Phelps M, Mazziota J. and Schelbert H, Raven press, 391–450 (1986).

Fujiwara T, Matsuzawa T, Kubota K, Abe Y, Itoh M, Fukuda H, Hatazawa J, Yoshioka S, Yamaguchi K, Ito K, Watanuki S, Takahashi T, Ishiwata K, Iwata R and Ido T, J, Nucl. Med. 30, 33–37 (1989).

Garlick PJ and Marshall I, J Neurochem. 19, 577–583 (1971).

Graeb DA, Steinbok P and Robertson WD, Radiology 144, 813–817 (1982).

Hall, *Radiobiology for the radiobiologist*, Lippincott (1987).

Halldin C, Schoeps KO, Stone-Elander S and Wiesel FA, Eur. J. Nucl. Med. 13, 288–291 (1987).

Hatanaka M, Augl C and Gilden RV, J. Biol. Chem. 245, 714–717 (1970).

Hawkins RA, Huang SC, Barrio JR, Keen RE, Feng D, Mazziotta JC and Phelps ME, J. Cereb. Blood Flow Metab. 9, 446–460 (1989).

Heiss WD, Heindel W, Herholz K, Rudolf J, Bunke J, Jeske J and Friedman G, J. Nucl. Med. 31, 302–310 (1990).

Hübner KF, King P, Gibbs WD, Partain CL, Washburn, Hayes RL and Holloway E, In: *Medical Radionuclide Imaging*, IAEA Vienna, 515–529 (1980).

Hübner KF, Krauss S, Washburn LC, Gibbs WD and Holloway EC, Clin. Nucl. Med. 6, 249–252 (1981).

Hunter DC, Weintraub M, Blackburn GL and Bistrian BR, Br. J. Surg. 76, 149–153 (1989).

Ido T, Wan CN and Fowler JS, J. Org. Chem. 42, 2341–2342 (1977).

Ishiwata K, Vaalburg W, Elsinga PH, Paans A and Woldring MG, J. Nucl. Med. 29, 1419–1427 (1988a)

Ishiwata K, Vaalburg W, Elsinga PH, Paans A and Woldring MG, J. Nucl. Med. 29, 524–529 (1988b).

Ishiwata K, Ido T, Takahashi T, Iwata R, Brady F, Hatazawa J and Itoh M J. Nucl. Med. Biol. 16, 371–374 (1989).

James W, Sender P, Garlick PJ and Waterlow JC, In: *Dynamic studies with radioisotopes in medicine*, IAEA Report No. 185, 461–472 (1975).

James W, Garlick P, Sender P and Waterlow J, Clin. Sci. Mol. Med. 50, 525–532 (1976).

Jones RM, Cramer S, Sargent T and Budinger, J. Nucl. Med. 26, P168 (1985).

Johnström P, Stone-Elander S, Ericson K, Mosskin M and Bergström M, J. Appl. Radiat. Isot. 38, 729–734 (1987).

Kairento AL, Brownell GL, Elmaleh DR and Swartz MR, Br. J. Radiol. 58, 637–643 (1985).

Karlson P, *Biochemie*, Thieme Verlag, 1977.

Kearfott KJ, Elmaleh DR, Goodman M, Correia JA, Alpert NM, Ackerman RH, Brownell GL and Strauss WH, J. Nucl. Med. Biol. 11, 15–22 (1984).

Keen RE, Barrio JR, Huang SC, Hawkins RA and Phelps ME, J. Cereb. Blood Flow Metab. 9, 429–445 (1989).

Kern KA, Brunetti A, Norton J, Chang AC, Malawer M, Lack E, Finn RD, Rosenberg SA and Larson SM, J. Nucl. Med. 29, 181–186 (1988).

Kirikae M, Diksic M and Yamamoto YL, J. Cereb. Blood Flow Metab. 9, 87–89 (1989).

Konings AWT, Radiat. Phys. Chem. 30, 339–349 (1987).

Kubota K, Yamada K and Fukuda H, Eur. J. Nucl. Med. 9, 136–150 (1984).

Kubota K, Matsuzawa T, Ito M, Fujiwara T, Abe Y, Yoshioka S, Fukuda H, Hatazawa J, Iwata R, Watanuki S and Ido T, J. Nucl. Med. 26, 37–42 (1985).

Kubota K, Matsuzawa T, Fujiwara T, Abe Y, Ito M, Hatazawa J, Ido T, Ishiwata K and Watanuki S, J. Comp. Ass. Tom. 12, 794–796 (1988).

Kubota K, Matsuzawa K, Takahashi T, Fujiwara T, Kinomura S, Ido T, Sato T, Kubota R, Tada M and Ishiwata K, J. Nucl. Med. 30, 2012–2016 (1989).

van Langevelde A, van der Molen HD, de Korver-Journée JG, Paans A, Pauwels E and Vaalburg W. Eur. J. Nucl. Med. 14, 382–387 (1988).

Långström B and Lundqvist H, J. Appl. Radiat. Isot. 27, 357–363 (1976).

Lear JL, Radiology 174, 328–330 (1990).

Lilja A, Bergström K, Hartvig P, Spännare P, Halldin C, Lundqvist C and Långström B, Am. J. Neuro. Rad. 6, 505–514 (1985).

Lilja A, Lundqvist H, Olsson Spännare B, Gullberg P and Långström B, Acta Radiologica 30, 121–128 (1989).

Lobley GE, Milne V, Lovie J, Reeds PJ and Pennie K, Br. J. nutr. 43, 491–502 (1980).

Lombardini JB and Talalay P, Adv. Enzyme Reg. 9, 349–384 (1971).

Luyten PR, Marien A, Heindel W, van Gerwen PH, Herholz K, den Hollander JA, Friedman G and Heiss WD, Radiology 176, 791–799 (1990).

Mazoyer BM, Levasseur M, Syrota A, Prenant C, Baron JC, Sette G, Verrey B and Samson Y, J. Nucl. Med. 30, 822 (1989).

Meikle AW and Klain GJ, Am. J. Phys. 222, 1246–1250 (1972).

Minn H, Joensuu H, Ahonen A and Klemi P, Cancer 61, 1776–1781 (1988a).

Minn H, Paul R and Ahonen A, J. Nucl. Med. 29, 1521–1525 (1988b).

Minn H and Soini, Eur. J. Nucl. Med. 15, 61–66 (1989).

Moldawer LL, Kawamura I, Bistrian BR and Blackburn GL, Biochem. J. 210, 811–817 (1983).

Mosskin M, von Holst H, Bergström M, Collins VP, Eriksson L, Johnström P and Norén G, Acta Radiologica 28, 673–681 (1987).

Mosskin M, Ericson K, Hindmarsh T, von Holst H, Collins VP, Bergström M, Eriksson L and Johnström P, Acta Radiologica 30, 225–232 (1989).

Nolop KB, Rhodes CG, Brudin LH, Beaney RP, Krausz T, Jones T and Hughes JM, Cancer 60, 2682–2689 (1987).

Nyhan WL and Busch H, Cancer Res. 18, 385–393 (1958).

Ogawa T, Uemura K, Shisido F, Yamaguchi T, Murakami M, Inugami A, Kanno I, Sasaki H, Kato T, Hirata K, Kowada M, Mineura K and Yasuda T, J. Comp. Ass. Tom. 12, 290–297 (1988).

Oldendorf WH, Am. J. Phys. 221, 1629–1639 (1971).

Overgaard J, Matsui M, Lindegaard JC, Grau C, Zachariae C, Johansen IM, von der Maase H and Nielsen OS, In: *Rodent tumor models in experimental cancer therapy*, Pergamon, 128–135 (1987).

Pardridge WM and Oldendorf WH, Biochim. Biophys. acta. 401, 128–136 (1975).

Patronas NJ, Di Chiro G, Brooks RA, DeLaPaz RL, Kornblith BH, Smith BH, Rizolli RV, Kessler RM, Manning RG, Channing M, Wolf AP and O'Connor CM, Radiology 144, 885–889 (1982).

Paul R, Aho K, Bergman J, Haaparanta M, Kulmana J, Reissel A and Solin O, J. Nucl. Med. Biol. 16, 449–453 (1989).

Phelps ME, Huang SC, Hoffman EJ, Selin C, Sokoloff L and Kuhl DE, Ann. Neurol. 6, 371–388 (1979).

Phelps ME, Barrio JR, Huang SC, Keen RE, Chugani H and Mazziotta JC, Ann Neurol. 15, S192–S202 (1984).

Phillips PC, Dhawan V, Strother SC, Sidtis JJ, Evans AC, Allan JC, and Rottenberg DA, Ann. Neurol. 21, 59–63 (1987).

Sauer LA, Stayman JW and Dauchy RT, Cancer Res. 42, 4090–4097 (1982).

Reiman RE, Huvos AG, Benua RS, Rosen G, Gelbard AS and Laughlin JS, Cancer 48, 1976–1981 (1981).

Reiman RE, Benua RS, Gelbard AS, Allen JC, Vomero JJ and Laughlin JS, J. Nucl. Med. 23, 682–687 (1982a).

Reiman RE, Rosen G, Gelbard AS, Benua RS and Lauglin JS, Radiology 142, 495–500 (1982b).

Reivich M, Kuhl DE, Wolf A, Greenberg J, Phelps M, Ido T, Casella V, Fowler J, Hoffman E, Alavi A, Som P and Sokoloff L, Circ. Res. 44, 127–137 (1979).

Rosenthal J, Angel A and Farkas J, Am. J. Phys. 226, 411–418 (1974).

Saga K and Shimojo T, J. Biochem. 92, 343–355 (1982).

Sauer LA, Stayman JW and Dauchy RT, Cancer Res. 42, 4090–4097 (1982).

Schlag P, Lehner B, Strauss LG, Georgi P and Herfarth C, Arch. Surg. 124, 197–199 (1989).

Schmall B, Cont PS, Bigler RE, Zanzonico PB, Reiman RE, Benua RS, Yeh S, Dahl JR, Lee R and Laughlin JS, Clin. Nucl. Med. 12, 22–26 (1987).

Schober O, Meyer GJ, Gaab MR, Müller JA and Hundeshagen H, J. Nucl. Med. 27, 890 (1986).

Shanbhoque R, Bistrian B, Lakshman K, Crosby L, Swenson S, Wagner D, Jenkins RL and Blackburn GL, Metabolism 36, 1047–1053 (1987).

Simon O, Münchmeyer R, Bergner H, Zebrowska T and Buraczewska L, Br. J. Nutr. 40, 243–252 (1978).

Smith CB, Davidsen L, Deibler G, Patlak C, Pettigrew K and Sokoloff L, Trans. Am. Soc. Neorochem. 11, 94 (1980).

Sokoloff L, Reivich M, Kennedy C, Des Rosiers MH, PatlaK CS, Pettigrew KD, Sakurada O and Shinokaza M, J. Neurochem. 28, 897–916 (1977).

Som P, Atkins HL, Bandyopadhyay D, Fowler JS, MacGregor RR, Matsui K, Oster ZH, Sacker DF, Shiue CY, Turner H, Wan CN, Wolf AP and Zabinski SV, J. Nucl. Med. 21, 670–675 (1980).

Strauss LG, Clorius JH, Schlag P, Lehner B, Kimmig B, Engenhardt R, Marin–Grez M, Helus F, Oberdorfer F, Schmidlin P and van Kaick G, Radiology 170, 329–332 (1989).

Syrota A, Duquesnoy N, Paraf A and Kellerhohn C, Radiology 143, 249–253 (1982).

O'Tuama LA, Phillips PC, Strauss LC, Carson BJ, Uno Y, Smith QR, Dannals RF, Wilson AA, Ravert HT, Loats S, Loats HA, LaFrance ND and Wagner HN, Pedriat. Neurol. 6, 163–170 (1990).

Tyler JL, Diksic M, Villemure JG, Evans AC, Meyer E, Yamamoto YL and Feindel T, J. Nucl. Med. 28, 1123–1133 (1987).

Tyler JL, Diksic M, Villemure JG, Evans AC, Meyer E, Yamamoto YL and Feindel T, J. Nucl. Med. 29, 422–423 (1988).

Valk PE, Budinger TF, Levin VA, Silver P, Gutin PH and Doyle WK, J. Neurosurg. 69, 830–838 (1988).

de Vis K, Schelstraete K, Deman J, Vermeulen FL, Sambre J, Goethals P, van Haver D, Slegers G, Vandecasteele C and de Schrijver A, Acta Oncologica 26 105–111 (1987).

Wagle SR, Morris HP and Weber G, Cancer Res. 23, 1003–1007 (1963).

Washburn LC, Wieland BW, Sun TT, Hayes RL and Butler TA, J. Nucl. Med. 19, 77–83 (1978).

Warburg O, Posener K and Negelein E, Biochem. Z. 152, 309–344 (1924).

Weber G, N. Eng. J. Med. 296, 541–551 (1977).

CHAPTER 2

A COMPARATIVE PET STUDY USING DIFFERENT ^{11}C-LABELLED AMINO ACIDS IN WALKER 256 CARCINOSARCOMA-BEARING RATS.

Bernard J.G. Daemen, Philip H. Elsinga, Kiichi Ishiwata, Anne M.J. Paans and Willem Vaalburg

[published in Nuclear Medicine and Biology 18, 197–204 (1990)]

ABSTRACT

In Walker 256 carcinosarcoma–bearing rats, the dynamic distribution of L–[1–^{11}C]tyrosine, L–[methyl–^{11}C]methionine, L–[1–^{11}C]methionine and D–[1–^{11}C]methionine has been measured by PET. An equivalent tumor–imaging potential was observed for each of the three L–amino acids. Thirty minutes after injection, the tumors accumulated 57% ($P<0.01$) more ^{11}C–activity from L–[1–^{11}C]methionine than from L–[methyl–^{11}C]methionine. At the same point of time, the livers showed a 33% ($P<0.001$) higher ^{11}C–uptake with L–[methyl–^{11}C]methionine than with L–[1–^{11}C]methionine. The dynamic tissue data are in agreement with the findings in experiments with ^{14}C–analogs.

INTRODUCTION

One of the most interesting fields of positron emission tomography (PET) in oncology is the application of ^{11}C–labelled amino acids. On account of an elevated growth rate, most tumor cells have an increased demand for amino acids. When offered, ^{11}C–labelled amino acids will often be concentrated by tumor tissues. This physiochemical phenomenon can be visualized by PET and may provide answers to important clinical issues. Visualization of tumors with ^{11}C–amino acids may yield accurate coordinates for stereotactic surgery of brain tumors (Lilja *et al.* 1985). Furthermore, the effect of therapeutic interventions on tumor can be evaluated in terms of alterations in ^{11}C–amino acid uptake (Dunzendorfer *et al.* 1981, Daemen *et al.* 1989a,b). The amount of ^{11}C–amino acid accumulated into tumor may be an indicator for the grade of malignancy of the tissue (Schober *et al.* 1986).

L–[methyl–^{11}C]methionine can be synthesized easily; no complex purification procedure is necessary, and the radiochemical yield is high. Therefore, this particular ^{11}C–amino acid has been used most often for the detection of a great variety of tumors (Lilja *et al.* 1985, Kubota *et al.* 1985, Bergström *et al.* 1987, Schober *et al.* 1986, 1987). Because methionine is the main source of the active methyl–group, investigations in brain (Jones *et al.* 1985) and tumor (Ishiwata *et al.* 1988b) have shown that L–[methyl–^{14}C]methionine is utilized to a fair extent, as a methyl–group donator. Therefore methyl–labelled methionine appears to be less suitable for investigating protein synthesis by PET. Carboxylic–labelled amino acids have greater potential for measuring the protein synthesis process (Banker and Cotman 1971). Metabolic studies with L–[1–^{14}C]tyrosine and L–[1–^{14}C]methionine showed that these two amino acids have a low amount of labelled metabolites and a high incorporation of ^{14}C–activity into proteins during the time span of a PET study (Ishiwata *et al.* 1988a,b). In patients, using L–[1–^{11}C]tyrosine, good visualization of meningioma, liver metastasis and breast cancer was accomplished, which demonstrated the clinical importance of this ^{11}C–amino acid for PET (Bolster *et al.* 1986a). Because of their uptake into tumor tissue, D–amino acids, especially D–[^{11}C]–methionine, are compounds of interest for PET. Although D–methionine is not incorporated into proteins, Takeda *et al.* (1984) observed a high uptake of D–[3,4–^{14}C]methionine into tumors, and even an incorporation of its ^{14}C–radioactivity into proteins.

In tumors and normal tissues, much is known about the fate of the

individual, above-mentioned amino acids, especially of the ^{14}C-labelled ones. In this study, knowledge is to be extended with a comparative PET study, using the different ^{11}C-labelled amino acids, in the same experimental tumor model.

Therefore, the aims of the current study are:

1. To compare the dynamic uptake of ^{11}C-activity of L-[1-^{11}C]tyrosine (L-1-tyr), L-[methyl-^{11}C]methionine (L-me-met), L-[1-^{11}C]methionine (L-1-met) and D-[1-^{11}C]methionine (D-1-met) in tumor and normal tissues of the Walker 256 carcinosarcoma-bearing rat, using a longitudinal positron camera.
2. To compare the dynamic PET data of the ^{11}C-amino acids with the data obtained from experiments using ^{14}C-amino acids after dissection of the animal.

MATERIALS AND METHODS

Radiopharmaceuticals

$^{11}CO_2$ was produced by irradiating a nitrogen target with 18 MeV protons, using the $^{14}N(p,\alpha)^{11}C$ reaction. L-me-met was synthesized from $^{11}CH_3I$ and L-homocysteine thiolactone, according to Comar *et al.* (1976). L-me-met was prepared with a radiochemical yield of 60%, a specific activity > 2 GBq/μmol and a radiochemical purity of 97%, and was obtained in saline. L-1-tyr was synthesized, following the isocyanide route, according to Bolster *et al.* (1986a). In brief, after lithiating p-methoxyphenylethylisocyanide, carboxylation was carried out with $^{11}CO_2$. After acid hydrolysis, the racemic mixture was purified, and the enantiomers were separated on a chiral column by HPLC. Radiochemically pure L-1-tyr with a radiochemical yield of 3-5% and a specific activity >3.7 GBq/μmol was obtained in saline. D,L-1-met was synthesized using the isocyanide route as well (Bolster *et al.* 1986b). The lithiated methylthio-3-propylisocyanide anion was carboxylated with $^{11}CO_2$. Hereafter, the separation of the enantiomers, using a chiral buffer and HPLC, was carried out as described by Ishiwata *et al.* (1988c). Radiochemically pure L-1-met or D-1-met, with a radiochemical yield of 3-5%, and a specific activity of >3.7 GBq/μmol were obtained in 0.1 M NaH_2PO_4 buffer (pH 4.6). L-[1-^{14}C]tyrosine with a specific activity of 2.07 GBq/mmol (56 mCi/mmol) was purchased from Amersham International (U.K.).

Animals

The Walker 256 carcinosarcoma tumor model has already been reviewed extensively (Earle 1935). Male Wistar rats, weighing 160–180 g, were given an i.m. injection, containing 10^6 Walker 256 carcinosarcoma cells suspended in 0.2 ml phosphate buffer, into the rectus femoris of the left hind leg, according to the standardization of growth method of Talalay *et al.* (1952). After 7 days, the diameter of the left hind leg increased from 0.9 to 1.9 cm. At that point, the tumors contained, besides vital tissue, substantial areas of necrosis. Animals received a standard diet and water ad libitum.

PET experiments

The tumor–bearing animal was intraperitoneally anaesthetized with 0.3 ml sodium pentobarbital (6g/100ml) and was kept under light anaesthesia. The right femoral vein was catheterized using a polyethylene catheter (o.d. 0.65 mm, i.d. 0.35 mm). This was done to be sure of a complete administration of the tracer. The anaesthetized rat was fixed on a heating blanket to restrain the animal from moving during the PET experiments, and to maintain the body temperature at a normal physiological level. An amount of 1.85 MBq (50 μCi) amino acid was rapidly injected with a volume of less than 0.4 ml (average 0.2 ml). Immediately after the injection, the catheter was flushed with 0.05 ml saline to achieve complete administration of radioactivity. No disturbances of blood flow, blood pressure and renal function were observed with these volumes. At the moment of injection, the camera was activated to acquire dynamic PET data. During the 1 h study, the rate of framing was 1 frame/min for the first 10 min , and 1 frame/5 min for the following 50 minutes.

Data acquisition and analysis

A longitudinal PET camera with a resolution of 5.5 mm was used as imaging device (Paans *et al.* 1982). This positron–imaging system consists of two uncollimated scintillation cameras, operating in a coincidence mode. A hardware backprojection option was used, which allows for dynamic studies in one selectable tomographic plane. Since all coincident events are backprojected onto this plane, the overlaying tissue structures will be measured by their integral value. This so–called "blurring effect" will be

minimized in thin animals and can be compared to a partial volume effect. The field of view was 39 cm in diameter with a matrix of 64 x 64 pixels. All measured coincidences were projected onto one focal plane that was defined at the middle of the tumor. For correction of the non–uniform response of the system and for physical decay, the PET data were processed on a PDP 11/34 computer (Digital Equipment Corporation). Ancillary calibration experiments revealed, that because the rat is a thin animal, the loss of counts, due to attenuation, was negligible (<5%). Regions of interest (ROIs) were graphically defined for brain, liver, left kidney, striated muscle in the right hind leg and for tumor. The volume of the ROI was calculated by multiplying the surface of the ROI (S_{roi}) by the thickness of the rat in the ROI (T_{roi}). This thickness was measured externally by a vernier caliper.

Uptake was calculated as a differential absorption ratio DAR(PET):

$$DAR(PET)_{roi} = \frac{C_{roi}}{C_{rat}} \times \frac{W_{rat}}{S_{roi} \times T_{roi}} .$$

In this formula, the amount of radioactivity in the ROI and the rat is represehted by C_{roi} and C_{rat} respectively, and the weight of the rat by W_{rat}.

An adapted formula was used for calculation of the DAR(PET) in the Walker 256 tumor. In ROIs of equal size (S_{roi}), the radioactivity of the unaffected contralateral hind leg (C_m) was subtracted from the radioactivity in the tumor (C_t), followed by division by the difference in thickness between the two ROI's (T_t–T_m).

$$DAR(PET)_{tumor} = \frac{(C_t - C_m)}{C_{rat}} \times \frac{W_{rat}}{(T_t - T_m) \times S_{roi}}$$

L–[1–^{14}C]tyrosine experiments

Rats were anaesthetized as described above. An amount of 7.5 kBq (2 μCi) L–[1–^{14}C]tyrosine was injected into the catheterized femoral vein. At 5, 10, 15, 30 and 60 min after injection, animals were sacrificed by cervical dislocation, and blood was removed by heart puncturing. Five animals were used for each point of time. Tissue samples of brain, liver, kidney, muscle and

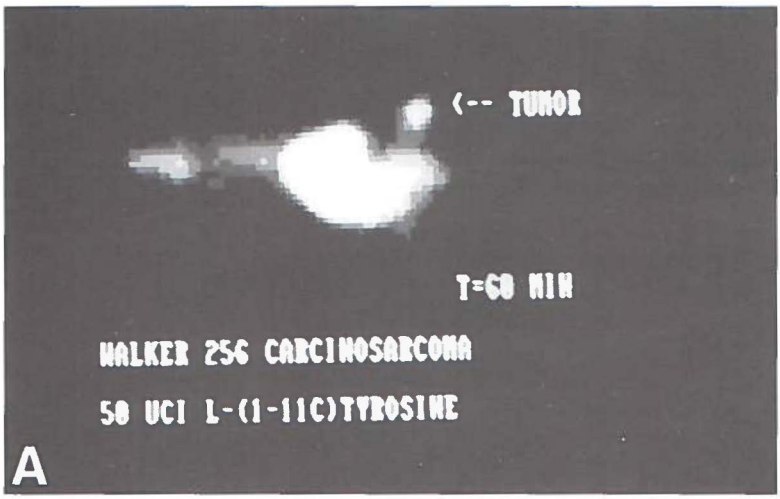

Figure 1a *The distribution of L-1-tyr in the Walker 256 carcinosarcoma-bearing rat at 60 min after injection.*

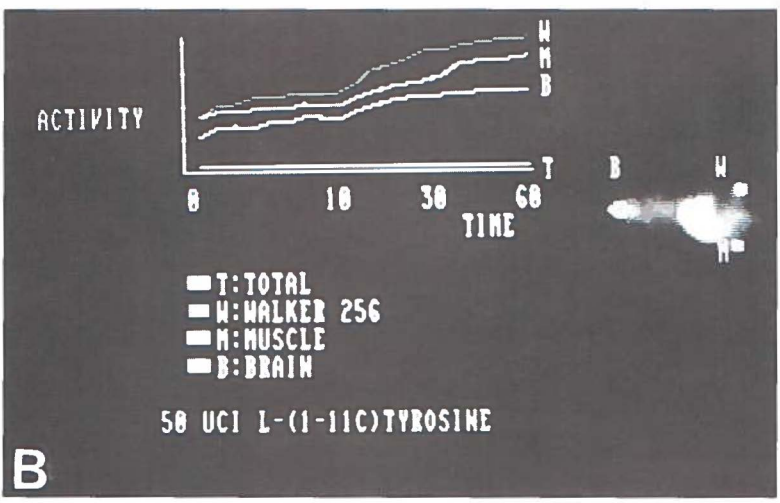

Figure 1b *Time activity curves in selected ROIs of the same study (fig. 1a) during the first 60 minutes after injection.*

vital tumor, weighing 50–100 mg, were rinsed with saline and blotted. The samples were dissolved in 1.5 ml NCS Tissue Solubiliser© (Amersham International, U.K.). After addition of 10 ml Plasmasol© (Packard Instruments, U.S.A.), the total ^{14}C–radioactivity of the sample was measured by liquid scintillation counting. The uptake was calculated as differential absorption ratio (DAR): (counts/g tissue) x (g body weight/total injected counts).

RESULTS

Despite the size of Walker 256 carcinosarcoma–bearing rats that weighed 200 g, vizualization of organs with all four ^{11}C–amino acids was achieved for brain, liver, muscle and kidney by PET. Tumor was visualized, provided that the tumor was well separated from the rest of the body, especially from the peritoneum (see fig. 1a). Furthermore, it was possible to measure

Table 1. *Uptake of L–1–tyr, L–me–met, L–1–met and D–1–met in tissue after i.v. injection in Walker 256 carcinosarcoma–bearing rats*

Tissue	Tracer	Time after injection				
		5 min	10 min	15 min	30 min	60 min
Brain	L–1–tyr	0.54±0.04	0.54±0.08	0.55±0.07	0.60±0.06	0.68±0.07
	L–me–met	0.56±0.08	0.56±0.09	0.54±0.10	0.62±0.10	0.72±0.09
	L–1–met	0.56±0.06	0.60±0.06	0.60±0.06	0.65±0.06	0.73±0.09
	D–1–met	0.60±0.10	0.62±0.11	0.63±0.10	0.65±0.07	0.73±0.09
Liver	L–1–tyr	1.16±0.41	1.24±0.24	1.29±0.27	1.51±0.25	1.74±0.22
	L–me–met	2.19±0.48	2.37±0.43	2.48±0.44	2.98±0.45	3.39±0.54
	L–1–met	1.67±0.16	1.76±0.15	1.76±0.17	2.00±0.19	2.36±0.21
	D–1–met	1.40±0.20	1.49±0.19	1.56±0.18	1.80±0.22	2.17±0.38
Kidney	L–1–tyr	1.34±0.41	1.36±0.35	1.37±0.26	1.63±0.28	1.94±0.40
	L–me–met	1.97±0.48	1.96±0.39	2.02±0.40	2.17±0.31	2.20±0.39
	L–1–met	1.62±0.20	1.67±0.24	1.74±0.26	1.97±0.24	2.29±0.34
	D–1–met	1.73±0.31	1.73±0.29	1.83±0.30	2.06±0.25	2.33±0.24
Muscle	L–1–tyr	0.67±0.19	0.71±0.19	0.72±0.20	0.79±0.23	0.86±0.27
	L–me–met	0.66±0.19	0.69±0.17	0.68±0.19	0.71±0.19	0.74±0.19
	L–1–met	0.72±0.12	0.80±0.10	0.81±0.13	0.87±0.13	0.95±0.16
	D–1–met	0.83±0.13	0.89±0.17	0.91±0.12	1.00±0.15	1.14±0.11
Tumor	L–1–tyr	0.60±0.22	0.64±0.20	0.69±0.20	0.78±0.29	0.89±0.25
	L–me–met	0.45±0.14	0.51±0.14	0.50±0.21	0.63±0.21	0.86±0.28
	L–1–met	0.77±0.16	0.76±0.16	0.86±0.11	0.99±0.13	1.11±0.18
	D–1–met	0.58±0.15	0.60±0.15	0.66±0.15	0.72±0.16	0.78±0.17

Uptake as DAR(PET), errors are SD, N=5 for tyrosine, N=6 for methionines.

quantitatively the dynamic distribution of L–1–tyr, L–me–met, L–1–met and D–1–met by PET (see fig. 1b). After injection of 1.85 MBq (50 μCi) ^{11}C–amino acid, characteristic count rates of 2500–3500 counts/s were measured at the beginning of the PET study. The ROI of the muscle had the lowest count rate (40–60 counts/s), while the ROI of the liver had the highest count rate (200–250 counts/s). Table 1 shows the uptake values of each of the ^{11}C–amino acids for the five tissues mentioned above, measured at 5, 10, 15, 30 and 60 min after injection. The values are expressed as DAR(PET).

The dynamic uptake curves revealed a biphasic pattern. Between 0 and 5 min after injection, the first phase was observed as a rapid distribution of radioactivity into tissue, for each of the ^{11}C–amino acids. About 75% of the value of the ^{11}C–activity, measured at the end of the study, was already observed, in the respective tissues, at 5 min after the start of the study. Between 5 and 60 min, a slow linear increase of radioactivity was observed as the second phase.

Table 1 shows that in brain, kidney and striated muscle no significant differences in uptake values were found between L–1–tyr, L–me–met, L–1–met and D–1–met. For all 4 amino acids, liver and kidney showed the highest uptake; for tumor, muscle and brain a significantly lower uptake was found. At 1 h after injection, 44% ($P<0.02$) more radioactivity of L–me–met was measured in liver as compared to L–1–met. Furthermore, in this tissue, at 30 min after injection, ^{11}C–activity from L–me–met and L–1–met accumulated respectively 95% ($P<0.001$) and 36% ($P<0.02$) higher than from L–1–tyr. At 60 minutes, the tumor showed 42% ($P<0.01$) higher uptake of radioactivity with L–1–met than with its enantiomer D–1–met.

Table 2. *Uptake of L–[1–^{14}C]tyrosine in tissue after i.v. injection into Walker 256 carcinosarcoma–bearing rats.*

Tissue	Time after injection				
	5 min (N=5)	10 min (N=5)	15 min (N=5)	30 min (N=5)	60 min (N=5)
Brain	0.93±0.20	0.79±0.06	0.75±0.12	0.65±0.07	0.61±0.07
Liver	3.76±0.88	3.73±0.30	4.25±0.80	3.44±0.38	3.10±0.46
Kidney	2.55±0.53	2.47±0.19	2.40±0.18	2.60±0.20	3.09±0.47
Muscle	0.57±0.19	0.57±0.05	0.64±0.11	0.60±0.19	0.46±0.07
Tumor	2.44±0.81	2.02±1.04	2.00±0.78	2.36±0.55	3.27±0.60

Uptake as DAR, errors are SD.
Published in part by Ishiwata *et al.* (1988a).

In table 2, the DAR values for L-[1-^{14}C]tyrosine of the same 5 organs that were measured in the PET studies are presented for 5, 10, 15, 30 and 60 min after injection. Tumor, liver and kidney showed DAR values for L-[1-^{14}C]tyrosine of about 3; markedly lower values were observed in brain and striated muscle.

In fig. 2, a graphical comparison of the results of the two techniques for measuring the differential absorption ratio is shown. In tumor, the ^{14}C-values of L-[1-^{14}C]tyrosine were higher than the ^{11}C-values of L-1-tyr with an average factor of 3.7. Compared to PET data, both liver and kidney showed respectively 2.6 and 1.7 times higher DAR values with L-[1-^{14}C]tyrosine. Small differences were observed in muscle and brain.

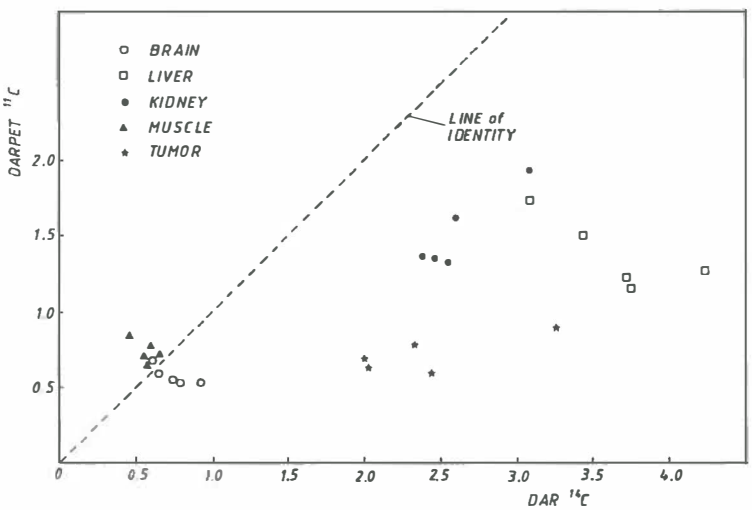

Figure 2 *Differential absorption ratios measured with L-[1-^{14}C]tyrosine after dissection into organs (X-axis) and L-1-tyr measured by PET (Y-axis) in brain, liver, muscle, kidney and tumor. The comparison was made per tissue at the same 5 points of time (5, 10, 15, 30, 60 min) after injection.*

DISCUSSION

Using PET, we investigated the dynamics of L-1-tyr, L-me-met, L-1-met and D-1-met quantitatively in brain, liver, kidney, muscle and tumor of the standardized Walker 256 carcinosarcoma-bearing rat.

The higher uptake of L-me-met in liver, compared to the uptake of

L–1–met, is also observed in experiments with their ^{14}C–analogues (Aquilar *et al.* 1974, Ishiwata *et al.* 1988b). This is explained by the fact that of all rat tissues, liver has the highest level of the enzyme L–methionine–S–adenosyltransferase, which converts methionine to S–adenosyl–methionine (SAM) (Baldessarini and Kopin 1966). After conversion of L–me–met to L–[methyl–^{11}C]SAM, the ^{11}C–methyl group of L–[methyl–^{11}C]SAM is donated to a variety methyl–group acceptors, consequently the ^{11}C–label is mainly retained in the liver tissue. The analogous L–[1–^{11}C]SAM, unlike L–[methyl–^{11}C]SAM, is decarboxylated, and the ^{11}C–label is rapidly cleared from the liver tissue as $^{11}CO_2$. In liver, both methyl– and carboxylic–labelled methionine accumulated at higher rates than L–1–tyr. This difference can also be ascribed to the dominant role of the transmethylation processes in this tissue.

The higher uptake of L–1–met in tumor, compared to the uptake of L–me–met, was observed in the ^{14}C–experiments as well (Ishiwata *et al.*1988b). The explanation for this difference is that in the Walker 256 carcinosarcoma, the level of SAM is 11 times lower than in the liver of the Wistar rat (Lombardini and Talalay 1971). Probably, in this tumor, transmethylation is a less important metabolic pathway as is the case in liver. Sequential PET studies with L–1–met and L–me–met might have potential for investigating the transmethylation processes in liver and tumor.

In normal tissue, stereospecificity in uptake for D–1–met or L–1–met has not been observed in the PET experiments, where the total tissue radioactivity was measured. In mammalian tissue, label of ^{14}C–D–methionine is incorporated into protein (Takeda *et al.* 1984, Lauenstein *et al.* 1987). In fact, D–methionine is oxidized by D–amino oxidase to α–keto–γ–methiol–butyrate followed by stereospecific transamination to the L–form (Berg 1953). Consequently, over the time course, the percentage label from D–methionine incorporated into protein is lower as compared to L–methionine. In tumors, the differences in accumulation between L– and D– methionine are unpredictable. In mice bearing solid Ehrlich ascites tumors, uptake of D–methionine was 3 times higher compared to L–methionine (Takeda *et al.* 1984). In the Walker 256 carcinosarcoma we found the opposite; a 42% higher accumulation of the L–form than of the D–form. In patient studies with malignant glioma, Schober *et al.* (1987) found no differences in accumulation between the two enantiomers. Bergström *et al.* (1987) however, found 2.4 times higher accumulation rates for L– compared to D–methionine in gliomas.

L–1–tyr is one of the important amino acids for measuring protein synthesis rates by PET. Because of the high turnover rate and the high incorporation into proteins, tyrosine has a small free pool in plasma and tissue (Garlick 1973). In the Walker 256 tumor, at 5 min after injection of L–[1–^{14}C]tyrosine, Ishiwata *et al.* (1988b) found that 41.5% of the label was incorporated in the acid insoluble fraction. At 60 min, this fraction amounted to 87.6%. Therefore, the rapid increase of ^{11}C–activity between 0 and 5 min, observed in the PET studies, can be ascribed to rapid transport of the amino acid into the cell. Furthermore, the slower increase of ^{11}C–activity in tumor tissue, between 5 and 60 min, can be attributed to trapping of the label by protein synthesis. This was also found in PET studies with another experimental tumor model, the ocular melanoma bearing hamster, which demonstrated high uptake of L–1–tyr in tumor tissue. In this tumor, 30 min after injection of L–[1–^{14}C]tyrosine, 85% of the radioactivity was already measured in the acid insoluble fraction (van Langevelde *et al.* 1988). The two major non–protein metabolic pathways, (1) transamination to [1–^{11}C]p–hydroxyphenylpyruvic acid followed by oxidation to homogentisic acid, and (2) hydroxylation to [1–^{11}C]3,4–dihydroxyphenylalanine followed by decarboxylation to 3,4–dihydroxyphenylethylamine, predominantly yield the radioactive metabolite $^{11}CO_2$, which is rapidly cleared from tissue (Banker and Cotman 1971). In studies using L–[1–^{14}C]tyrosine in Walker 256 carcinosarcoma–bearing rats, only 2.4% of total radioactivity of the tumor tissue was measured as non–carbon dioxide metabolite, at 60 min after injection. Therefore, Ishiwata *et al.* (1988b) suggest a four–compartment model for L–[1–^{11}C]tyrosine for calculating protein synthesis rates in tumor.

The differences, registered in fig. 2, between L–1–tyr and L–[1–^{14}C]tyrosine were also observed between the L–^{11}C–methionines and their ^{14}C–analogues. Therefore, the examplatory tyrosine data are considered sufficient for the discussion of the differences between the two techniques in general.

The Walker 256 carcinosarcoma is a rapidly growing tumor, and necrosis of part of the tumor will occur early. In fact, necrotic tissue was always present at the time of the experiments. In the ^{14}C–experiments visually vital tumor tissue was sampled. Inevitably, in the non–invasive PET experiments, the tumor, including the necrotic part, was measured as a whole. This difference in sampling technique explains the differences in the values of the differential absorption ratios; the heterogeneity of the tumor tissue causes a

problem for the quantification of metabolism of vital tissue using the PET technique. For PET studies with rats, histologically homogeneous tumors are therefore more preferable.

Although ROIs of liver and kidney can clearly be defined, the PET data in these organs show lower values, as compared to the ^{14}C–values. When stretched, rats are thin animals, and alignment of the animal to the horizontal focal plane in our longitudinal camera was not a problem, as it would be in a vertical ring system. Because radioactivity was measured in one plane, and the thickness of the ROI varied, corrections for thickness of the ROIs were obligatory. This will lead to partial volume effects. The elimination of partial volume effects requires spatial resolution in three dimensions which is beyond the present limits. Consequently, the ROIs of liver and kidney contain other tissues, such as dorsal and ventral striated muscle, skin, and fat. Therefore, the tissue activity level, as measured by the integral value of the overlying tissues, is underestimated.

These disadvantages of experimental PET in small animals are outweighed by its advantages. In contrast to dissection methods, experimental PET yields dynamic tissue uptake curves from single animals, which greatly reduces the interindividual variation. Quantitative differences in metabolism between specific ^{11}C–amino acids, in particular tissues, will therefore be detected more effectively. The PET method appears to be less time consuming, and more animal lives are saved compared to the dissection methods. Furthermore, the dynamics of several different ^{11}C–amino acids can be compared consecutively in the same animal. This perspective also offers the possibility of evaluating ^{11}C–amino acid uptake into tumor of the same animal before and after therapeutic intervention. Although quantification is not exact, relative differences in amino acid kinetics may be detected. Provided that the proper calibration of the measurements of radioactivity in tissues is possible, kinetic modelling studies with ^{11}C–amino acids can be performed. Rats, unlike human beings, can be dissected, and with ^{14}C–amino acids more detailed biochemical insight in tumor metabolism can be obtained for understanding ^{11}C–PET data

In conclusion, the findings in studies with ^{14}C–analogues (Ishiwata *et al.* 1988a, 1988b) are in agreement with the dynamic PET studies using ^{11}C–amino acids in Walker 256 carcinosarcoma bearing rats. The tumor–imaging potential of L–1–met, L–me–met and L–1–tyr is nearly equal. Because of the intricate metabolism of methionine, L–1–tyr is a better tracer for

investigating protein synthesis in tumor by PET. In the future, the method will be used to generate dynamic PET data in tissue of rats for the kinetic modeling of L–1–tyr. These tissue data will also be used to evaluate the efficacy of therapy protocols in tumor.

ACKNOWLEDGEMENTS

This research was funded by the Dutch Cancer Foundation "Koningin Wilhelmina Fonds". The cooperation of staff of the Kernfysisch Versneller Instituut (Professor Dr R.H. Siemssen) and the considerable help of the operating team of the cyclotron are gratefully acknowledged.

REFERENCES

Aquilar T.S., Benevenga N.J. and Harper A.E. (1974) Effect on dietary methionine level on its metabolism in rats. J. Nutr. **104**, 761–771.

Baldessarini R.J. and Kopin I.J. (1966) S–Adenosylmethionine in the brain and other tissues. J. Neurochem. **13**, 769–777.

Banker G. and Cotman C.W. (1971) Characteristics of different amino acids as protein precursors in mouse brain: advantages of certain carboxyl–labeled amino acids. Arch. Biochem. Biophys. **142**, 505–573.

Berg C.P. (1953) Physiology of D–amino acids. Physiol. Rev. **33**, 145–189.

Bergström M., Lundqvist H., Ericson K., Lilja A., Jonstrom P., Långström B., von Holst H., Eriksson L. and Blomqvist G. (1987) Comparison of the accumulation kinetics of L–(methyl–11C)–methionine and D–(methyl–11C)–methionine in brain tumors studied with positron emission tomography. Acta Radiol. Fasc.I **28**, 389–393.

Bolster J.M., Vaalburg W., Paans A.M.J., van Dijk Th.H., Elsinga Ph.H., Zijlstra J.B., Piers D.A., Mulder N.H., Woldring M.G. and Wynberg H. (1986a) Carbon–11C labelled tyrosine to study tumor metabolism by positron emission tomography (PET). Eur. J. Nucl. Med. **12**, 321–324.

Bolster J.M., Vaalburg W., Elsinga Ph.H., Ishiwata K., Vissering H. and Woldring MG. (1986b) The preparation of 11C–carboxylic labelled L–methionine for measuring protein synthesis. J. Labelled. Compd. Radiopharm. **23**, 1081–1082.

Comar D., Cartron J.C., Maziere M. and Marazano C. (1976) Labelling and metabolism of Methionine–Methyl–11C. Eur. J. Nucl. Med. **1**, 11–14.

Daemen B.J.G., Paans A.M.J., Elsinga Ph.H., Wieringa R.A., Konings A.W.T. and Vaalburg W. (1989a) Hyperthermia induced suppression of protein synthesis in tumors measured by PET. In: Nuclear Medicine, Trends and possibilities in Nuclear Medicine, Eds. Schmidt H.A.E. and Buraggi G.L., Stuttgart, New York, Schattauer Verlag, p 77–80.

Daemen B.J.G., Elsinga Ph.H., Paans A.M.J., Wieringa R.A., Konings A.W.T. and Vaalburg W. (1989b) The effect of radiotherapy on L–[1–11C]tyrosine and 18FDG metabolism of tumors as measured by PET. J. Nucl. Med. **30**, 789.

Dunzendorfer U., Schmall B., Bigler R.E., Zanzonico P.B., Conti P.S., Dahl J.R., Kleinert E. and Whitmore W.F. (1981) Synthesis and body distribution of alpha–amino–isobutyric acid–L–11C in normal and prostate cancer bearing rat after chemotherapy. Eur. J. Nucl. Med. **6**, 535–638.

Earle W.R. (1935) A study of the Walker rat mammary carcinoma 256, in vivo and in vitro. Am. J. Cancer **24**, 566–612.

Garlick P.J. (1973) Protein turnover in the whole animal and specific tissues. In : Florkin M., Stotz E.H. (eds) Comprehensive Biochemistry, vol 19B. Amsterdam, Elseviers, 77–153.

Ishiwata K., Vaalburg W., Elsinga Ph. H., Paans A.M.J., Woldring M.G. (1988a) Metabolic studies with L–[1–14C]tyrosine for the investigation of a kinetic model to measure protein synthesis rates with PET. J. Nucl. Med. **29**, 524–529.

Ishiwata K., Vaalburg W , Elsinga Ph.H., Paans A.M.J and Woldring M.G. (1988b) Comparison of L–[1–11C]methionine and L–Methyl–[11C]methionine for measuring in vivo protein synthesis rates with PET. J. Nucl. Med. **29**, 1419–1427.

Ishiwata K., Ido T. and Vaalburg W. (1988c) Increased amounts of D–enantiomer dependent on alkaline concentration in the synthesis of L–[methyl–11C]methionine. J. Appl. Radiat. Isot. **39**, 311–314.

Jones R.M., Cramer S., Sargent T. and Budinger T.F. (1985) Brain protein synthesis rates measured in vivo using methionine and leucine [Abstract]. J. Nucl. Med. **26**, P168.

Kubota K., Matsuzawa T., Ito M., Ito K., Fujiwara T., Abe Y., Yoshioka S., Fukuda H., Hatazawa J., Iwata R., Watanuki S. and Ido T. (1985) Lung tumor imaging by positron emission tomography using C–11 L–methionine. J. Nucl. Med. **26**, 37–42.

Langevelde van A., van der Molen H.D., Journee–de Korver J.G., Paans A.M.J., Pauwels E.K.J. and Vaalburg W. (1988) Potential radiopharmaceuticals for the detection of ocular melanoma Part III. A study with 14C and 11C labelled tyrosine and dihydroxyphenylalanine. Eur. J. Nucl. Med. **14**, 382–387.

Lauenstein L., Meyer G–J., Sewing K–F., Schober O. and Hundeshagen H. (1987) Uptake kinetics of 14C L–Leucine and 14C L– and D–methionine in rat brain and incorporation into protein. Neurosurg. Rev. **10**, 147–150.

Lilja A., Bergström K., Hartvig P., Spånnare B., Halldin C., Lundqvist H. and Långström B. (1985) Dynamic study of supratentorial gliomas with L–methyl–11C–methionine and positron emission tomography. Am. J. Neurol. Rad. **6**, 505–514.

Lombardini J.B. and Talalay P. (1971) Formations, functions and regulatory importance of S–adenosyl–L–methionine. Adv. Enzyme Reg. **9**, 349–384.

Paans A.M.J., De Graaf E.J., Welleweerd J., Vaalburg W. and Woldring M.G. (1982) Performance parameters of a longitudinal tomographic positron imaging system. Nucl. Instrum Methods **192**, 491–500.

Schober O., Meyer G–J., Gaab M.R., Muller J.A. and Hundeshagen H. (1986) Grading of brain tumors by C–11–methionine PET. J. Nucl. Med. **27**, P890.

Schober O., Duden C., Meyer G–J., Muller J.A. and Hundeshagen H. (1987) Non selective transport of [11C–methyl]–L– and D–methionine into a malignant glioma. Eur. J. Nucl. Med. **113**, 103–105.

Takeda T., Goto R., Tamemasa O., Chaney J.E. and Digenis G.A. (1984) Biological evaluation of radiolabeled D–methionine as a parent compound in potential nuclear imaging. Radioisotopes **33**, 213–217.

Talalay P., Takano G.M.V. and Huggins C. (1952) Studies on the Walker tumor. I. Standardization of the growth of a transplantable tumor. Cancer Res. **12**, 834–837.

CHAPTER 3

SUITABILITY OF RODENT TUMOR MODELS FOR EXPERIMENTAL PET WITH L-[1-^{11}C]TYROSINE AND 2-[^{18}F]FLUORO-2-DEOXY-D-GLUCOSE

Bernard J.G. Daemen, Philip H. Elsinga, Anne M.J. Paans, Willy Lemstra, Antonius W.T. Konings and Willem Vaalburg.

[Accepted for publication in Nuclear Medicine and Biology (1991)]

ABSTRACT

The applicability of five different rodent tumors for experimental PET has been investigated. L–[1–^{11}C]tyrosine was a better indicator for the growth activity of the tumors than ^{18}FDG. For experimental PET, the three mice models studied appeared inappropriate; the Lewis lung tumor and the fibrosarcomateous FIO 26 had too low a tyrosine utilization, while the lymphosarcomateous LY showed insufficient tumor to background ratios. Of the two rat models, the necrotic Walker 256 carcinosarcoma was less suitable. By using L–[1–^{11}C]tyrosine, the solid, rhabdomyosarcoma tumor offers good possibilities of monitoring therapeutic interventions with PET.

INTRODUCTION

An important clinical issue arising during and after therapeutic cancer treatment is, whether the intervention will be successful or not. Positron emission tomography (PET), a non–invasive diagnostic method, may provide answers to that question. In order to examine these possibilities with the PET technique in patients, experiments with animals are a prerequisite. Tumor–bearing mice and rats may be suitable models for this purpose (Wiebe 1983). Animal experiments with radiolabeled compounds, especially designed to be complementary to experimental PET studies are very scarce.

In general, tumor cells possess higher dividing rates, as compared to the cells they originate from (Weber 1977). As a consequence, most tumors have a rather high amino acid and glucose metabolism. PET may employ this difference in metabolism to discriminate between tumor and normal tissue. Up to now, many amino acids and glucose derivatives have been labeled with positron–emitting radionuclides. From kinetic tracer models, protein synthesis rates and glycolytic rates can be calculated (Sokoloff 1986).

The amino acid that has been used most widely for PET is L–[methyl–^{11}C]methionine. However, in the cell, the methyl–group of methionine is transferred to a number of methyl–acceptors, and therefore, methionine is less suitable for measuring the protein synthesis process. To circumvent these problems and to determine protein synthesis activity in tumors, carboxylic–labeled amino acids have been proposed, such as methionine (Ishiwata *et al.* 1988a), leucine (Hawkins *et al.* 1989) and tyrosine (Ishiwata *et al.* 1988b). The main metabolite of these amino acids is ^{11}C–carbon dioxide, which is produced through decarboxylation. This ^{11}C–carbon dioxide exchanges rapidly from the cell into the plasma bicarbonate pool. After expiration from the lung into the air, ^{11}C–carbon dioxide does not interfere anymore with the tissue measurements. From the amino acids mentioned above, L–[1–^{11}C]tyrosine (^{11}C–tyr) and L–[1–^{11}C]leucine were found to have nearly equal incorporation rates into mouse brain proteins (Banker and Cotman 1971), and both compounds can be considered most appropriate for measuring protein synthesis in tumors. Furthermore, in tissues of the Walker 256 carcinosarcoma–bearing rat, ^{11}C–tyr was found to have lower amounts of metabolites, as compared to L–[1–^{11}C]methionine (Ishiwata *et al.* 1988a,b). ^{11}C–tyr was therefore selected for these studies.

In order to compare protein synthesis in tumors with tumor carbohydrate

metabolism, we synthetized 2-[^{18}F]fluoro-2-deoxy-D-glucose (^{18}FDG). ^{18}FDG is extensively used in PET and may be considered as an established standard to indicate enhanced metabolic activities in cells and as such suitable to compare with other PET tracers. ^{18}FDG has proven to be a useful probe in a variety of animal tumors to indicate glycolytic activity (Gallagher *et al.* 1978, Som *et al.* 1980, Kearfott *et al.* 1984, D 'Argy *et al.* 1988).

The aim of the current study was the following:

1. To determine tissue distribution of the ^{14}C- and ^{18}F-labels of L-[1-^{14}C]tyrosine (^{14}C-tyr) and ^{18}FDG, including tumor tissue of the different animal models.
2. To determine the incorporation of the ^{14}C-label of ^{14}C-tyr into protein of the different animal tissues including tumor tissue.
3. To characterize a number of physiological tumor properties of the different animal models (e.g. growth rates and tissue homogeneity).
4. To compare the suitability of three mice and two rat tumor models for tumor visualization and quantitation by using ^{11}C-tyr and ^{18}FDG as metabolic probes.

MATERIALS AND METHODS

Animals

Lewis lung tumors (LL) were prepared by injecting 3-month-old, female C57Bl mice (20-25 g) subcutaneously in the left flank with 4 x 10^6 viable cells suspended in 0.2 ml Simms solution. Within 2 weeks LL grew to a volume between 0.5-1.0 ml. Tumors with a volume larger than 0.5 ml contained areas of necrosis (Woerdenbag *et al.* 1987a)

The fibrosarcomateous FIO 26 tumors (FIO 26) were transplanted by injecting in the left flank, subcutaneously, a suspension of 2 x 10^6 viable cells in 3-month-old, female C57Bl mice (20-25 g). After 3 weeks, FIO 26 tumors developed to a volume between 0.5 and 1.0 ml, and appeared to be solid. No necrotic areas were observed (Woerdenbag *et al.* 1987b).

Lymphosarcoma tumors (LY) were obtained by injecting 10^5 lymphosarcomateous isologeous spleen cells intraperitoneally into 3-month-old, female C57Bl mice. After 7 days, due to growth of LY cells, weight of the spleen increased from 0.1 to 0.8-1.0 g. Animals with spleen weights of more than 0.8 g were selected for experiments. These spleens contained more than

90% LY cells (De Vries and Vos 1958).

Female, 2–months–old Wag/Rij rats (TNO, Rijswijk, The Netherlands) that weighed 140 g, were inoculated subcutaneously with 100 mg of solid rhabdomyosarcoma tissue (RMS) (TNO, Rijswijk, The Netherlands). Within 18 days, solid, homogeneous tumors developed to a volume of 4 ml (Barendsen and Broerse 1969).

Male Wistar rats, that weighed 200 g, were intramuscularly injected with 10^6 Walker 256 carcinosarcoma cells in the left hind leg (Earle 1935, Talalay *et al.* 1952). After 7 days, tumors were palpable (about 1 cm dia) and ready for the experiments.

Animals were subjected to a normal day and night rhythm and had free access to water and food (RMH pellets, Hope Farms, Woerden, The Netherlands). For all experiments, the same dietary status of the animals was pursued.

Materials

^{14}C–tyr with a specific activity of 2 MBq/μmol (56 mCi/mmol) was purchased from the Radiochemical Centre, Amersham International plc, Buckinghamshire, U.K. Radiochemical pure ^{11}C–tyr was synthetized using the isocyanide route according to Bolster *et al.* (1986), with a specific activity of at least 3.7 GBq/μmol (100 Ci/mmol). ^{18}FDG was synthetized, no carrier added, according to Hamacher *et al.* (1986), with a radiochemical purity >98%. Plasmasol© was purchased from Packard Instruments Inc., Downers Grove, Ill., U.S.A. and Protosol© from Dupont, Boston, Mass, U.S.A.

Measurement of Radioactivity in Tissue

Mice and rats were anaesthetized with sodium pentobarbital (6 mg/100 g animal). Doses of 18.5 kBq (0.5 μCi) ^{14}C–tyr per mouse, and of 93 kBq (2.5 μCi) per rat were injected into a tail vein. After 60 min animals were sacrificed by a heart puncture and subsequently, vital tumor, muscle, liver, brain and blood were sampled as main tissues. Washed and blotted organ samples weighing 50–100 mg were dissolved in Protosol© and total uptake of radioactivity was measured by scintillation counting. An amount of 50 mg tissue was homogenized in 0.4 ml 10% trichloro acetic acid (TCA). The precipitate was washed 2 times with 0.4 ml 5% TCA and measured as the percentage of ^{14}C–radioactivity incorporated into proteins. Blood samples were

centrifuged and 100 μl of plasma obtained was dissolved in Plasmasol© to assay total plasma radioactivity. Another 100 μl plasma was treated with TCA to estimate the incorporation of ^{14}C radioactivity into plasma proteins.

An i.v. dose of 740 kBq (20 μCi) ^{18}FDG per mouse, and of 3.7 MBq (100 μCi) ^{18}FDG per rat was injected into a tail vein. After 60 min, animals were sacrificed by heart puncturing, followed by sampling of vital tumor, muscle, liver, brain, heart, kidney and blood. The ^{18}F-radioactivity of 50-100 mg tissue was determined in a NaI well counter and corrected for decay to the time of injection.

Uptake values were expressed as Differential Absorption Ratio (DAR):

$$DAR = \frac{\text{radioactivity sample}}{\text{radioactivity injected}} \; X \; \frac{\text{weight animal}}{\text{weight sample}}$$

Positron emission tomography

As imaging device a stationary double-headed positron camera was used (Paans *et al.* 1982). This system, with a resolution of 5.5 mm, uses two uncollimated gamma cameras in a coincidence mode, which enables dynamic studies in multiple planes. The sensitivity for extended sources (rodents) amounted 2.7 cps/kBq (100 cps/μCi) with a maximum in coincidence count rate of 7.5 kHz. In one tomographic plane defined at the position of the animal, the acquired data were reconstructed with a field size of 19.5 x 19.5 cm^2. The matrix size used was 64 x 64. When stretched, rodents are thin animals, therefore the attenuation correction is small (<5%), as was measured in calibration experiments. Due to the good energy resolution (10% FWHM) and the fact that only photo-peak events are selected, the scatter fraction (<5%) is limited using thin animals in this system. For both effects, attenuation and scatter, no corrections were performed. In the calibrated situation, the data are available in terms of kBq/cm^2. In order to translate these numbers into volumetric data, external measurements of the size of the tumors were performed in three dimensions with a vernier caliper (Daemen *et al.* 1991).

Animals, bearing tumors with different sizes, were anaesthetized with sodium pentobarbital (6 mg/100 g body weight). Being aligned to the focal plane of the positron camera, the animals were intravenously injected through a catheter (inserted into a tail vein) with ^{11}C-tyr dissolved in 0.1 M NaH_2P0_4 (pH 4.6) or ^{18}FDG in saline solution. The dose of radioactivity administered

amounted to 3.7 MBq (100 μCi) in a maximum volume of 0.5 ml for a rat and 740 kBq (20 μCi) in a maximum volume of 0.2 ml for a mouse. Immediately after injection, the catheter was flushed with saline (<0.05 ml). For acquisition of dynamic PET data, the camera was activated at the time of injection. During 1 h after injection, distribution of tracer and visualization of tumor was monitored.

RESULTS

Tissue distribution of radioactivity

Uptake values for ^{14}C–tyr in tumor and other tissues at 60 min after i.v. injection are shown in table 1. In order to enable comparisons between animals with different body weights, all uptake values are expressed as differential absorption ratios (DAR). The amount of ^{14}C–label incorporated into protein is also given in this table. The three mice models used, do not show identical

Table 1. *Uptake of L–[1–^{14}C]tyrosine in different tissues and its incorporation into proteins at 60 min after i.v. injection.*

	Uptake (incorporation as percentage)				
	Mice			Rats	
	LL (n=4)	FIO 26 (n=5)	LY (n=5)	W256# (n=5)	RMS (n=5)
Plasma	0.39±0.02 (58±7)	0.60±0.10 (68±5)	0.64±0.11 (44±11)	1.54±0.17 (85±2)	1.36±0.12 (94±1)
Brain	0.25±0.02 (30±8)	0.31±0.03 (52±2)	0.42±0.06 (49±13)	0.61±0.03 (80±2)	0.43±0.01 (87±3)
Liver	2.35±0.39 (55±6)	2.64±0.12 (91±2)	3.69±0.19 (90±2)	3.10±0.21 (94±1)	2.89±0.18 (94±1)
Muscle	0.33±0.04	0.31±0.03	0.35±0.05	0.46±0.03	0.29±0.03
Tumor	0.33±0.06 (63±4)	0.37±0.08 (48±1)	3.07±0.29 (79±8)	3.27±0.27 (88±1)	1.65±0.12 (81±2)

Uptake values expressed as DAR. Values are mean ± SEM.
Percentage incorporated into protein is between parentheses.
data from Ishiwata *et al.* (1988b).

Table 2. *Uptake of ^{18}FDG in different tissue at 60 min after i.v. injection expressed as DAR.*

	Mice			Rats	
	LL	FIO 26	LY	W256	RMS
Blood	0.55±0.05	0.62±0.07	0.75±0.17	0.36±0.05	0.66±0.04
Brain	0.99±0.11	1.07±0.10	2.03±0.40	2.92±0.77	2.21±0.04
Liver	0.92±0.06	0.91±0.11	2.72±0.42	0.50±0.07	1.05±0.14
Heart	10.4±1.48	7.17±1.33	3.18±2.06	11.2±2.20	8.28±1.56
Kidney	1.65±0.21	1.62±0.23	1.42±0.36	1.60±0.22	2.13±0.17
Muscle	0.51±0.07	0.31±0.02	0.27±0.05	0.61±0.16	0.31±0.02
Tumor	2.05±0.27	2.09±0.27	3.63±0.46	3.58±0.82	3.97±0.73

Uptake expressed as DAR. Values are mean ± SEM.
Five animals per data point.

uptake values for ^{14}C-tyr in tumor tissue. The LL and FIO26 tumors have DAR values of 0.33 and 0.37, respectively, whereas the LY tumor has a DAR value of 3.07. The percentage ^{14}C incorporated into proteins of the mouse models was the highest in the LY tumor. With respect to the two rat models, the W256 has a DAR value of 3.27, which is about 2 times higher when compared to data of the RMS. In the rat models, high percentages of ^{14}C-label incorporated into proteins are found; 88% for the W256 and 81% for the RMS. The higher uptake of ^{14}C-label for the rat models, as compared to the mice, does not only apply for tumor tissue, but is also observed for a number of normal tissues. As expected the highest ^{14}C-uptake within the normal tissues is found in the liver. With respect to the incorporation of amino acids into protein, the rat tissues are generally more active within the time span studied.

Table 2 presents the uptake values of ^{18}FDG in tumor and normal tissues of the five different animal models. The LL and FIO26 tumors show uptake values of about 2; the uptake by the LY tumor is markedly higher. These differences between the tumors tally with the differences in the uptake values for ^{14}C-tyr (table 1). In rats, the W256 and RMS tumors both show high ^{18}FDG uptake values of 3.58 and 3.97 respectively. The high ^{18}FDG uptake values of the heart are as expected (Gallagher *et al.* 1977, Yamada *et al.* 1985). Another observation which is notable in table 2, is the elevated uptake value of the liver in the LY model, which is about 3 times higher as compared to the livers in the LL and FIO26 bearing mice.

From the tumor tissue values in tables 1 and 2, the ratio of ^{18}FDG and ^{14}C-tyr uptake has been calculated and compared with measured doubling times.

The doubling times were the same as published previously by different authors (Barendsen and Broerse 1969, Tribukait *et al.* 1981, Woerdenbag *et al.* 1987a,b , McCredie *et al.* 1965). This ratio is presented in table 3 and shows a large variety with a range from 1.1 (W256) to 6.2 (LL). The shortest tumor doubling time is for the LY (0.5 day) and the longest for the RMS (3.5 days).

Table 3. *Tumor doubling time and ratio of tracer uptake of ^{18}FDG and $L-[1-^{14}C]tyrosine$.*

tumor	doubling time	^{18}FDG	^{14}C–tyr	ratio
LL *	2 days	2.05	0.33	6.2
FIO 26 †	3 days	2.09	0.37	5.6
LY ‡	12 hours	3.63	3.07	1.2
W256 §	18–24 hours	3.58	3.27	1.1
RMS ¶	3.5 days	3.97	1.65	2.4

* Woerdenbag *et al.* (1987a), † Woerdenbag *et al.*(1987b), ‡ Tribukait *et al.* (1981), § McCredie *et al.* (1965), ¶ Barendsen *et al.* (1969).

Positron emission tomography

It was observed that in an early stage the LL tumor is already far more necrotic than the FIO 26. For that reason the latter tumor model seems more suitable for experimental PET studies. The LY tumor, although very active in amino acid uptake and protein synthesis, cannot be used, because of its anatomic location (close to the liver). With respect to the rat tumors, the RMS had much less necrotic areas as compared to the W256. Therefore the FIO 26 and the RMS models have been evaluated further for PET experimentation especially in terms of tumor volume necessary for successful visualization.

In fig. 1, PET images of two FIO 26 bearing mice are given. At the left hand of the figure, ^{11}C–tyr uptake is shown for a small (A, 0.7 cm^3) and a large (C, 3.0 cm^3) tumor at 60 min after injection of the label. At the right hand of the figure, the corresponding ^{18}FDG images of the same mice (B,D) are shown. No tumor visualization could be realized with the smaller FIO 26 tumors (A,B 0.7 cm^3). The arrows, in fig. 1, indicate the expected position of the tumor. The larger tumor (C,D 3.0 cm^3) is clearly visible with both metabolic tracers. In figure 2, a PET image of a rat with 2 RMS tumors, after injection of ^{11}C–tyr, is depicted. The small tumor (L, 0,8 cm^3) is only just visible, whereas the large tumor (R, 5.2 cm^3) is clearly visible on the PET image. More

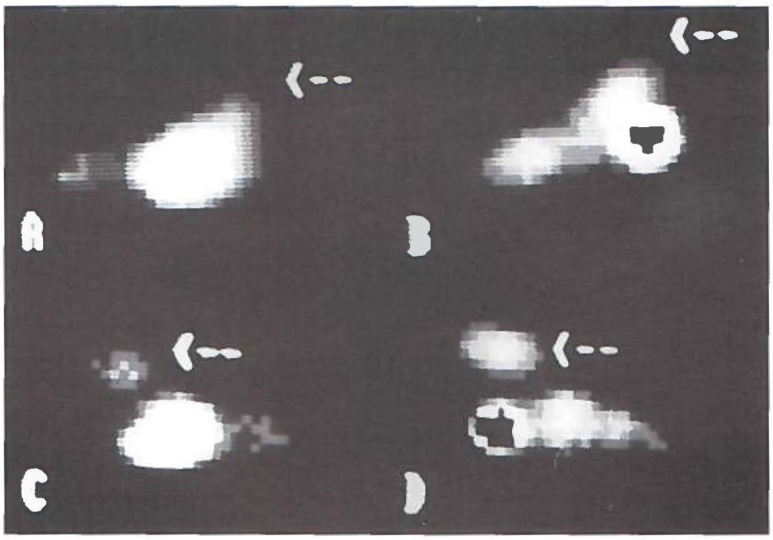

Figure 1. *PET images showing the distribution of $^{11}C-tyr$ and ^{18}FDG in FIO 26 bearing mice at 60 min after injection of the label. Small tumors (0.7 ml) were neither visible with $^{11}C-tyr$ (A) nor with ^{18}FDG (B). Arrows indicate the expected position. Larger tumors (3.0 ml) were clearly visible with $^{11}C-tyr$ (C) and ^{18}FDG (D).*

radioactivity was observed in the RMS tumors of the ^{18}FDG injected rats than in the corresponding ^{11}C–tyr studies. This is expected from the values of the tissue distribution studies with ^{18}FDG (table 2).

In order to use PET for monitoring the effect of a therapeutic intervention, mere visualization of the tumor is not sufficient. Suitable parameters like DARs of tracers in tissue to quantitate the effect of treatment on tumor metabolism are needed. These parameters have to be derived from the measured amounts of counts. In the FIO 26 tumor, at 60 min after an injection of 0.74 MBq (20 μCi) ^{11}C–tyr, we were able to measure 4–5 x 10^3counts/ml tissue within 5 min. Because these amounts have a relative error of less than 1.5%, these figures are acceptable for quantitative work. This is also true for the rat model. In the RMS tumor we measured 2–2.5 x 10^4 counts/ml tumor within a period of 5 min, at 60 min after an injection of 3.7 MBq (100 μCi) ^{11}C–tyr.

In analogy to the tissue distribution studies an ^{18}FDG/^{11}C–tyr ratio can

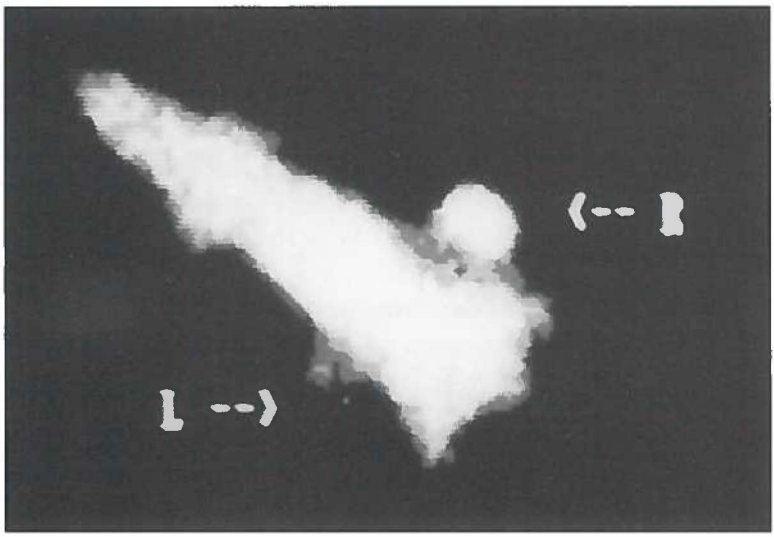

Figure 2. *PET image showing the distribution of $^{11}C-tyr$ at 60 min after injection in a Wag/Rij rat with a rhabdomyosarcoma at each flank of the animal. A volume of 0.8 ml (L) is just visible and a volume of 5.2 ml (R) is clearly visible.*

also be calculated from the quantitative PET data. For the FIO 26 and RMS tumor we found ratios of 4 and 2, respectively. These PET ratios are in fair agreement with the ratios obtained with the invasive approach (table 3).

DISCUSSION

To investigate the applicability of PET during and after therapeutic treatment of tumors, suitable animal models are required. For this purpose we investigated five different tumor-bearing rodents. Important parameters to be considered were metabolic activity, visualization by PET, location and volume of the respective tumors.

Our studies in mice showed a notable lower uptake of ^{14}C-tyr and also a lower incorporation into proteins for the LL and FIO26 tumors, as compared to the LY tumor. This can be explained by the fact that the accumulation of amino acids and incorporation into proteins is a reflection of the dividing rate of

the tumor cells. The LL and FIO26 have longer doubling times, as compared to the LY (see table 3). Studies with tissue slices of hepatomas with different growth characteristics, show that the extent of the incorporation of amino acids into proteins correlates well with the doubling time of the different tumors (Bhargava *et al.* 1976, Wagle *et al.* 1963). Such a correlation was also observed in our studies with the tumor bearing rats. The W256 has a high uptake of ^{14}C–tyr which was accompanied by a short doubling time, while in the RMS a reverse situation was found.

The high uptake values for ^{18}FDG in heart tally with the findings of other investigators in mice (Gallagher *et al.* 1977) and rats (Yamada *et al.* 1985). In the mice studies the high uptake of ^{18}FDG was ascribed to extensive glucose consumption by the heart.

The elevated ^{18}FDG uptake in liver of LY–bearing mice can be ascribed to metastasized LY cells originating from the LY tumor in the spleen (Tribukait *et al.* 1981). In patients with liver metastases, Yonekura and co–workers (1982) found ratios of metastasized to normal liver of about 4. These relatively high signals make ^{18}FDG a useful tool to discover liver tumors by PET. The LY mouse model has potential for investigations on metastasizing rates with radiolabeled compounds.

The low protein synthesis activity in the brain, as indicated by the uptake of radiolabeled tyrosine, corresponds with the absence of proliferation in this tissue. On the other hand, glucose is the main source of energy for the brain and is required in large quantities. Consequently, in the brain relatively high ^{18}FDG/^{14}C–tyr ratios are observed.

Uptake ratios in tumors treated with multiple metabolic tracers are considered suitable diagnostic parameters to indicate the degree of malignancy and grade of differentiation (D'Argy *et al.* 1988). An important question is whether these ratios are also appropriate indicators of tumor response after therapy. In our study we calculated the ^{18}FDG/^{14}C–tyr uptake ratios for five different rodent tumors and compared these data with the volume doubling times of the tumors. Irrespective of growth, more or less the same uptake values of ^{18}FDG in all five tumors tested was observed. Therefore the ratio is mainly determined by the ^{14}C–tyr uptake value. In tumor the measured ^{18}F–activity is present as ^{18}FDG and ^{18}FDG–PO_4. At 60 min after injection the latter form prevails. The activity of the enzyme hexokinase determines the amount of ^{18}FDG–PO_4 produced. Studies with slices of hepatomas with different growth characteristics showed no correlation of the activity of hexokinase with

growth rate (Sweeney *et al.* 1963). From these and from our own experiments it can be deduced that ^{18}FDG is not a proper indicator for growth activity of tumors and a less elegant tool to be used in the follow up of therapy. We consider that the uptake of ^{11}C–tyr, as measured by PET, is a better parameter describing the growth activity of a tumor than the ^{18}FDG/^{11}C–tyr ratio, and a far better parameter than the ^{18}FDG uptake values alone. Minn and co–workers (1988) compared ^{18}FDG uptake in human tumors with the percentage of S–phase cells and found a good correlation between the two parameters. Their method for estimating tumor growth rates (flow cytometry) was more indirect as compared to our volume measurement method. Multiparameter studies in patients with gliomas using L–[methyl–^{11}C]methionine and ^{18}FDG give evidence that, compared to ^{18}FDG, the measurement of amino acid uptake is a better way for predicting the tumor growth and even for estimating the grade of malignancy of the tumor (Schober *et al.* 1988).

For PET, visualization and quantitation is not only a resultant of the metabolic activity of the tumor but also of tumor volume and tumor location. Despite the adequate resolution of the PET camera (5.5 mm), PET studies with ^{11}C–tyr, in equal sized RMS and FIO 26 tumors at volumes <1 ml, showed only detection of the former tumor. This is explained by the higher protein synthesis rate of the RMS. Visualization of the FIO 26 tumor was achieved at volumes >3 ml. Visualization of the tumor also depends on the environment of the tumor. For example, the LY tumor cannot be delineated with ^{11}C–tyr, because the uptake of the amino acid in the adjacent liver gives rise to unfavorable tumor to background ratios. The location of the tumor tissue influences quantitation as well. For a proper evaluation of data obtained by PET, a good correlation of the amount of vital tumor with the magnitude of the PET signal is required. Despite a good visualization with ^{11}C–tyr (Daemen *et al.* 1991), the W256 tumor, encased in striated muscle, is largely necrotic and quantitation of metabolic activity in the W256 tumor by PET is therefore seriously impaired.

From the results discussed above it appears that the FIO26 tumor model in the mouse and the RMS rat tumor model are the two experimental systems suitable for further consideration. In prospective studies it will be necessary to compare PET data obtained in tumors before and after therapy with data on growth delay. This approach implicates that for the FIO 26 the tumor volume at the start of therapy must be about 3 ml, and for the RMS about 1 ml. To obtain a value for the doubling time, measurements of tumor volume are

required at volumes much larger than those at the moment of treatment. It is also desired that these measurements of tumor volumes take place within the time period of progressive growth. Because of the large starting volume this is not possible anymore for the FIO 26 tumor in mouse, but may be conveniently obtained with the RMS in rat.

On the basis of ^{14}C-tyr and ^{18}FDG uptake data as well as the ^{11}C-tyr and ^{18}FDG studies with PET, it is concluded that the rhabdomyosarcoma in the rat meets the main requirements for experimental PET. This model offers the possibility of investigating the follow up of treatment. At the moment we are using the RMS model with the tumor in the flank to explore the effects of hyperthermia and radiotherapy on tumor growth. Data on growth delay will be correlated with data from ^{11}C-tyr metabolism as obtained by PET.

ACKNOWLEDGEMENTS

This investigation was supported by a grant of the Dutch Cancer Society "Koningin Wilhelmina Fonds". The authors are grateful for the cooperation of the staff and the cyclotron operators of the Kernfysisch Versneller Instituut.

REFERENCES

Banker G. and Cotman C.W. (1971) Characteristics of different amino acids as protein precursors in mouse brain: advantages of certain carboxyl-labeled amino acids. Arch. Biochem. Biophys. **142**, 565-573.

Barendsen G.W. and Broerse J.J. (1969) Experimental radiotherapy of a rat with 15 MeV neutrons and 300 KeV X-rays. I. Effect of single exposures. Eur. J. Cancer **5**, 373-391.

Bhargava P.M., Szafarz D., Bornecque C.A. and Zajdela F. (1976) A comparison of the ability of normal liver, a solid hepatoma and the Zajdela ascitic hepatoma, to take up amino acids in vitro. J. Membrane Biol. **26**, 31-41.

Bolster J.M. Vaalburg W., Paans A.M.J., van Dijk T.H., Elsinga Ph.H., Zijlstra J.B., Piers D.A., Mulder N.H., Woldring M.G. and Wijnberg H.(1986) Carbon-11 labelled tyrosine to study tumor metabolism by positron emission tomography (PET). Eur. J. Nucl. Med. **12**, 321-324.

Daemen B.J.G., Elsinga Ph.H., Ishiwata K., Paans A.M.J. and Vaalburg W. (1991) A comparative PET study using different 11C-labelled amino acids in Walker 256 carcinosarcoma-bearing rats. Nucl. Med. Biol. **18**, 197-204.

D'Argy R., Paul R., Frankenberg L., Stålnacke C-G., Lundqvist H., Kangas L., Halldin C., Nagren K., Roeda D., Haaparanta M., Solin O. and Långström B. (1988) Comparative double-tracer whole body autoradiography: uptake of 11C-, 18F- and 3H-labeled compounds in rat tumors. Nucl. Med. Biol. **15**, 577-585.

De Vries M.J. and Vos O.(1958) Treatment of mouse sarcoma by total body X–irradiation and by injection of bone marrow and lymph node cells. J. Natl. cancer Inst. **21**, 1117–1129.

Earle W.R. (1935) A study of the Walker 256 in vivo and in vitro. Am. J. Cancer **24**, 566–612.

Gallagher B.M., Ansari A., Atkins H., Casella V., Christman D.R., Fowler J.S., Ido T., MacGregor R.R., Som P., Wan C.N., Wolf A.P., Kuhl D.E. and Reivich M. (1977) Radiopharmaceuticals XXVII. 18F–Labelled 2–deoxy–2–fluoro–D–glucose as a radiopharmaceutical for measuring regional myocardial glucose metabolism in vivo: tissue distribution and imaging studies in animals. J. Nucl. Med. **18**, 990–996.

Gallagher B.M., Fowler J.S., Gutterson N.I., MacGregor R.R., Wan C–N. and Wolf A.P. (1978) Metabolic Trapping as a principle of radiopharmaceutical design: some facts for the biodistribution of [18F]deoxy–2–fluoro–D–glucose. J. Nucl. Med. **19**, 1154–1161.

Hamacher K., Coenen H.H. and Stocklin G. (1986) Efficient stereospecific synthesis of no–carrier added 2–[18F]–fluoro–2–deoxy–D–glucose using aminopolyether supported nucleophilic substitution. J. Nucl. Med. **27**, 235–238.

Hawkins R.A., Huang C.S., Barrio J.R., Keen R.E., Feng D., Maziotta J.C. and Phelps M.E. (1989) Estimation of local cerebral protein synthesis rates with L–[1–11C]leucine and PET: methods, model, and results in animals and humans. J. Cereb. Bl. Flow Metab. **9**, 446–460.

Ishiwata K., Vaalburg W., Elsinga Ph. H., Paans A.M.J., and Woldring M.G.(1988a) Comparison of L–[1–11C]methionine and L–methyl–[11C]methionine for measuring protein synthesis rates with PET. J. Nucl. Med. **29**, 1419–1427.

Ishiwata K., Vaalburg W., Elsinga Ph. H., Paans A.M.J., and Woldring M.G. (1988b) Metabolic studies with L–[1–14C]tyrosine for the investigation of a kinetic model to measure protein synthesis rates with PET. J. Nucl. Med. **29**, 524–529.

Kearfott K.J., Elmaleh D.R., Goodman M., Correia J.A., Alpert N.M., Ackerman R.H., Brownell G.L. and Strauss W.H. (1984) Comparison of 2– and 3–18F–Fluoro–deoxy–D–glucose for studies of tissue metabolism. Nucl. Med. Biol. **11**, 15–22.

McCredie J.A., Inch W.R., Kruuv J. and Watson T.A. (1965) The rate of growth of tumours in animals. Growth **29**, 331–347.

Minn H., Joensuu H., Ahonen A. and Klemi P. (1988) Fluorodeoxyglucose imaging: a method to assess the proliferative activity of human cancer in vivo. Cancer **62**, 1776–1781.

Paans A.M.J., de Graaf E.J., Welleweerd J., Vaalburg W. and Woldring M.G. (1982) Performance parameters of a longitudinal tomographic positron imaging system. Nucl. Instr. Meth. **192**, 491–500.

Schober O., Meyer G.–J., Gaab M.R., Dietz H. and Hundeshagen (1988) Multi–parameter studies in brain tumors by PET. J. Nucl. Med. **29**, 853 (Abstract).

Sokoloff L. (1986) Cerebral circulation, energy metabolism, and protein synthesis: general characteristics and principles of measurement. In: Positron emission tomography and autoradiography: principles for the brain and the heart, Eds. Phelps M., Mazziotta J. and Schelbert H., Raven Press, New York, pp 1–71.

Som P., Atkins H.L., Bandyopadhyay D., Fowler J.S., MacGregor R.R., Mats K., Oster Z.H., Sacher D.F., Shiue C.Y., Turner H., Wan C–N., Wolf A.P. and Zabinski S.V. (1980) Fluorinated glucose analog, 2–fluoro–2–deoxy–D–glucose (F–18): nontoxic tracer for rapid tumor detection. J. Nucl. Med. **21**, 670–675.

Sweeney M.J., Ashmore J., Morris H.P. and Weber G. (1963) Comparative biochemistry of hepatomas IV. Isotope studies of glucose and fructose metabolism in liver tumors of different growth rates. Cancer Res. **23**, 995–1002.

Talalay P., Takano G.M.V. and Huggins C. (1952) Studies on the Walker tumor I. Standardization of the growth of a transplantable tumor. Cancer Res. **12**, 834–837.

Tribukait B., Veninga T., Lemstra W., Linder I. and Sundius G. (1981) Kinetics of cell proliferation in a rapidly growing murine lymphosarcoma. Acta Radiol. Oncol. **20**, 39–49.

Wagle S.R., Morris H.P. and Weber G. (1963) Comparative biochemistry of hepatomas V. Studies on amino acid incorporation in liver tumors of different growth rates. Cancer Res. **23**, 1003–1007.

Weber G. (1977) Enzymology of cancer cells (part 2). New Engl. J. Med. **296**, 541–551.

Wiebe L.I. (1983) Small animal oncological models for screening diagnostic radiotracers. In: Animal models in radiotracer design, Eds. Lambrecht R.M. and Eckelman W.C., Springer Verlag, New York, Heidelberg, Tokyo, pp 107–147.

Woerdenbag H.J., Lemstra W., Hendriks H., Malingré Th. H. and Konings A.W.T. (1987a) Investigation of the anti–tumour action of eupatoriopicrin against Lewis Lung tumour. Pl. Med. 318–322.

Woerdenbag H.J., Malingre Th.M., Lemstra W. and Konings A.W.T. (1987b) Cytostatic activity of Eupatoriopicrin in fibrosarcoma bearing mice. Phytother. Res. **1**, 76–78.

Yamada K., Endo S., Fukuda H., Abe Y., Yoshioka S., Itoh M., Kubota K., Hatazawa J., Satoh T., Matsuzawa T., Ido T., Iwata R., Ishiwata K. and Takahashi T. (1985) Experimental studies on myocardial glucose metabolism of rats with 18F–2–fluoro–2–deoxy–D–glucose. Eur. J. Nucl. Med. **10**, 341–345.

Yonekura Y., Benua R.S., Brill A.B., Som P., Yeh S.D.J., Kemeny N.E., Fowler J.S., MacGregor G.G., Stamm R., Christman D.R. and Wolf A.P. (1982) Increased accumulation of 2–deoxy–2–[18F]fluoro–D–glucose in liver metastases from colon carcinoma. J. Nucl. Med. **23**, 1133–1137.

CHAPTER 4

PET MEASUREMENTS OF HYPERTHERMIA-INDUCED SUPPRESSION OF PROTEIN SYNTHESIS IN TUMORS IN RELATION TO EFFECTS ON TUMOR GROWTH

Bernard J.G. Daemen, Philip H. Elsinga, Jaap Mooibroek, Anne M.J. Paans, Andre R. Wieringa, Antonius W.T. Konings and Willem Vaalburg.

[Accepted for publication in the Journal of Nuclear Medicine (1991)]

ABSTRACT

Hyperthermia-induced metabolic changes in tumor tissue have been monitored by positron emission tomography. Uptake of L-[1-^{11}C]tyrosine in rhabdomyosarcoma tissue of Wag/Rij rats was dose dependently reduced after local hyperthermia treatment at 42, 45 or 47 °C. Tumor blood flow, as measured by PET with $^{13}NH_3$, appeared to be unchanged. The L-[1-^{11}C]tyrosine uptake data were compared to uptake data of L-[1-^{14}C]tyrosine and with data on the incorporation of L-[1-^{14}C]tyrosine into tumor proteins. After iv injection, the ^{14}C-data were obtained from dissected tumor tissue. Heat-induced inhibition of the incorporation of L-[1-^{14}C]tyrosine into tumor proteins tallied with the L-[1-^{11}C]tyrosine uptake data. Heat-induced inhibition of amino acid uptake in the tumor correlated well with regression of tumor growth. It is concluded that PET using L-[1-^{11}C]tyrosine is eligible for monitoring the effect of hyperthermia on tumor growth.

INTRODUCTION

Since positron emission tomography (PET) is a non-invasive tool able to monitor quantitatively metabolic activities of tissues, the effects of therapy on tumor tissues can be investigated with this technique.

Relatively few investigators have applied positron-emitting tracers in experiments with tumor-bearing animals subjected to therapy. In the majority of these studies, uptake of tracer was determined in dissected tumor tissue before and after treatment. The effects of chemotherapeutics on tumor tissue have been investigated in terms of amino acid transport using L-^{11}C-α-isobutyric acid (1). Radiotherapeutic effects on glycolysis in tumor tissue have mainly been assessed by applying 2-^{3}H-deoxyglucose (2) and ^{18}F-2-fluoro-2-deoxyglucose (3). Recently, the response of the amino acid transport system of tumor to ionizing radiation has been investigated with L-[methyl-^{11}C]methionine (4). Using a pinhole-collimated gamma camera, Knapp and co-workers (5,6) investigated the uptake of ^{13}N-glutamate in relation to tumor blood flow in the Walker 256 carcinosarcoma before and after chemotherapy and radiotherapy.

Application of heat to tissues, induces many changes on cellular structures and on metabolic activities (7). From the literature it is known that protein synthesis is inhibited by hyperthermia in a heat dose dependent way (8,9,10). Especially the rate of recovery of protein synthesis seems to correlate with the extent of cell survival after hyperthermia. Heat-induced inhibition of tumor growth has been shown in a number of animal studies (11). Studies on the in vivo inhibition of protein synthesis in tumors, parallel with the measurement of tumor growth during hyperthermia, are important in order to explore to what extent PET is a prognostic tool for tumor growth by measuring alterations in protein synthesis For this purpose, L-[1-^{11}C]tyrosine (^{11}C-tyr) is available as a tracer (12,13).

In tumor tissue, hyperthermia may change the tumor blood flow which might affect the uptake of radiolabelled compounds and the removal of heat (14,15,16). These changes can be investigated with $^{13}NH_3$ (17).

The aims of the current study are:

1. To investigate the effects of different thermal doses on protein synthesis in tumors using L-[1-^{14}C]tyrosine (^{14}C-tyr) in rhabdomyosarcoma(RMS)-bearing rats, and to correlate these effects with the corresponding effects on ^{11}C-tyr uptake as measured by PET.

2. To investigate the effects of the thermal doses on tumor growth and to correlate these with the ^{11}C–tyr data obtained by PET.

MATERIALS AND METHODS

Chemicals

$^{13}NH_3$ was prepared according to Vaalburg *et al.* (18). Briefly, during irradiation of distilled water with 18 MeV protons, ^{13}N–activity was generated, no carrier added, in the form of ^{13}N–nitrites and ^{13}N–nitrates. These were reduced to $^{13}NH_3$, using Devarda's alloy in strong alkaline solution. L–[1–^{11}C]tyrosine was prepared according to Bolster *et al.* (19). After carboxylation with 7.4 GBq (200 mCi) $^{11}CO_2$ of the lithiated p–methoxy–phenylethyl–isocyanide, 110–140 MBq (3–4 mCi) enantiomerically pure L–[1–^{11}C]tyrosine were obtained with a specific activity of at least 3.7 GBq/μmol (100 Ci/mmol).

Animals

The rhabdomyosarcoma tumor in the Wag/Rij rat was used as a tumor model (20). Cubic pieces (100 mg) of solid, homogeneous, rhabdomyosarcoma tissue were grafted into the left flanks of 2–month–old female Wag/Rij rats that weighed 140 g. A volume of between 4 and 5 ml was measured 18 days after transplantation. At this stage, the ellipsoid–shaped tumors were free of necrotic parts, and therefore histologically homogeneous. Animals were fed on a standard diet and given water ad libitum.

L–[1–^{14}C]tyrosine uptake and incorporation

Tumor–bearing rats were intraperitoneally anaesthetized with a dose of 3 mg sodium pentobarbital (3g / 100 ml saline) per 100 g body weight. A supplement of 1 mg anaesthetic was given every two hours. The tumor was locally heated for 15 minutes at 42, 45 or 47 °C. Rats were given an intraveneously injected dose of 93 kBq (2.5 μCi) L–[1–^{14}C]tyrosine (Amersham International, Buckinghamshire, UK) dissolved in 0.2 ml saline with a specific activity of 2 GBq/mmol (56 mCi/mmol) at intervals of 10, 30, 60 or 120 minutes

after treatment. Five animals were used per thermal dose and per point in time. Rats were sacrificed by a heart puncture 60 minutes after the ^{14}C–tyr injection. Tumors were excised, and 7 tumor tissue samples with a weight of 50–100 mg each were randomly selected. Five of these tumor samples were used for the measurement of the total tissue activity. These samples were weighed and dissolved in Protosol© (Dupont, Boston, Mass, USA). After addition of 10 ml Plasmasol© scintillation liquid (Packard Instruments, Downers Grove, Ill, USA), the total ^{14}C–radioactivity was measured by liquid scintillation counting. The tumor uptake was expressed as differential absorption ratio (DAR): i.e. (counts/g tissue) x (g body weight/total injected counts). The values of the 5 samples were averaged. In order to determine the protein synthetizing activity of the tumor tissue at different times after hyperthermia, the incorporation of ^{14}C–tyr into proteins was measured. Therefore, the 2 remaining tumor samples were homogenized and treated with trichloro acetic acid (TCA) at 0 °C. Subsequently, the TCA–insoluble fraction was determined. From the total ^{14}C–uptake and the TCA–insoluble fraction, the accumulated ^{14}C–radioactivity incorporated into protein was calculated and expressed as DAR. For 10 untreated rats the uptake and incorporation of ^{14}C–tyr was also determined; these animals served as controls.

Hyperthermia

A modified, commercially available Curadar 2000 (Enraf Nonius, Delft, The Netherlands) was used as hyperthermia device. This device emitted 2.45 GHz microwaves, which were locally applied on the tumor by means of a home–built 4 x 4 cm^2 applicator. Three thermocouples were placed into the tumor; one at the core and two at the peripheries. The desired temperature was attained within two minutes. The electric feedback from the thermocouples to the microwave generator, in combination with a predefined temperature threshold, regulated the amount of energy released from the microwave generator on the tumor. The tumor temperature was kept constant with an accuracy of 0.3 °C. Marked differences in temperature, registered at the three different positions of the thermocouples, were not observed. A fourth rectal thermocouple monitored whole body temperature. Notable elevation of the body temperature was not registered during the hyperthermia treatment.

PET experiments with L-[1-^{11}C]tyrosine and $^{13}NH_3$

Animals were anaesthetized with sodium pentobarbital, as described above. During experimentation, body temperature was measured rectally. It is known that anaesthesia causes a drop in temperature of the body. To prevent this, body temperature was maintained above 37 °C by the use of infra red lamps. A catheter with a low volume (<0.05 ml) was inserted into a tail vein. Complete administration of tracer was achieved by flushing the catheter with 0.05 ml saline after each injection. The rat was dorsally positioned in a longitudinal positron camera (21). The PET data were acquired as described previously by Daemen *et al.* (22,23). A dose of 0.37 MBq (10 μCi) $^{13}NH_3$ in a volume of 0.1 ml saline was administered to the untreated rat via the catheter as a fast bolus. 10 minutes after the injection, the uptake of the ^{13}N-radioactivity into the RMS tumor was measured by PET. Subsequently, after physical decay of the ^{13}N-activity to a negligible background value (<0.5%), an injection of 1.1 MBq (30 μCi) ^{11}C-tyr in 0.2 ml phosphate buffer (pH 4.6) was administered to the same animal. 60 minutes after this injection, the uptake of ^{11}C-tyr into tumor tissue was measured. The rat was removed from the camera and the tumor was given a local thermal dose. Hereafter, the treated rat was repositioned in the positron camera, and was given a second injection of 0.37 MBq (10 μCi) $^{13}NH_3$ 10 minutes after hyperthermia. In analogy to the pretreatment measurement, the ^{13}N-uptake in tumor was determined 10 minutes after injection. 30 minutes after hyperthermia, the rat was given a second injection of 1.1 MBq (30 μCi) ^{11}C-tyr. The ^{11}C-uptake into the tumor tissue was measured 60 minutes after injection. The time interval between the $^{13}NH_3$ injection and the ^{11}C-measurement was 80 minutes. The contribution of the ^{13}N-background in the second L-[1-^{11}C]tyrosine measurement is less than 0.4% and therefore considered to be negligible. The PET data were corrected for physical decay and non-uniform response of the system. The uptake in tissue was calculated as differential absorption ratio DAR(PET): i.e. (Counts tumor/Volume tumor) x (Weight rat/Counts rat).

Volume measurements and growth delay

The three principal diameters of the tumor, growing in situ, were measured with a vernier calliper. The volume of the tumor was calculated by the formula: $V = \frac{1}{6}\pi$ x (product of 3 orthogonal diameters) (24). Data obtained

from the tumor volume measurements in time course were used to construct the growth curves. From the growth curves, the tumor doubling times (time to double a certain volume, TD) were calculated. The growth delay (GD) was determined for the treated animals. GD is defined as the number of doubling times saved by therapy and is calculated by the formula: $GD = (TD_{tr} - TD_c)/TD_c$. The TD_{tr} is the doubling time of the treated tumors. These values were determined for 19 animals (7 at 42 °C, 6 at 45 °C and 6 at 47 °C). The TD_c is the doubling time of a second control group which consisted of 9 untreated animals. The statistical significances of the growth delays were analyzed with Fisher's distribution free sign test (25).

RESULTS

L-[1-^{14}C]tyrosine experiments

Data on the total uptake of ^{14}C-tyr into the tumor and its incorporation into tumor proteins are presented in table 1. The tumor tissue has been exposed to ^{14}C-tyr during a time span of 60 minutes (time between injection

Table 1. *Total ^{14}C-uptake of L-[1-^{14}C]tyrosine and incorporation of this amino acid into proteins of rhabdomyosarcoma tissue at different points of time after hyperthermia.*

		Time after hyperthermia			
Thermal dose		70 min	90 min	120 min	180 min
15 min 42 °C	Total-^{14}C	1.55±0.20	1.37±0.08	1.17±0.06*	1.44±0.19
	Protein-^{14}C	1.12±0.15	1.05±0.10	0.66±0.11*	1.18±0.19
15 min 45 °C	Total-^{14}C	0.73±0.15*	0.86±0.11*	1.12±0.05*	1.58±0.12
	Protein-^{14}C	0.30±0.07	0.28±0.09	0.53±0.16	1.19±0.15
15 min 47 °C	Total-^{14}C	0.89±0.03*	0.71±0.08*	0.74±0.10*	1.09±0.18*‡
	Protein-^{14}C	0.50±0.09	0.33±0.08	0.44±0.08	0.64±0.22*‡
Untreated	Total-^{14}C	1.58±0.05†			
	Protein-^{14}C	1.30±0.12†			

Total uptake of L-[1-^{14}C]tyrosine and incorporation into protein are expressed as DAR (see materials and methods section), errors are SEM.
*P-values of 0.05 or less from Student's t-test for differences with untreated. N=5 per point of time, †N=10, ‡N=4.

and dissection). The measured endpoint values are to be considered as a resultant of multiple metabolic processes and redistribution phenomena.

Table 1 shows that treatment of the tumor at 42 °C for 15 minutes does not have a pronounced influence on the uptake of ^{14}C–tyr. A significant reduction in uptake of ^{14}C–tyr was only observed at 120 minutes after hyperthermia. Hyperthermia at 45 °C and 47 °C gave rise to statistically significant reductions of the ^{14}C–tyr uptake already measured 70 minutes after treatment. In the 45 °C experiments, this reduced uptake was restored to the control level after 180 minutes. In the 47 °C experiments, the reduction was more prolonged than in the 45 °C experiments.

From the total uptake values (table 1) and the percentages incorporated into proteins, the amount of accumulated ^{14}C–tyr that was converted to protein was calculated, representing the protein synthesizing activity of the tumor tissue. This parameter is presented in table 1. This table shows, that at 120 minutes after the 42 °C treatment, the amount of incorporated ^{14}C–tyr is reduced by a factor of 2, as compared to the untreated tumors. Even larger reductions were measured in the 45 °C and the 47 °C experiments, where fourfold reductions were found 90 minutes after treatment.

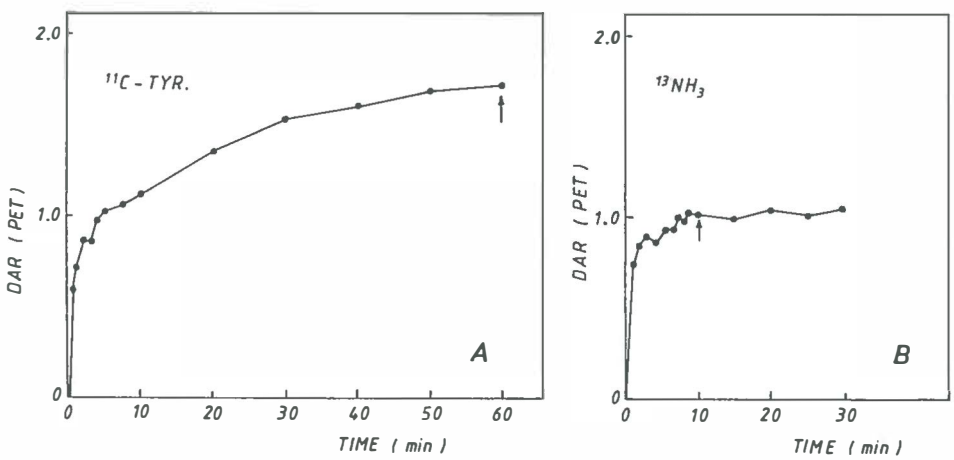

Figure 2. *(A) Uptake curve of ^{11}C–activity into untreated rhabdomyosarcoma tissue during 60 minutes after injection of ^{11}C–tyr. (B) Uptake curve of ^{13}N–activity into the tumor tissue during 30 minutes after injection of ^{13}NH$_3$. Uptake of radioactivity is expressed as DAR(PET). The arrows indicate the moments of radioactivity measurements for the hyperthermia experiments.*

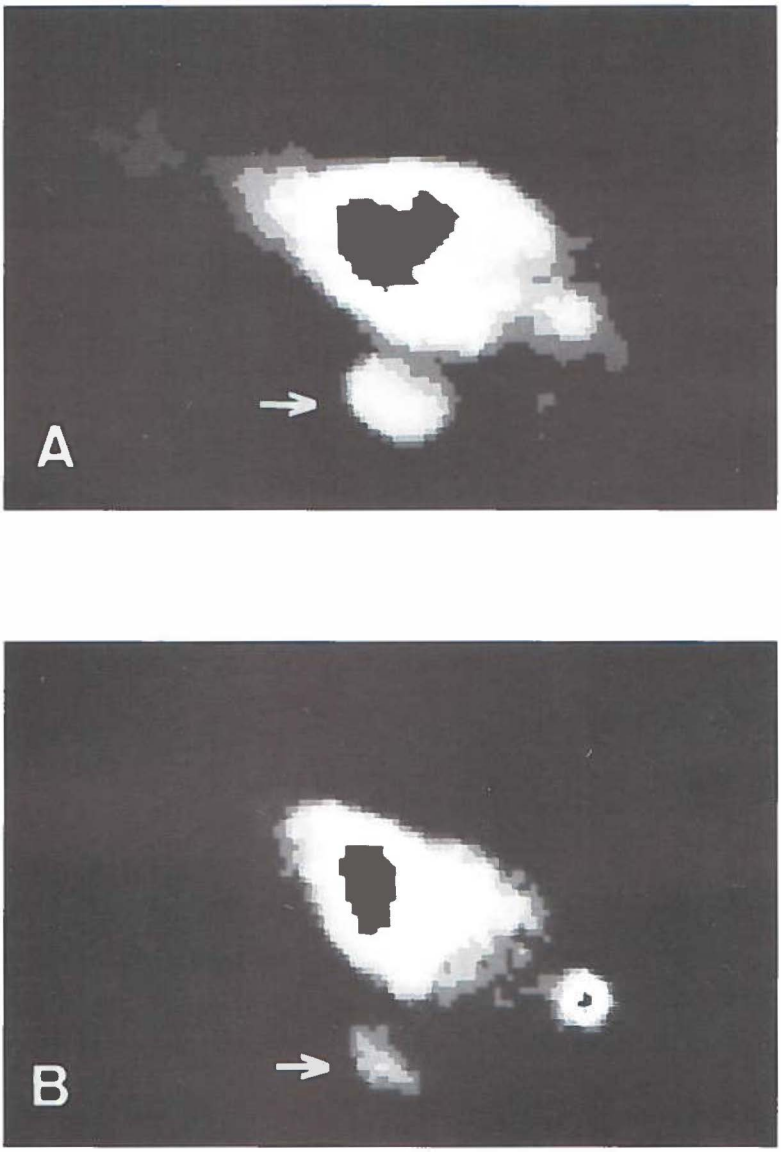

Figure 1. *(A) Distribution of $^{11}C-tyr$, measured by PET, 60 minutes after iv injection into the rat bearing a RMS tumor of 5 ml. (B) Distribution of $^{13}NH_3$, 10 minutes after injection into the same animal. Arrows indicate the position of the tumor. Black areas in the images (e.g., liver ($^{11}C-tyr$, $^{13}NH_3$) and bladder ($^{13}NH_3$)) are caused by windowing of the PET images, in order to obtain clearer visualization of the tumor.*

PET experiments with L-[1-^{11}C]tyrosine and $^{13}NH_3$

As can be seen in figure 1A (arrow), PET studies with ^{11}C-tyr in the rhabdomyosarcoma-bearing rat revealed good visualization of the tumors. In figure 2A, a curve of the kinetics of the uptake of ^{11}C-radioactivity into the untreated rhabdomyosarcoma tissue is shown. A typical biphasic pattern is observed. The first phase, between 0 and 5 minutes after injection, is observed as a rapid uptake of ^{11}C-radioactivity into the tumor. Between 5 and 60 minutes, a second phase is observed as a slow, linear increase of ^{11}C-radioactivity. The statistical error in the measurement of the ^{11}C-activity in the tumor, measured 60 minutes after injection, is less than 1% for the untreated situation. As PET data acquisition period, the period between 30-90 minutes after hyperthermia was chosen. The heat dose dependency on the reduction of ^{14}C-tyr uptake was best reflected in this period (see table 1).

In table 2A, ^{11}C-tyr PET data are shown obtained prior to and after administration of different thermal doses to the tumor. Uptake of ^{11}C-tyr into the tumor tissue was calculated as differential absorption ratio (DAR). In table 2A, it is observed that uptake of ^{11}C-tyr in the tumor after hypertermia is reduced as compared to the untreated situation. These statistically significant reductions amounted to 21%, 28% and 35% after hyperthermia at 42, 45 and 47 °C, respectively. The statistical significance of these reductions (P-values), as obtained with paired Student's t-tests, increased with the rise in thermal dose.

Table 2. *Uptake of L-[1-^{11}C]tyrosine (A) and $^{13}NH_3$ (B) into rhabdomyosarcoma tissue before and after hyperthermia as measured by PET.*

	Thermal dose	Before	(%)	After	(%)	P-value	Number
A.	15 min 42 °C	1.72±0.11	(100)	1.35±0.12	(79±5)	0.05	n=6
	15 min 45 °C	1.63±0.12	(100)	1.17±0.06	(72±3)	0.01	n=5
	15 min 47 °C	1.75±0.10	(100)	1.14±0.09	(65±4)	0.002	n=6
B.	15 min 42 °C	1.04±0.11	(100)	1.18±0.14	(104±7)	n.s.	n=6
	15 min 45 °C	1.10±0.15	(100)	1.13±0.15	(110±16)	n.s.	n=5
	15 min 47 °C	0.93±0.10	(100)	0.99±0.07	(112±12)	n.s.	n=6

Uptake values expressed as DAR(PET). Values are mean ± sem.
Percentual amounts between brackets.
Probability values from paired Student's t-test, n.s. is not significant.

Studies with $^{13}NH_3$ in the RMS–bearing rat revealed that ^{13}N–activity was rapidly taken up by the tumor tissue (figure 2B) which resulted in a good visualization of the tumor on the PET image (see figure 1B). Between 5 and 10 minutes after injection, the level of ^{13}N–activity, which was corrected to the time of injection, reached a plateau value (fig. 2B). This plateau value was observed between 10 and 30 minutes after injection. The plateau value, which was measured at 10 minutes after injection of $^{13}NH_3$, was taken as control parameter for tumor blood flow.

In table 2B, the $^{13}NH_3$–uptake values of the RMS tumor prior to and after hyperthermia are presented. No statistically significant differences in uptake of ^{13}N–activity were observed at each of the three different doses of heat. The profile of the $^{13}NH_3$–uptake curves did not change after hyperthermia treatment (not shown).

A comparison between the uptake values of ^{11}C–tyr and ^{14}C–tyr in the RMS at the 30–90 minutes period after hyperthermia is given in figure 3. It was observed that at 42 and 45 °C treatments, no statistically significant differences between the PET and the dissection experiments were found. With the 47 °C treatments, the reduction in uptake in the dissection experiments with ^{14}C–tyr was more pronounced than the reduction as measured by PET using ^{11}C–tyr.

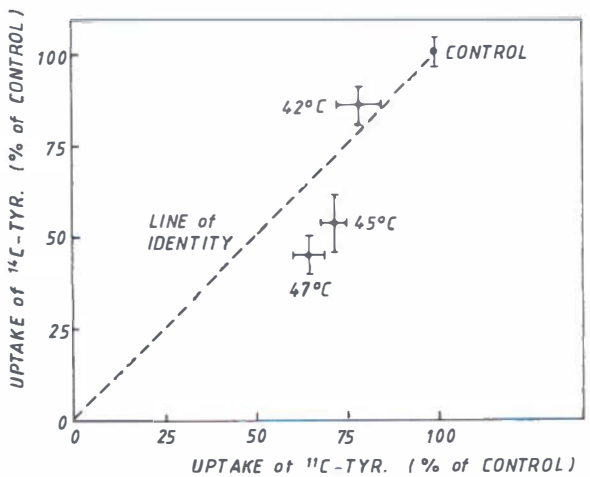

Figure 3. *Comparison between the PET method ($^{11}C-tyr$) and the dissection method ($^{14}C-tyr$) for measuring differences in uptake of radioactivity in tumor tissue as a result of hyperthermic treatment. In both methods, radioactivity was measured in the same period (30–90 min) after hyperthermia. The uptake values after hyperthermia were normalized to the untreated situation (100%).*

Growth delay

Tumors with volumes between 4 and 5 ml were heated, and subsequently growth curves were measured. In table 3, the effects of the different hyperthermia treatments on tumor growth are summarized. After the 42 °C treatments no significant growth delays were observed. Growth delays of 0.17 ($P<0.11$) and 0.18 ($P<0.016$) respectively were measured at the 45 and 47 °C treatments.

Table 3. *Effects of different thermal doses on tumor growth of the rhabdomyosarcoma tumor represented as growth delay values.*

Treatment	Growth Delay (GD)	P–value	Number
15 min at 42 °C	0.07±0.14	n.s.	n=7
15 min at 45 °C	0.17±0.04	0.11	n=6
15 min at 47 °C	0.18±0.03	0.016	n=6

Values are mean ± sem. For definition of GD see method section.
Probability values from Fisher's distribution free sign test.
n.s. is not significant.

DISCUSSION

In this report, the possible use of PET to monitor the effect of hyperthermia on tumor growth is described in experiments with rhabdomyosarcoma–bearing Wag/Rij rats.

In these experiments, carboxylic–labelled tyrosine was used to measure amino acid uptake and incorporation into protein of tumor tissue. In the current studies, ^{11}C–tyr was preferred above the more widely used L–[methyl–^{11}C]methionine. The advantages of ^{11}C–tyr are a higher incorporation into proteins and a lower amount of metabolites (13,26). Moreover, the predominant metabolite $^{11}CO_2$ is washed rapidly from the tissue into the plasma bicarbonate pool and consequently does not contribute to the amount of ^{11}C–radioactivity measured in the tumor tissue.

From in vitro studies, it is known that hyperthermia reduces the incorporation of amino acids into proteins (8,9). In our studies with the RMS tumor, this inhibition was also observed. The suppressed incorporation of ^{14}C–tyr was accompanied by a decreased uptake of total ^{14}C–radioactivity. In cultured cells, Magun (27) also observed such a decreased amino acid uptake,

which could be ascribed to a suppressed demand of amino acid caused by inhibition of protein synthesis and not to a hyperthermia–induced effect on amino acid transport.

The absorbed dose of heat by the tumor is a function of the elevation of tumor temperature and of the duration of this elevation. Panniers and Henshaw (10) observed that immediately after temperature elevation in Ehrlich Ascites cells, inhibition of protein synthesis increased steeply over a range of elevated temperatures. Henle and Leeper (28) found a similar result with Chinese Hamster Ovary cells. In their study, an increase of the treatment time at the same temperature was accompanied with an augmented reduction in incorporation of amino acid into tumor protein shortly after hyperthermia. These findings are in agreement with our observation that in the 30–90 minutes period after hyperthermia, the decreased uptake correlated positively with the increase of temperature and consequently with the thermal dose.

The inhibition of protein synthesis caused by treatment is observed to be reversible. The restoration of protein synthesis in the experiments with ^{14}C–tyr has a time lag which appeared to be dose dependent (see table 1). Studies with cultured cells (10,28) also indicated that the higher thermal dose the longer the period required for restoration of protein synthesis.

In the corresponding PET studies, reduced uptake of ^{11}C–tyr was observed after application of different thermal doses, as was expected from the ^{14}C–tyr studies. The reduction of ^{11}C–tyr uptake was dose dependent up to a maximum of 35% in the 47 °C experiments.

When compared, the PET method and the dissection method gave similar reductions in uptake of radiolabelled tyrosine after hyperthermia at 42 and 45 °C. At the 47 °C treatments, the reduction in uptake of ^{11}C–tyr was smaller than the reduction in uptake of ^{14}C–tyr after dissection. One explanation might be that only after hyperthermia at 47 °C the RMS became edemateous. This hyperthermic effect was also observed by Mooibroek and co-workers (29) who found edema after heating the RMS tumor at 43 °C for 120 minutes. Edema, due to enlargment of the tumor volume, leads to the lowering of the concentration of radioactivity in the tumor tissue. In the ^{11}C–tyr studies, unlike the ^{14}C–tyr studies, this effect was not accounted for. Therefore, the uptake values of ^{11}C–tyr are overestimated in the 47 °C experiments, yielding an underestimation of the hyperthermia–induced reduction of amino acid uptake.

In a tumor, after first pass extraction, $^{13}NH_3$ is trapped via binding to amino acids such as glutamic acid. Within 10 minutes after injection, the

level of ^{13}N–radioactivity in the RMS tumor rapidly reaches a plateau level. This plateau was also found by Schelstraete (17) in a number of tumors of human origin. The effect of hyperthermia on blood flow was extensively reviewed by Reinhold and Endrich (16) who pointed out that hyperthermia, especially above 42 °C, might decrease the blood flow in tumors. But not all blood vessels in tumors respond to hyperthermia in the same manner. Using labelled microspheres, after a 60–minute treatment at 45 °C, Song and co–workers (30) found no alterations of flow in the Walker 256 carcinosarcoma. In our studies with the RMS tumor, hyperthermia did not change tumor blood flow at temperatures between 42 and 47 °C as monitored during 10–20 minutes after hyperthermia. From these results, it is concluded that shortly after treatment, the hyperthermia–induced reductions in uptake of ^{11}C–tyr are not caused by a change in blood flow.

Reductions on tumor growth were observed after 15 minutes treatments at 45 and 47 °C, but not at 42 °C. These data (table 3) correspond with results of Zywietz (31) obtained after treatment of a RMS tumor at 43 °C for 30 minutes, where similar delays in tumor growth were observed.

In the 45 and 47 °C treatments, a reduced uptake of ^{11}C–tyr was accompanied by a delay in tumor growth. Therefore, we conclude that the hyperthermia–induced suppression of protein synthesis, as measured by PET, is an appropriate prognostic indicator for the effect of heat on tumor growth.

ACKNOWLEDGEMENTS

This research was supported by the Dutch Cancer Society "Koningin Wilhelmina Fonds". The cooperation of staff of the Kernfysisch Versneller Instituut (Prof Dr R.H. Siemssen) and the considerable help of the operating team of the cyclotron are gratefully acknowledged.

REFERENCES

(1) Dunzendorfer U, Schmall B, Bigler RE, *et al.* Synthesis and body distribution of alpha–aminoisobutyric acid–L–11C in normal and prostate cancer bearing rat after chemotherapy. *Eur J Nucl Med* 1981; 6:535–538.

(2) Iosilevsky G, Front D, Bettman L, Hardorff R, Ben–Arieh Y. Uptake of Gallium–67 citrate and [2–3H]deoxyglucose in the tumor model, following chemotherapy and radiotherapy. *J Nucl Med* 1985; 26:278–282.

(3) Abe Y, Matsuzawa T, Fujiwara T, *et al.* Assessment of radiotherapeutic effects on experimental tumor using 18F–2–fluoro–2–deoxy–D–glucose. *Eur J Nucl Med* 1986; 12:325–328.

(4) Kubota K, Matsuzawa T, Takahashi T, *et al.* Rapid sensitive response of Carbon–11–L–methionine tumor uptake to irradiation. *J Nucl Med* 1989; 30:2012–2016.

(5) Knapp WH, Helus F, Layer K, Panzer M, Höver K–H, Ostertag H. N–13 glutamate uptake and perfusion in Walker 256 carcinosarcoma before and after single dose irradiation. *J Nucl Med* 1986; 27:1604–1610.

(6) Knapp WH, Panzer P, Helus F, Layer K, Sinn HJ, Ostertag H. Effect of methotrexate on perfusion and Nitrogen–13 glutamate in the Walker–256 carcinosarcoma. *J Nucl Med* 1988; 29:208–216.

(7) Konings AWT. Effects of heat and radiation on mammalian cells. *Radiat Phys Chem* 1987; 30:339–349.

(8) Mc Cormick W, Penman S. Regulation of protein synthesis in HeLa cells: translation at elevated temperatures. *J Mol Biol* 1969; 39:315–333.

(9) Mondovi B, Finazzi Agro' A, Rotilio G, Strom R, Moricca G, Rossi Fanelli A. The biochemical mechanism of selective heat sensitivity od cancer cells II. Studies with nucleic acids and protein synthesis. *Europ J Cancer* 1969; 5:137–146.

(10) Panniers R, Henshaw EC. Mechanism of inhibition of polypeptide chain initiation in heat–shocked Ehrlich ascites tumour cells. *Eur J Biochem* 1984; 140:209–214.

(11) Overgaard J, Suit HD, Walker AM. Multifractionated hyperthermia treatment of malignant and normal tissue in vivo. *Cancer Res* 1980; 40:2045–2050.

(12) Garlick PJ. Protein turnover in the whole animal and specific tissues. In: Florkin M, Stotz EH, eds. *Comprehensive Biochemistry* Vol 19B. Amsterdam Elsevier; 1973:77–153.

(13) Ishiwata K, Vaalburg W, Elsinga PH, Paans AMJ, Woldring MG. Metabolic studies with L–[1–14C]tyrosine for the investigation of a kinetic model to measure protein synthesis rates with PET. *J Nucl Med* 1988; 29:524–529.

(14) Song CW. Effect of local hyperthermia on blood flow and micro environment: a review. *Cancer Res* 1984; 44:4721S–4730S.

(15) Vaupel P, Müller–Klieser W, Otte J, Manz R, Kallinowski F. Blood flow, tissue oxygenation, and pH–distribution in malignant tumors upon localized hyperthermia. *Strahlentherapie* 1983; 159:73–81.

(16) Reinhold HS, Endrich E. Tumour microcirculation as a target for hyperthermia. *Int J Hyperthermia* 1986; 2:111–137.

(17) Schelstraete K. Circulatory and metabolic studies in extracranial malignant tumors. In: Heiss WD, Pawlik G, Herholz K, eds. *Clinical Efficacy of Positron Emission Tomography.* Dordrecht, Boston, Lancaster: Martinus Nijhoff; 1987:345–359.

(18) Vaalburg W, Kamphuis JAA, Beerling–van der Molen HD, Reiffers S, Rijskamp A, Woldring MG. An improved method for the cyclotron production of 13N–labelled ammonia. *Int J Appl Rad Isot* 1975; 26:316–317.

(19) Bolster JM, Vaalburg W, Paans AMJ, *et al.* Carbon–11 labelled tyrosine to study tumor metabolism by positron emission tomography (PET). *Eur J Nucl Med* 1986: 12:321–324.

(20) Barendsen GW, Broerse JJ. Experimental radiotherapy of a rat rhabdomyosarcoma with 15 MeV neutrons and 300 KeV X-rays. I Effects of single exposures. *Europ J Cancer* 1969; 5:373–391.

(21) Paans AMJ, De Graaf EJ, Welleweerd J, Vaalburg W, Woldring MG. Performance parameters of a longitudinal tomographic positron imaging system. *Nucl Instr Meth* 1982; 192:491–500.

(22) Daemen BJG, Elsinga PH, Ishiwata K, Paans AMJ, Vaalburg W. A comparative PET study using different 11C–labelled amino acids in Walker 256 carcinosarcoma–bearing rats. *J Nucl Med Biol* 1991; 18:197–204.

(23) Daemen BJG, Elsinga PH, Paans AMJ, Lemstra W, Konings AWT, Vaalburg W. Suitability of rodent tumor models for experimental PET with L–[1–11C]tyrosine and 2–[18F]–fluoro–2–deoxy–D–glucose. *J Nucl Med Biol* 1991 (in press).

(24) Steel GG. Growth rate of tumours. In: Steel GG, ed. *growth kinetics of tumours*. Oxford: Clarendon; 1977:5–55.

(25) Hollander M, Wolf DA. Nonparametric statistical methods. New York, London, Sydney, Toronto: John Wiley & Sons; 1973: 39–41.

(26) Ishiwata K, Vaalburg W, Elsinga PH, Paans AMJ, Woldring MG. Comparison of L–[1–11C]methionine and L–Methyl–[11C]methionine for measuring protein synthesis rates with PET. *J Nucl Med* 1988; 29:1419–1427.

(27) Magun BE. Inhibition and recovery of macromolecular synthesis, membrane transport, and lysosaomal function following exposure of cultured cells to hyperthermia. *Rad Res* 1981; 87:657–669.

(28) Henle KJ, Leeper DB. Effects of hyperthermia (45 °C) on macromolecular synthesis in Chinese hamster ovary cells. *Cancer Res* 1979; 39:2665–2674.

(29) Mooibroek J, Dikomey E, Zywietz F, Jung H. Thermotolerance kinetics and growth rate changes in the R1H tumour heated at 43 °C. *Int J Hyperthermia* 1988; 4:677–686.

(30) Song CW, Kang MS, Rhee JG, Levitt SH. The effect of hyperthermia on vascular function, pH, and cell survival. *Radiology* 1980; 137:795–803.

(31) Zywietz F. Effect of microwave heating on the radiation response of the rhabdomyosarcoma. *Strahlentherapie* 1982; 158:255–257.

CHAPTER 5

RADIATION-INDUCED INHIBITION OF TUMOR GROWTH AS MONITORED BY PET USING L-[1-^{11}C]TYROSINE AND ^{18}FDG

Bernard J.G. Daemen, Philip H. Elsinga, Anne M.J. Paans, Andre R. Wieringa, Antonius W.T. Konings and Willem Vaalburg.

[Submitted for publication]

ABSTRACT

The potential use of PET to monitor radiotherapeutic effects on tumors has been evaluated with L-[1-^{11}C]tyrosine and ^{18}FDG. Single X-ray doses of 10, 30 or 50 Gy have been applied to rhabdomyosarcoma tumors, growing in the flank of rats. Dose-dependent reductions of tracer uptake were registered by PET 4 and 12 days after treatment. These later effects on tracer uptake appeared to correlate with changes in tumor volume. Therefore, PET using L-[1-^{11}C]tyrosine and ^{18}FDG is apposite to monitor kinetics of tumor growth and tumor regression after radiotherapy. Direct effect on tracer uptake was not observed within 8 hours after irradiation. This indicates that, using PET, early predictions on the outcome of radiotherapy are not possible. When combining a radiation treatment with hyperthermia, radiation-induced inhibition of tumor growth was clearly enhanced. Possibly due to invasion of host cells, the uptake of tracer remained at the pretreatment value. From these experiments it can be concluded that it is difficult to monitor a combined treatment of radiation and hyperthermia by PET.

INTRODUCTION

In clinical practice, it is difficult to give a reliable prognosis concerning the curative outcome of a radiotherapeutic treatment. With positron emission tomography (PET) it is possible to investigate and to quantify metabolic processes in tissues, such as synthesis of macromolecules and glycolysis. For this reason, PET might be an elegant technique in monitoring tumor metabolism before and after treatment.

Irradiation of tumors is known to result in inhibition of DNA synthesis, whereas protein synthesis and carbohydrate metabolism are only marginally influenced at the doses used in clinical practice (1,2,3,4). Direct radiation effects on glycolysis, protein synthesis or amino acid transport can only be expected at high doses (>100 Gy) (5,6,7). Hyperthermia rapidly suppresses protein synthesis in tumor tissue (8,9), and this phenomenon appeared to be useful for the prediction of tumor growth by PET after a hyperthermic treatment (10). In the case of radiotherapy it may be expected that PET measurements used to monitor immediate radiation effects on protein synthesis are less profitable for prognosis of radiation effects on tumor growth.

However, PET in combination with 2-[^{18}F]fluoro-2-deoxy-D-glucose (^{18}FDG), an indicator of glycolytic activity in tissue (11), has been used to follow effects of radiotherapy in tumors (12,13,14). With this tracer PET has been useful in the early differentiation between radiation-induced necrosis and tumor recurrence in intracranial tumors. In patients with extracranial head and neck cancer, using ^{18}FDG, Minn *et al.* (15) were able to discriminate between radiotherapy responding and resisting tumors. These studies monitored indirect long-term radiation effects.

In rats, Knapp *et al.* (16) measured acute reductions of ^{13}N-glutamate uptake into Walker 256 carcinosarcomas 30 minutes after 8 Gy ^{60}Co-irradiation. Also in tumor-bearing rats, Kubota *et al.* (17) found a relatively rapid decrease of L-[methyl-^{11}C]methionine uptake within 6 hours after 20 Gy ^{60}Co-irradiation. This prompted us to evaluate, in an experimental animal model, direct and indirect radiation-induced changes of amino acid utilization of tumors by PET. To correlate amino acid uptake with protein synthesis in the tumor tissue, parallel studies with ^{14}C-labelled amino acids are necessary in which the percentages of amino acid incorporated into proteins are determined.

It is difficult to determine the actual tumor volume in patients undergoing radiotherapy. In the above-mentioned PET studies in patients, PET

data were merely coupled with the clinical outcome of treatment, but not with the tumor volume present at the time of the PET measurement. It is therefore important to correlate PET data obtained in tumors before and after radiotherapy with the actual radiobiological effects on tumor growth at the time of PET. To realize this, an experimental animal model was chosen: the rhabdomyosarcoma(RMS)–bearing rat.

Hyperthermia suppresses protein synthesis in tumors and it has a sensitizing effect on treatment with ionizing radiation (18,19). It is therefore of interest to evaluate the effects of the combined treatment of radiation and hyperthermia on L–[1–^{11}C]tyrosine (^{11}C–tyr) and ^{18}FDG uptake and to correlate these data with the effects on tumor growth.

The aims of the current study are:

1. To investigate the effects of radiotherapy as well as the combination of radiotherapy and hyperthermia on tumor uptake of ^{11}C–tyr and ^{18}FDG with PET, and to compare the ^{11}C–tyr data with L–[1–^{14}C]tyrosine (^{14}C–tyr) data on uptake and incorporation as obtained after dissection of tumor.
2. To determine the effects of the respective treatments on tumor growth and to correlate these with the PET data.

MATERIALS AND METHODS

Radiotracers

According to Bolster *et al.* (20), the radiopharmaceutical ^{11}C–tyr with a radiochemical purity of >99% and a specific activity of >3.7 GBq/μmol (100 Ci/mmol) was synthetized via the isocyanide route. ^{18}FDG was synthetized according to Hamacher *et al.* (21). The radiochemical purity of ^{18}FDG was >97%.

Animals

Rhabdomyosarcoma–bearing rats (22) were purchased from TNO, Rijswijk, The Netherlands. Cubic pieces of rhabdomyosarcoma tissue, that weighed 100 mg, were dissected from these animals and subcutaneously grafted into the left flank of 2–month–old female Wag/Rij rats with a weight of 140 g. Eighteen days after transplantation, the tumors developed to ellipsoid–shaped volumes between 4 and 5 ml. At these volumes, the tumors were free of necrotic tissue.

The rats had free access to water and food (RMH pellets, Hope Farms, Woerden, The Netherlands).

Radiotherapy and hyperthermia

Prior to a radiotherapy, the tumor-bearing animal was sedated with an intraperitoneally injected dose of 1.5-2.0 mg sodium pentobarbital (1.5 g/100 ml saline) per 100 g body weight. The body of the rat was protected by a telescoping lead cylinder with a total shielding thickness of 4 mm. From these lead shields, the tumor protruded through a slit. For irradiation a Philips-Muller Mg 300 Röntgen source, operated at 200 kV and 15 mA, was used. Only the tumor was irradiated. X-rays were filtered with 0.5 mm Cu and 0.5 mm Al. The dose rate was 3 Gy/min. Each animal received a single dose of 10, 30 or 50 Gy, respectively. Ten minutes after irradiation, a number of the animals that were exposed to 30 Gy received a hyperthermia treatment at 45 °C for 15 minutes. Hyperthermia was carried out as described previously (10).

L-[1-^{14}C]tyrosine experiments

At 8 hours, 4 days or 12 days after radiotherapy, rats with tumors exposed to doses of 10 Gy, 30 Gy or 50 Gy, were investigated with ^{14}C-tyr. At these points in time, rats were anaesthetized as described below and intraveneously injected with 93 kBq (2.5 μCi) ^{14}C-tyr (specific activity 2 MBq/μmol, Amersham International, Buckinghamshire, UK). Forty-five minutes after this injection, the rats were killed by a heart puncture, and the tumors were rapidly dissected. Seven samples (50-100 mg) were obtained from the dissected tumors, except from the tumors investigated 12 days after 10 Gy single-dose radiotherapy. In the latter case the volumes were larger than 10 ml, and growth necrosis amounted to 10% of the total tumor weight. From this necrotic tissue four samples were taken as well. Each of the five tumor samples and the two necrosis samples were dissolved in 1.5 ml Protosol© (Dupont, Boston, Mass, USA) and after addition of 10 ml Plasmasol© scintillation liquid (Packard Instruments, Downers Grove, Ill, USA), the ^{14}C-radioactivity of the samples was measured by liquid scintillation counting. The uptake of ^{14}C-tyr into the tissue was calculated as Differential Absorption Ratio (DAR), i.e. (activity sample/activity injected) x (weight rat/weight sample). The remaining two tumor samples and the two necrotic

samples were used to determine the incorporation of ^{14}C–tyr into tumor proteins. These samples were homogenized and the ^{14}C–labelled proteins were precipitated with trichloro acetic acid. The acid insoluble fraction was expressed as a percentage of the total ^{14}C–activity of the tumor. Tumor tissues of eight untreated animals served control.

PET experiments

Animals were intraperitoneally anaesthetized with 3–4 mg sodium pentobarbital (3 g/ 100 ml saline) per 100 g body weight, and received a catheter temporarily inserted into a tail vein to facilitate complete injections of tracer. In order to sustain anaesthesia, rats were given an additional dose of 1 mg per 2 hours. Anaesthesia had a lowering effect on body temperature. To maintain body temperature within the physiological range, animals were irradiated with infra red lamps.

PET data were acquired with a stationary double–headed positron camera (23). The method to obtain quantitative data in tumor–bearing animals has been described previously (24,25). The time schedule for the consecutive PET measurements is given in figure 1. After positioning the untreated rat into the PET camera, an iv dose of 1.1 MBq (30 μCi) ^{11}C–tyr in a volume of 0.2 ml was administered as a fast bolus, and PET data were acquired for 45 minutes. After each injection the catheter was flushed with 0.05 ml saline. Three hours after the ^{11}C–tyr study, in the same tumor–bearing rat, a second PET study was performed with 1.1 MBq (30 μCi) ^{18}FDG during 45 minutes. After regaining consciousness, the rat was allowed to recuperate for 1 day and was then subjected to radiotherapeutic and hyperthermic treatment. Eight hours after

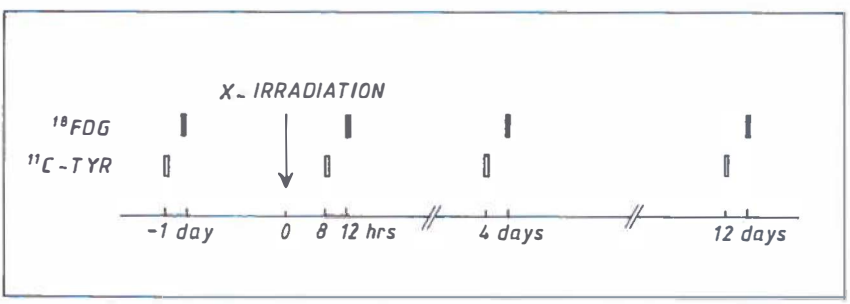

Figure 1. *Time schedule of the experimental procedure for PET measurements. ^{11}C–tyr (▯) and ^{18}FDG (▮) data were acquired during 45 minutes.*

these treatments, the tumor-bearing rat was monitored with ^{11}C-tyr as described above. Twelve hours after treatment, when ^{11}C-activity was reduced to a negligible background level, the animal was also investigated with ^{18}FDG. Identical PET studies with ^{18}FDG and ^{11}C-tyr were carried out 4 days and 12 days after treatment. At the end of experimentation, each individual animal had undergone a total of 8 scans, 4 with ^{11}C-tyr and 4 with ^{18}FDG. The radioactivity uptake into the tumor at 45 minutes after injection was calculated as a Differential Absorption Ratio, i.e. DARPET: (counts tumor/volume tumor) x (weight animal/counts animal).

Growth curves and growth delays

The three principal diameters of the tumors were measured in mm by the use of vernier calipers while the animal was under ether anaesthesia. From these measured diameters, the volumes of the ellipsoid-shaped tumors were calculated using the formula: $V = \frac{1}{6}\pi$ x length x width x thickness (26). These data were plotted as growth curves and the tumor doubling times (TD) were calculated. TD is the time needed for a tumor to double its treatment volume. The treatment effect on the tumor volume can be expressed as growth delay (GD). GD is calculated with the formula: $GD = (TD_{tr} - TD_c)/TD_c$, in which TD_{tr} is the doubling time for the treated tumors, and TD_c is the doubling time obtained in a control group of untreated animals. Statistical significance was analyzed with Fisher's distribution free sign test (27).

RESULTS

PET experiments

PET images, as presented in figure 2, show the distributions of ^{11}C-tyr and ^{18}FDG in a Wag/Rij rat with a rhabdomyosarcoma. In panel A and B, the uptake of ^{11}C-tyr and ^{18}FDG into untreated tumors is shown for 45 minutes after injection. The tumors are indicated with a horizontal line. In panel C and D, distributions of ^{11}C-tyr and ^{18}FDG at 12 days after 50 Gy irradiation are shown. From these images it can be observed that the tumor volume as well as the amount of radioactivity per unit of volume is decreased after treatment.

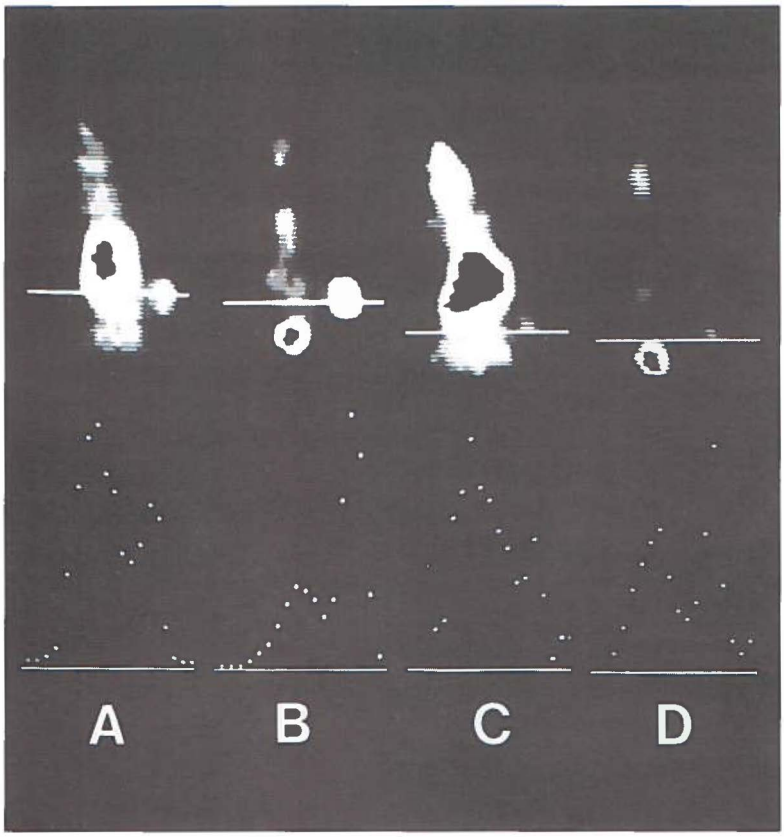

Figure 2. *Distribution of $^{11}C-tyr$ (A) and ^{18}FDG (B) as measured by PET at 45 minutes after iv injection into the same untreated RMS-bearing rat. Corresponding distribution of $^{11}C-tyr$ (C) and ^{18}FDG (D) acquired 12 days after 50 Gy irradiation. Tumors are indicated by horizontal lines. Black areas in the images are caused by windowing in order to obtain clearer visualization of the tumor.*

The uptake values of ^{11}C-tyr and ^{18}FDG into rhabdomyosarcoma tissue were calculated as DARPET. The data are summarized in table 1. The average DARPET values for ^{11}C-tyr and ^{18}FDG of 28 untreated tumors were 1.59 and 3.49, respectively. From these values, an ^{18}FDG/^{11}C-tyr uptake ratio of about 2 was

Table 1. *PET measurements on uptake of $^{11}C-tyr$ and ^{18}FDG into tumor tissue of rhabdomyosarcoma-bearing Wag/Rij rats before and after radiotherapy only and radiotherapy combined with hyperthermia.*

Treatment	Tracer	Before	Time after treatment 8/12 hours	4 days	12 days	number
10 Gy	$^{11}C-tyr$	1.63±0.17 (100±0)	1.78±0.16 (107±5)	1.64±0.18 (99±8)	1.61±0.12 (100±4)	n=8
	^{18}FDG	3.43±0.21 (100±0)	3.76±0.27 (110±7)	3.53±0.39 (103±13)	3.73±0.30 (110±10)	
30 Gy	$^{11}C-tyr$	1.70±0.13 (100±0)	1.52±0.12 (92±9)	1.28±0.13* (79±5)	1.89±0.25 (113±14) †	n=8
	^{18}FDG	3.74±0.27 (100±0)	3.73±0.23 (103±7)	2.57±0.27* (64±10)	3.51±0.49† (96±10)†	
50 Gy	$^{11}C-tyr$	1.60±0.06 (100±0)	1.57±0.11 (98±4)	1.36±0.15* (83±8)	0.94±0.08* (58±3)	n=7
	^{18}FDG	3.84±0.29 (100±0)	3.64±0.26 (102±10)	2.84±0.32* (79±12)	2.08±0.27* (55±8)	
30 Gy + HT§	$^{11}C-tyr$	1.35±0.07 (100±0)	1.34±0.13 (100±11)	1.48±0.17 (113±17)	1.41±0.15 (107±13)	n=5
	^{18}FDG	2.72±0.17 (100±0)	2.62±0.50 (103±25)	2.82±0.32 (111±23)	3.02±0.43 (120±31)	

Uptake values expressed as DARPET, percentual amounts between brackets.
Values are mean ± SEM.
* P-values of 0.05 or less with paired Student's t-test for differences with the untreated situation.
† 8 hours for $^{11}C-tyr$, 12 hours for ^{18}FDG. ‡ For this value n=7.
§ HT is hyperthermia for 15 minutes at 45 °C.

calculated. This ratio was observed at all points of time after the treatments. Consequently, the relative changes in uptake for both tracers are about the same, and therefore only results of $^{11}C-tyr$ are described.

It can be observed that the relative uptake of $^{11}C-tyr$ into the 10 Gy exposed tumors was not changed after treatment. Four days after the 30 and 50 Gy treatments, reductions of about 20 % were measured. After 12 days, the tumors treated with 30 Gy showed complete restoration of $^{11}C-tyr$ uptake to the level of the untreated situation, whereas the 50 Gy irradiated tumors showed further decline in $^{11}C-tyr$ uptake.

The combined treatment of 30 Gy X-radiation with hyperthermia did not have any significant effect on the relative $^{11}C-tyr$ uptake. Four days after treatment, a statistically significant difference in tracer uptake was observed between the tumors treated with 30 Gy only and the tumors treated with 30 Gy in combination with hyperthermia.

L-[1-^{14}C]tyrosine studies

Wag/Rij rats with untreated tumors and with tumors exposed to 10, 30 or 50 Gy were injected with ^{14}C-tyr. For reasons of comparison, the ^{14}C-tyr assays were carried out at the same points of time as in the PET studies using ^{11}C-tyr, namely 8 hours, 4 and 12 days after irradiation. Uptake of ^{14}C-tyr and incorporation of ^{14}C-radioactivity into proteins were measured in dissected tumor tissue obtained 45 minutes after injection. Total uptake was calculated as DAR. The incorporation into proteins was calculated as percentage of the amount of accumulated ^{14}C-activity (table 2). All tissue samples were homogeneous and appeared to be representative for the total

Table 2. *Uptake of ^{14}C-tyr into tumor tissue and its incorporation into tumor proteins of rhabdomyosarcoma-bearing rats after radiotherapeutic treatments at different points of time. Data were measured 45 minutes after iv injection of tracer.*

Treatment	Time after radiotherapy			
	0 hours (n=8)	8 hours (n=5)	4 days (n=6)	12 days (n=5)
Untreated	1.86±0.18†	–	–	–
	(78±6)	–	–	–
10 Gy	–	2.11±0.37	1.47±0.31	V. 1.76±0.12*
	–	(80±6)	(73±3)	(87±4)
				N. 0.85±0.40*
				(82±3)
30 Gy	–	1.68±0.14	1.24±0.29	2.01±0.34
	–	(80±4)	(73±8)	(82±3)
50 Gy	–	1.68±0.21	1.07±0.3	1.22±0.10
	–	(77±4)	(68±8)	(78±5)

† Uptake of ^{14}C-tyr is expressed as DAR and incorporation of accumulated ^{14}C-tyr activity as percentage (between brackets). Values are mean ± SD.
* V is vital tissue, N is tissue with growth necrosis.

tumor, except at 12 days after 10 Gy, when a clear distinction could be made between areas with necrotic and vital tissue. In the last column, separate data are presented for necrotic and vital tissue. In general, the ^{14}C-uptake data obtained after dissection of the tumor tally with the ^{11}C-tyr uptake data as measured by PET (see table 1). The amount of ^{14}C-tyr in the tissue with

growth necrosis (N; last column in table 2), measured at 12 days after 10 Gy irradiation, was about half the value of the untreated tumors. It is also notable that the pieces of necrotic tissue have much lower amounts of ^{14}C–tyr than the vital parts (V) of the tumors. Since the volume of necrotic tissue is about 10% of the total, it is estimated that the total ^{14}C–tyr uptake is about 1.7. Therefore, the small amount of necrotic tissue has no significant effect on the total ^{14}C–tyr uptake or the total ^{11}C–tyr uptake.

At 4 days after irradiation with 10, 30 or 50 Gy, dose dependent reductions of ^{14}C–tyr uptake of 21% ($P<0.05$), 33% ($P<0.01$) and 43% ($P<0.001$) respectively, were observed. Twelve days after treatment the uptake of ^{14}C–tyr into tumors exposed to 10 and 30 Gy was restored to the value of the control group, while in the 50 Gy irradiated tumors, uptake was still significantly reduced with 35%.

The percentage of ^{14}C–tyr incorporated into proteins is considered to be a reflection of the protein synthesis in the tumor tissue. The incorporation values measured at different points of time after the respective irradiations (68%–87%) did not differ much from the values measured in the untreated situation (78%).

Growth curves and growth delays

The effects of irradiation on tumor growth were evaluated by measuring tumor volumes in time course. To compare the effects of the respective irradiation doses on tumor growth, tumor volumes measured after treatment were normalized to the volumes at the time of treatment (100%). The data on relative tumor volumes were plotted to obtain the growth curves as shown in figure 3. This figure shows that for a duration of 7 days after 10 Gy, tumor growth had stopped. During this period, the tumors that were exposed to 30 and 50 Gy showed decreasing volumes. After 12 days, the 10 Gy as well as the 30 Gy irradiated tumors were in progressive growth, in contrast to the 50 Gy tumors. Recurrence of growth of the latter tumors started at about 2 weeks after treatment. The tumors exposed to doses of 10, 30 and 50 Gy had doubled their volumes present at the time of treatment (100%) after 18, 24 and 30 days, respectively. Since growth delays caused by the different treatments are dependent on the change in doubling time, growth delays of 1.98, 3.54 and 4.47 were calculated for the tumors treated with 10, 30 and 50 Gy, respectively (see table 3).

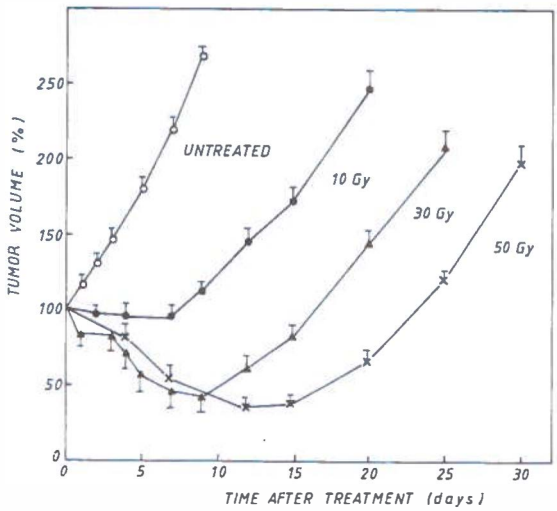

Figure 3. *Growth curves of rhabdomyosarcoma tumors exposed to doses of* 10 *Gy*(●, $n=8$), 30 *Gy* (▲, $n=6$) *and* 50 *Gy* (x, $n=6$) *and untreated tumors* (○, $n=9$). *The measured volumes* (*mean* ± *sem*) *are normalized to the value at the time of treatment* (100%).

It is of interest to examine the combined effect of X-irradiation and hyperthermia on tumor growth. In figure 4, growth curves are given for untreated tumors, tumors treated with hyperthermia during 15 min at 45 °C, tumors treated with a dose of 30 Gy of ionizing radiation, and tumors treated with the combination. Hyperthermia alone had only a small effect on tumor

Table 3. *Effect of radiotherapeutic and hyperthermic treatments on tumor growth of the rhabdomyosarcoma.*

Treatment	Growth Delay (GD)	P-value	Number
10 Gy	1.98±0.09	P<0.004	n=8
30 Gy	3.54±0.32	P<0.016	n=6
50 Gy	4.47±0.38	P<0.016	n=6
15 min at 45 °C	0.17±0.04*	P<0.11	n=6
30 Gy + 15 min at 45 °C	6.75±0.04	P<0.07	n=4

Values are mean ± SEM.
P-values obtained with Fisher's distribution free sign test (27).
* Data from reference (10).

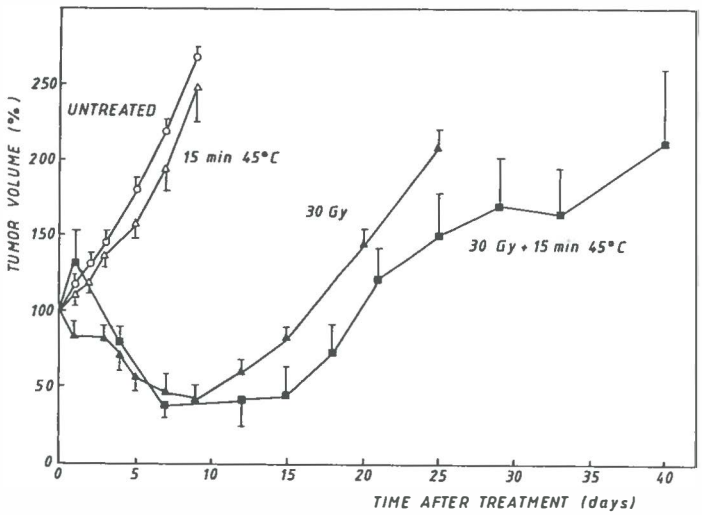

Figure 4. *Growth curves of untreated rhabdomyosarcoma tumors* (○, $n=9$), *tumors exposed to* 30 *Gy* (▲, $n=6$), *tumors treated with hyperthermia for* 15 *minutes at* 45 °C (▲, $n=6$), *and tumors treated with the combination* (■, $n=4$). *The measured volumes* (*mean* ± *sem*) *are normalized to the volume at the moment of treatment.*

growth as indicated by a GD of 0.17 (see table 3). Hyperthermia in combination with 30 Gy however, resulted in significantly more inhibition of tumor growth than caused by 30 Gy alone. The radiosensitizing effect of hyperthermia can be quantified by using growth delay data. The GD of the combination of radiotherapy and hyperthermia, 6.75 as shown in table 3, appeared to be larger than the summation of the GD's of the individual treatments (0.17 and 3.54). Consequently, a thermal enhancement ratio (6.75/3.71) of 1.8 may be calculated, quantifying the sensitizing effect of hyperthermia on the radiation treatment. A temporary increase in tumor volume, caused by edema, of about 30 percent was measured only on the first day after the combined treatment.

DISCUSSION

Tumors of rhabdomyosarcoma-bearing Wag/Rij rats were subjected to different doses of X-rays or to a combined treatment of radiation and

hyperthermia. Using PET, acute and indirect treatment effects were evaluated with ^{11}C–tyr and ^{18}FDG as metabolic tracers. For comparative reasons, radiation damage was also assessed with ^{14}C–tyr which is a probe to monitor amino acid uptake and incorporation into tumor proteins (28). The radio–biological effects on tumor growth were correlated with the metabolic data.

The ^{11}C–tyr data as measured by PET are in line with the effects on the ^{14}C–tyr uptake obtained in the corresponding dissection experiments. At 4 days after irradiation with 10 Gy, only a difference was observed between the ^{14}C–tyr data and the ^{11}C–tyr data. It is concluded that the ^{11}C–tyr data obtained by PET are a good reflection of tyrosine uptake and incorporation into proteins.

From in vitro studies it is generally understood that immediate acute effects on glycolysis and protein synthesis are not to be expected from radiation doses in a therapeutic range up to 60 Gy (3,4). The absence of significant changes in ^{14}C–tyr, ^{11}C–tyr and ^{18}FDG uptake into rhabdomyosarcoma tumors measured directly after irradiation are in affirmation with these conclusions.

In contrast to our observations, Kubota *et al.* (17) reported a rapid decreased uptake of L–[methyl–^{11}C]methionine into AH109A tumors already at 6 hours after 20 Gy ^{60}Co–irradiation. This discrepancy with our results may be explained by the difference in growth rate of the tumors. The AH109A tumor has a doubling time of 2 days, which is about half of the doubling time of the rhabdomyosarcoma tumor. Furthermore, in our study, the uptake of ^{11}C–tyr reflects protein synthesis. This was proved by the high incorporation percentages of ^{14}C–tyr into tumor proteins, as reported in this study. Kubota *et al.* (17) investigated only the uptake of L–[methyl–^{11}C]methione, and since this amino acid is involved in transmethylation it is unclear whether the rapid radiation–induced reduction of L–[methyl–^{11}C]methionine uptake reflects reduction of protein synthesis, transmethylation or amino acid transport.

After radiotherapy, unlike hyperthermia (10), only indirect metabolic effects on the tumor could be registered. Changes in uptake of tracer into the tumor tissue, observed days after the irradiation, can be correlated with changes in tumor volume. The decline in the ^{11}C–tyr, ^{18}FDG and ^{14}C–tyr uptake, observed as indirect effects after the 30 and 50 Gy irradiations were accompanied with declining tumor volumes. Furthermore, in the 30 Gy experiments, restoration of tracer uptake to the value of the untreated situation, occurring between 4 and 12 days after treatment, was paralleled by

a reverse in kinetics of tumor growth: from declining tumor volumes to progressive growth. In a rhabdomyosarcoma rat model, closely related to our animal system, Jung *et al.* (29) observed that X-irradiation-induced decline in tumor volume was accompanied by a depopulation of the tumor cells per unit of volume, while after treatment recurrence of tumor growth was associated with repopulation. It is concluded that ^{11}C-tyr and ^{18}FDG are suitable indicators for depopulation and repopulation processes in tumors during and after radiotherapeutic treatment.

The fraction of ^{14}C-tyr incorporated into tumor proteins is not markedly affected after X-irradiation. This indicates that, although the tumor is depopulating or repopulating, the cellular protein synthesis is about constant. Notably, an unchanged fraction of ^{14}C-tyr incorporated into proteins was also found in necrotic parts of tumors 12 days after exposure to 10 Gy.

The extent of tumor growth delay is an indication for the effectivity of the treatment. In our investigation, the calculated GD correlated almost linearly with the dose of the irradiation.

Hyperthermia given as an adjuvant treatment to irradiation usually increases the effectivity of the irradiation (23). From the growth curves in figure 4 it can be deduced that hyperthermia sensitizes the tumor tissue for radiation damage. This finding corresponds closely with the results of the study of Zywietz *et al.* (30) who found a thermal enhancement ratio of 1.7 in the rhabdomyosarcoma tumor after a combined treatment of 30 Gy X-irradiation and hyperthermia at 43 °C for 60 minutes.

When comparing the growth data of the combined treatment with the corresponding ^{11}C-tyr and ^{18}FDG uptake data, correlations, as observed in the single-dose irradiation experiments, were not found. During a period of three days after the combined treatment, a pronounced edema of the tumor tissue was observed, giving rise to invasion of host cells such as macrofages. Since these cells have high metabolic activities, they largely contribute to the uptake values of ^{11}C-tyr and ^{18}FDG of the treated tumor tissue.

In conclusion, immediate radiation-induced effects on protein synthesis and glycolysis of tumor were absent. Indirect radiation effects on ^{11}C-tyr and ^{18}FDG uptake into tumor tissue correlated with radiation effects on tumor volume. Therefore, PET is apposite for investigations on tumor growth kinetics during and after a radiotherapeutic treatment, indicating tumor regression or recurrence of tumor growth. Since radiation-induced changes in ^{11}C-tyr uptake into rhabdomyosarcoma tissue are proportionate to changes in ^{18}FDG uptake,

both tracers have an equivalent potential for assessing radiation damage to tumors by PET. In this study, radiotherapy in combination with hyperthermia did not affect tissue utilization of ^{11}C-tyr and ^{18}FDG. Therefore, PET data obtained during such combined treatments have to be interpreted with caution.

ACKNOWLEDGEMENTS

This research was supported by a grant from the Dutch Cancer Society. The authors gratefully acknowledge the cooperation with the staff of the Kernfysisch Versneller Instituut (Prof Dr R.H. Siemssen) and the skilled help from the operating team of the cyclotron.

REFERENCES

(1) Maass H, Künkel HA. Biochemische Veränderungen in Tumorzellen nach Einwirkung von Röntgenstrahlen, Jodessigsäure, Wasserstoffperoxyd und Äthyleniminobezochinonen. *Int J Rad Biol* 1960; 2:269–279.

(2) Gerbaulet K, Maurer W, Brückner J. Autoradiographische Untersuchung über die Inkorporation von [^{3}H]Aminosäuren im Zellkernen während der G1–Phase und der S–Phase bei normalen und röntgen–bestrahlten Mäusen. *Biochim Biophys Acta* 1963; 68:462–471.

(3) Streffer C. Strahlen–Biochemie. Springer Verlag, Berlin, Heidelberg, New York, 1969, pp 22–105.

(4) Altman KI, Gerber GB, Okada S. Radiation Biochemistry Vol I and II. Academic Press, New York, London, 1970.

(5) Dose K, Dose U. Mechanisms of glycolysis by X–rays in ascites tumour cells. I. Alterations in steady–state concentrations of some intermediate nucleotides and in electrolyte equilibrium under various conditions of incubation. *Int J Rad Biol* 1960; 4:85–94.

(6) Cammarano P. Protein synthesis, glycolysis, and oxygen uptake in hepatoma cells irradiated in vitro. *Rad Res* 1963; 18:1–11.

(7) Archer E. Inactivation of amino acid transport systems in Ehrlich ascites carcinoma cells by Cobalt–60 gamma radiation. *Rad Res* 1968: 35:109–122.

(8) Mc Cormick W, Penman S. Regulation of protein synthesis in HeLa cells: translation at elevated temperatures. *J Mol Biol* 1969; 39:315–333.

(9) Mondovi B, Finazzi Agro' A, Rotilio G, Strom R, Moricca G, Rossi Fanelli A. The biochemical mechanism of selective heat sensitivity of cancer cells II. Studies with nucleic acids and protein synthesis. *Europ J Cancer* 1969; 5:137–146.

(10) Daemen BJG, Paans AMJ, Elsinga PH, Wieringa RA, Konings AWT, Vaalburg W. Hyperthermia–induced suppression of protein synthesis in tumors measured by PET. In:Schmidt HAE, Buraggi GL eds. *Nuclear Medicine, Trends and Possibilities in Nuclear Medicine.* Stuttgart, New York; Schattauer 1989: pp 77–80.

(11) Phelps ME, Huang SC, Hoffman EJ, Selin C, Sokoloff L, Kuhl D. Tomographic measurement of local cerebral glucose metabolic rate in humans with (F–18)2–fluoro–2–deoxy–D–glucose: validation of method. *Ann Neurol* 1979; 6:371–388.

(12) Patronas NJ, Di Chiro G, Brooks R *et al.* Work in Progress: [18F]fluorodeoxyglucose and positron emission tomography in the evaluation of radiation necrosis of the brain. *Radiology* 1982; 144:885–889.

(13) Doyle WK, Budinger TF, Valk PE, Levin VA, Gutin PH. Differentiation of cerebral radiation necrosis from tumor recurrence by [18F]FDG and 82Rb positron emission tomography. *J Comp Assist Tom* 1987; 11:563–570.

(14) Di Chiro G, Oldfield E, Wright DC *et al.* Cerebral necrosis after radiotherapy and/or intraarterial chemotherapy for brain tumors: PET and neuropathologic studies. *Am J Radiol* 1988; 150:189–197.

(15) Minn H, Paul R, Ahonen. Evaluation of treatment response to radiotherapy in head and neck cancer with fluorine–18 fluorodeoxyglucose. *J Nucl Med* 1988; 29:1521–1525.

(16) Knapp WH, Helus F, Layer K, Panzer M, Höver K–H, Ostertag H. N–13 glutamate uptake and perfusion in Walker 256 carcinosarcoma before and after single dose irradiation. *J Nucl Med* 1986; 27:1604–1610.

(17) Kubota K, Matsuzawa T, Takahashi T, *et al.* Rapid sensitive response of Carbon–11–L–methionine tumor uptake to irradiation. *J Nucl Med* 1989; 30:2012–2016.

(18) Konings AWT. Effects of heat and radiation on mammalian cells. *Radiat Phys Chem* 1987; 30:339–349.

(19) Overgaard J. The current and potential role of hyperthermia in radiotherapy. *Int J Rad Onc Biol Phys* 1989; 16:535–549.

(20) Bolster JM, Vaalburg W, Paans AMJ, *et al.* Carbon–11 labelled tyrosine to study tumor metabolism by positron emission tomography (PET). *Eur J Nucl Med* 1986: 12:321–324.

(21) Hamacher K, Coenen HH, Stocklin G. Efficient stereospecific synthesis of no–carrier added 2–[18F]–fluoro–2–deoxy–D–glucose using aminopolyether supported nucleophilic substitution *J Nucl Med* 1986; 27:235–238.

(22) Barendsen GW, Broerse JJ. Experimental radiotherapy of a rat rhabdomyosarcoma with 15 MeV neutrons and 300 KeV X–rays. I Effects of single exposures. *Europ J Cancer* 1969; 5:373–391.

(23) Paans AMJ, De Graaf EJ, Welleweerd J, Vaalburg W, Woldring MG. Performance parameters of a longitudinal tomographic positron imaging system. *Nucl Instr Meth* 1982; 192:491–500.

(24) Daemen BJG, Elsinga PH, Paans AMJ, Lemstra W, Konings AWT, Vaalburg W. Suitability of rodent tumor models for experimental PET with L–[1–11C]tyrosine and 2–[18F]–fluoro–2–deoxy–D–glucose. *J Nucl Med Biol* 1991 (in press).

(25) Daemen BJG, Elsinga PH, Ishiwata K, Paans AMJ, Vaalburg W. A comparative PET study using different 11C–labelled amino acids in Walker 256 carcinosarcoma–bearing rats. *J Nucl Med Biol* 1991; 18:197–204.

(26) Steel GG. Growth rate of tumours. In: Steel GG, ed. *growth kinetics of tumours*. Oxford: Clarendon; 1977:5–55.

(27) Hollander M, Wolf DA. Nonparametric statistical methods. New York, London, Sydney, Toronto: John Wiley & Sons; 1973:39–41.

(28) Ishiwata K, Vaalburg W, Elsinga PH, Paans AMJ, Woldring MG. Metabolic studies with L–[1–14C]tyrosine for the investigation of a kinetic model to measure protein synthesis rates with PET. *J Nucl Med* 1988; 29:524–529.

(29) Jung H, Beck HP, Brammer I, Zywietz F. Depopulation and repopulation of the R1H rhabdomyosarcoma of the rat after X–irradiation. *Eur J Cancer* 1981; 17:375–386.

(30) Zywietz F. Effect of microwave heating on the radiation response of the rhabdomyosarcoma. *Strahlentherapie* 1982; 158:255–257.

CHAPTER 6

PET STUDIES WITH L-[1-^{11}C]TYROSINE, L-[METHYL-^{11}C]METHIONINE AND ^{18}FDG IN PROLACTINOMAS IN RELATION TO BROMOCRYPTINE TREATMENT.

Bernard J.G. Daemen, Rolf Zwertbroek , Philip H. Elsinga, Anne M.J.Paans, Hieronymus Doorenbos and Willem Vaalburg.

[Submitted for publication]

ABSTRACT

Aspects of metabolism in prolactinomas were investigated by positron emission tomography using L–[1–^{11}C]tyrosine, L–[methyl–^{11}C]methionine and ^{18}FDG . Using L–[1–^{11}C]tyrosine, 4 patients were monitored prior to and 18 hours after an intramuscular injection of 50 mg bromocryptine. At 18 hours after bromocryptine intervention, L–[1–^{11}C]tyrosine uptake into tumor was lowered with 28% ($P<0.07$). A correlation analysis of the bromocryptine–induced decrease in L–[1–^{11}C]tyrosine uptake and the reduction of the serum prolactin levels indicated that the actions of bromocryptine on prolactin synthesis and on prolactin release are not coupled. In the untreated situation, the 4 patients were investigated with ^{18}FDG as well, but the prolactinomas could not be visualized. Three untreated patients were studied with L–[methyl–^{11}C]methionine. The tumor–imaging potential of L–[methyl–^{11}C]methionine and L–[1–^{11}C]tyrosine appeared to be nearly equivalent for prolactinomas. Unlike prolactinoma tissue, the salivary glands showed a pronounced preference for L–[1–^{11}C]tyrosine as compared to L–[methyl–^{11}C]methionine. L–[1–^{11}C]tyrosine is a valuable tool to obtain information on the metabolism and treatment of prolactinomas.

INTRODUCTION

Positron emission tomography (PET) using ^{11}C–labelled amino acids has prominent clinical applications in the field of oncology. PET measurements of the uptake of these radiopharmaceuticals into tumors have predictive value for the grade of malignancy (Schober *et al.* 1987; Derlon *et al.* 1989) and therefore implications for the choice of tumor therapy. After tumor treatment, ^{11}C–labelled amino acids also are suitable metabolic probes to assess the beneficial effects of surgery (Lilja *et al.* 1989) and radiotherapy (Derlon *et al.* 1989). The majority of the PET studies to establish these applications have been performed with L–[methyl–^{11}C]methionine (^{11}C–me–met), predominantly in gliomas and astrocytomas.

Ten to twenty percent of all intracranial lesions are prolactin–secreting pituitary tumors (Dollar and Blackwell 1986). These slowly growing prolactinomas cause high serum prolactin levels which inhibit the production of the sex hormones. Therefore secondary effects arise such as impaired sexual function and decreased libido. In particular, ammenorrhea and galactorrhea are encountered in the female prolactinoma patient. Prolactinomas are sensitive to treatment with dopamine agonists. In the last years, this form of treatment for prolactinomas has become first line treatment as compared to former conventional therapies such as surgery and radiotherapy (Grossman and Besser 1985).

In comparison to PET studies with malignant gliomas and astrocytomas, disproportionately few PET studies have been performed with prolactinomas. Bergström et al (1987a) reported a 4–patient study describing the bromocryptine induced reduction of ^{11}C–me–met uptake into these tumors. This effect could be attributed to binding of bromocryptine to D_2–receptors. In an earlier study, these D_2–receptors were already demonstrated with PET using ^{11}C–methylspiperone in 2 untreated patients with pituitary tumors (Muhr *et al.* 1986).

Besides protein synthesis, methyl–labelled methionine is involved in other metabolic pathways such as transmethylation, which might lead to accumulation of a variety of non–protein metabolites in tumor tissue (Daemen *et al.* 1990). Therefore carboxylic–labelled amino acids, such as L–[1–^{11}C]tyrosine (^{11}C–tyr) (Ishiwata *et al.* 1988) and L–[1–^{11}C]leucine (Keen *et al.* 1989) appear to be more appropriate compounds to determine protein synthesizing activity of tumor tissues. The main metabolite of these amino

acids is $^{11}CO_2$, which is cleared from tissue to plasma and rapidly expired from lung into air. Therefore, $^{11}CO_2$ does not contribute substantially to the ^{11}C–radioactivity in the tumor tissue, as measured by PET. In animal studies, ^{11}C–tyr has proven to be a sensitive probe for the follow–up of the effects of hyperthermia and radiotherapy on tumors (Daemen *et al.* 1989a,b). Therefore, ^{11}C–tyr was chosen for this study in order to monitor the effect of bromocryptine intervention on patients with prolactinomas.

To compare ^{11}C–amino acid uptake with carbohydrate metabolism, 2–[^{18}F]–fluoro–2–deoxy–D–glucose (^{18}FDG) was also selected for this study. This compound is widely used in PET as a suitable indicator of glycolytic activity of tumors. The determination of the grade of malignancy of intracranial tumors (Di Chiro 1986) and the early discrimination between radiation necrosis and recurrence of tumor after radiotherapy (Patronas *et al.* 1983) appear to be the major clinical applications of PET using ^{18}FDG in oncology. Until now, ^{18}FDG has not been applied for the investigation of prolactinomas and for the possibility to validate prolactinoma treatment.

The aim of the present study is:

1. To compare the visualization of prolactinomas with ^{11}C–tyr, ^{11}C–me–met and ^{18}FDG by PET.
2. To assess the effect of a pharmacological intervention with bromocryptine on prolactinomas in terms of ^{11}C–tyr uptake as measured by PET in relation to alterations in serum prolactin levels.

MATERIALS AND METHODS

Materials

Radiochemically pure L–[1–^{11}C]tyrosine was synthetized with a specific activity >3.7 GBq/μmol (100 Ci/mmol) (Bolster *et al.* 1986). ^{18}FDG was synthetized, no carrier added, with a radiochemical purity >98% (Hamacher *et al.* 1986). L–[methyl–^{11}C]methionine was synthetized with a specific activity of >2 GBq/μmol (55 Ci/mmol) and a radiochemical purity of 97% (Comar *et al.* 1976). Serum prolactin was determined with an immunoradiometric assay (Prolactin Maiaclone™, Serono Diagnostics, Woking, UK). As bromocryptine preparation was used Parlodel©LA (Sandoz, Basel, Switzerland).

Table 1. *Data of investigated patients with prolactinomas.*

Patient sex/age	Clinical status	MRI findings	Hormonal status*
1/F/21	Secondary ammenorrhea, galactorrhea	Intrasellar tumor	Estradiol 0.1
2/F/31	Secondary ammenorrhea, headache	Extension to scull base, displacement of optic chiasm	Estradiol 0.0
3/M/49	Hypogonadism, decreased libido	Tumor invasive into sphenoid sinus, displacement of right carotid artery	Testosterone 5.09
4/M/21	Hypogonadism, arrested puberty, normocytic anemia	Displacement of optic chiasm and bottom of 3rd ventricle	Testosterone 2.18, substituted thyroid insufficiency
5/M/39	Visual field defects, paralysis of abducent nerve, headache	Giant tumor, invasive into 3rd ventricle, displacement of right carotid artery	Testosterone 7.62
6/M/57	Bitemporal visual field defects	Invasive tumor into sphenoid sinus, displacement of chiasm	Testosterone 1.43, substituted thyroid insufficiency
7/F/22	Secondary ammenorrhea, visual field defects	Suprasellar extensions	Estradiol 0.0, substituted thyroid insufficiency

* Normal values: Estradiol 0.1–0.2 nmol/l (female), Testosterone 18–45 nmol/l (male).

Patients

In seven patients, 3 female and 4 male, whose ages ranged from 21 to 57 years, the presence of a prolactinoma was confirmed by the elevated serum prolactin level and MRI. The MRI images were obtained with a Philips Gyroscan S15 (Philips, The Netherlands). The patients had tumors of different sizes, one tumor appeared to be a microprolactinoma (∘ <10 mm), while the other six were macroprolactinomas with suprasellar extensions. Prior to the PET studies, the patients had not been receiving tumor treatment in any form. Data of the patients are summarized in table 1.

PET camera

The positron camera used was a double–headed rotating uncollimated camera system (Paans *et al.* 1985). This imaging apparatus has a spatial resolution of 7.5 mm FWHM and a sensitivity for a point source of 2.7 cps/kBq. The data were acquired in 18 steps of 10 degrees. The actual data acquisition time for each rotational step was corrected for the physical half–life of the radionuclide used. This procedure results in a same effective data acquisition time for each rotational step.Therefore, data acquisition time for one static image with ^{11}C– and ^{18}F–activity amounted 32 and 25 minutes, respectively. The image was backprojected into a volume of 30 x 30 x 30 cm^3 which was divided into 16 slices with thicknesses of nearly 2 cm. The matrix size used was 64 x 64 pixels per slice. The final images were obtained after deconvolution of the back–projected images for the system response function.

Data acquisition and analysis

Via an antecubital vein, the untreated patient (patient 1–4) was given a dose of 37 MBq (1 mCi) ^{11}C–tyr as a rapid bolus. After 30 minutes, the patient was positioned into the PET camera, and data were acquired between 30 and 62 minutes after injection. An ^{11}C–tyr study was comprised of 2–3 x 10^5 counts. From a catheter, temporarily inserted into a contralateral dorsal hand vein, blood samples were obtained in order to monitor the level of ^{11}C–radioactivity in plasma. The measured radioactivity in the plasma samples was corrected for physical decay to the time of injection, whereupon level of plasma radioactivity was calculated as Differential Absorption Ratio:

$$DAR = \frac{\text{activity plasma sample}}{\text{total activity injected}} \; X \; \frac{\text{weight patient}}{\text{weight plasma sample}} .$$

After three hours, which is 9 times the half–life of ^{11}C, the patient was administered an iv injection of 18.5 MBq (0.5 mCi) ^{18}FDG. While the patient was in the same position as in the ^{11}C–tyr study, PET data were acquired between 20 and 45 minutes after injection. Sensory stimuli (noise, light) were constant during time of the PET studies. In the ^{18}FDG studies, 3–4 x 10^5 counts were registered.

Within a few days, the patient was intragluteally injected with 50 mg

bromocryptine mesylate in a sustained-release formulation. A second PET study with ^{11}C-tyr was repeated 18 hours after bromocryptine intervention.

In order to compare with the ^{11}C-tyr PET studies, three patients (patients 5-7) were investigated with ^{11}C-me-met. The patients were injected with 37 MBq (1 mCi) ^{11}C-me-met and data were acquired between 30 and 62 minutes post-injection.

The serum prolactin levels at the moments of the PET studies were determined with an radioimmunometric assay.

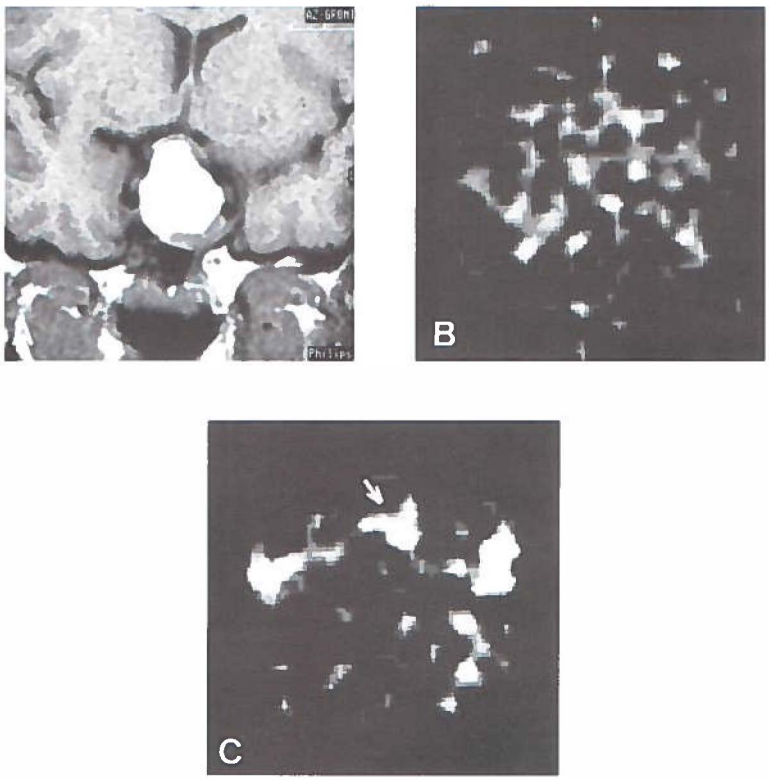

Figure 1. *(A) MRI study (patient 4) with clear visualization of the untreated prolactinoma in a coronal slice. (B) PET study with ^{18}FDG of the same untreated patient in a transaxial slice, no visualization of tumor was achievable. (C) Corresponding PET study using L-[1-^{11}C]tyrosine, position of the tumor is indicated with an arrow, the contralateral spots reflect uptake of ^{11}C-radioactivity into the parotid salivary glands.*

The localization of the prolactinoma on MRI was used to determine the position of the tumor on the PET images. Regions of interest (ROI) were graphically defined for tumor, cortex and cerebellum, and counts were then measured. ROI for cortex, which consisted mainly of white matter, was delineated in the slice 4 cm cranial to the pituitary tumor, while ROI for cerebellum was delineated 2 cm caudal to the pituitary tumor. The ROI's of the first ^{11}C–tyr study were also used for the radioactivity measurements of the second ^{11}C–tyr study. The uptakes of the ^{11}C–amino acids into the prolactinomas were expressed as tumor–to–non–tumor (T/NT) ratios.

RESULTS

Prolactinomas of four patients were consecutively investigated with MRI and PET using ^{11}C–tyr and ^{18}FDG respectively. MRI and PET studies with ^{11}C–me–met were performed in three other patients. Between these four imaging methods, discrepancies were observed. Prolactinomas could clearly be visualized with MRI, and PET using ^{11}C–tyr and ^{11}C–me–met. In figure 1, the prolactinoma of the untreated patient 4 is shown on MRI (A) and, as indicated

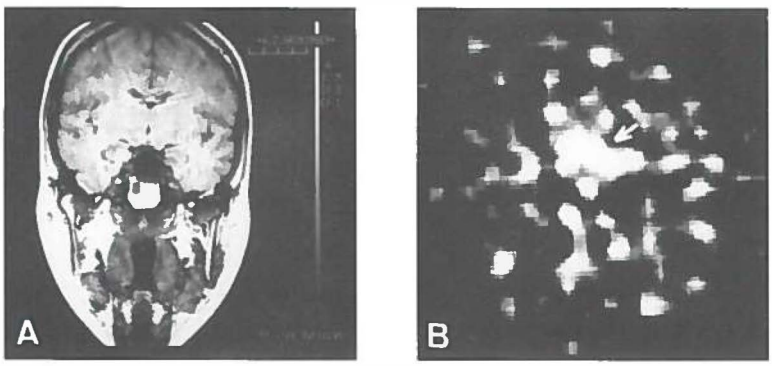

Figure 2. (*A*) *MRI study of prolactinoma (patient 7) in a coronal slice. The prolactinoma tissue shows a clear signal heterogeneity.* (*B*) *L–[methyl–^{11}C]methionine PET study in a transaxial slice, position of the* with the arrow, on the ^{11}C–tyr PET image (C). In each of the four ^{18}FDG *tumor is indicated with an arrow.*

studies, prolactinomas of the untreated patients could not be delineated. No localized hyper or hypometabolic regions could be discerned (see figure 1B). In order to visualize the ^{18}FDG and ^{11}C-tyr distribution different absolute scaling had to be used. This resulted in a visual overestimation of the amount of ^{18}FDG as presented in figure 1B with respect to the ^{11}C-tyr image (figure 1C). In figure 2, the visualization of prolactinoma (patient 7) is shown with MRI and with PET using ^{11}C-me-met.

The averaged plasma ^{11}C-radioactivity measured in the four ^{11}C-tyr PET studies in the untreated situation is given in figure 3. The concentration is given as DAR. This parameter corrects for the injected dose and weight of the patient. Within 15 minutes after iv injection, ^{11}C-tyr is distributed from plasma into tissue. During the time span of the PET study, between 30 and 60 minutes after injection, the plasma radioactivity level is observed to be constant.

The tumor-to-tissue uptake ratios of ^{11}C-tyr and ^{11}C-me-met ratios are presented in table 2. The mean tumor-to-cortex (T/Cor) ratio for ^{11}C-tyr and ^{11}C-me-met amounted 3.20 and 2.78, respectively. Mann-Whitney test revealed a P-value of 0.32 for the difference. The uptake of ^{11}C-tyr into the

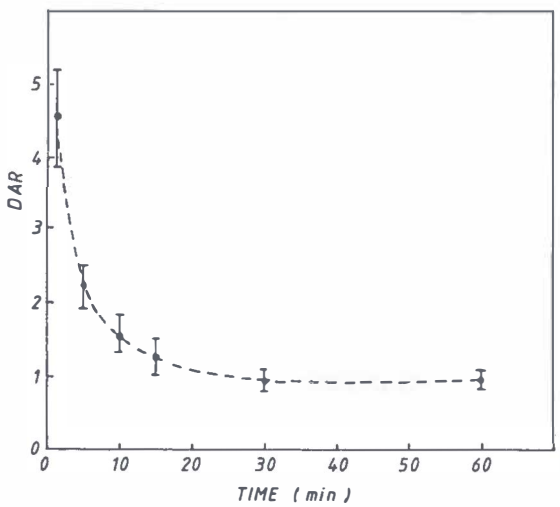

Figure 3. *Time activity curve of L-[1-^{11}C]tyrosine in plasma of four patients measured at* 1, 5, 10, 15, 30 *and* 60 *minutes after injection. Plasma activity was calculated as DAR and expressed as mean ± sem.*

Table 2. *Tissue uptake ratios of (A) L–[1–^{11}C]tyrosine measured prior to and 18 hours after bromocryptine administration (patient 1–4) and (B) L–[methyl–^{11}C]methionine (patient 5–7).*

	Untreated			18 h after bromocryptine		
Patient	T/Cor (%)	T/Cer (%)	Cor/Cer	T/Cor (%)	T/Cer (%)	Cor/Cer
A. L–[1–^{11}C]tyrosine						
1	2.73 (100)	3.41 (100)	1.25	2.02 (74)	2.02 (59)	1.00
2	2.00 (100)	1.76 (100)	0.88	1.65 (83)	1.49 (85)	0.90
3	4.05 (100)	2.58 (100)	0.64	3.07 (76)	2.37 (92)	0.77
4	4.00 (100)	2.62 (100)	0.65	2.18 (55)	1.31 (50)	0.60
mean	3.20	2.59	0.86	2.23	1.80	0.82
sem	0.50	0.34	0.15	0.30	0.25	0.09
B. L–[methyl–^{11}C]methionine						
5	3.81	3.58	0.94	-	-	-
6	2.23	2.04	0.91	-	-	-
7	2.27	1.95	0.86	-	-	-
mean	2.78	2.52	0.90			
sem	0.52	0.53	0.02			

Abbreviations: T = tumor, Cor = cortex, Cer = cerebellum.
Percentual amounts for T/Cor and T/Cer ratios between parentheses.

Table 3. *Bitemporal diameter on MRI in coronal slices and serumprolactin levels of 7 patients with untreated prolactinomas. In 4 patients, serum prolactin was also determined 18 hours after administration of bromocryptine.*

Patient	Ø MRI	Before	(%)	After 18 h	(%)
1	7	1256	(100%)	251	(20.0%)
2	22	18180	(100%)	1792	(9.9%)
3	30	51000	(100%)	5335	(10.5%)
4	24	15700	(100%)	4191	(26.7%)
5	55	422000	-	-	-
6	37	46600	-	-	-
7	26	39600	-	-	-

MRI diameters in mm, serum prolactin levels in mU/l.
Between parentheses prolactin level as a percentage.
Normal values: female 165 (range 50–520), male 110 (range 40–290).

prolactinoma, after bromocryptine administration, is also listed in this table. At 18 hours after bromocryptine injection, the T/Cor and tumor–to–cerebellum (T/Cer) ratios were decreased in each individual patient, with an average of 28% and 29% respectively for the whole group. A 4–paired–sample sign test indicates that bromocryptine is effective on the ^{11}C–tyr uptake ($P<0.07$). The tumor extent on the ^{11}C–tyr images was observed not to change 18 hours after intervention with bromocryptine. Based on the measured counts in the ROIs, the stastical errors in the T/NT ratios are estimated to be 6%. Consequently, the errors in the bromocryptine–induced differences as observed in ^{11}C–tyr studies are about 10%.

The serum prolactin levels for each patient are presented in table 3. In the untreated situation, the measured serum prolactin levels showed a large variation, with a range between 1.3 x 10^3 and 411 x 10^3 mU/l. A coarse correlation was observed between the volume of the tumor, as estimated with MRI, and the serum prolactin level. At 18 hours after administration of bromocryptine serum prolactin was rapidly reduced to an average residual level

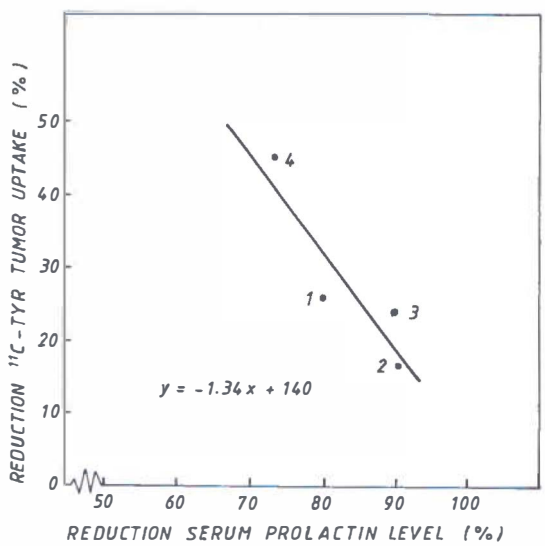

Figure 4. *Graphical comparison in four patients of the percentual reduction of the L–[1–^{11}C]tyrosine tumor uptake (Y–axis) and the percentual reduction of the serum prolactin level (X–axis) due to an intramuscular bromocryptine injection, and measured at* 18 *hours after administration. Numbers in the figure are the respective patients.*

of 16 ± 8% (±sd), as compared to the untreated situation.

In figure 4, a graphical comparison is shown between the percentual reduction of the ^{11}C–tyr T/Cor ratio and the percentual reduction of the serum prolactin level per individual patient. A correlation was observed between the decreases in ^{11}C–tyr T/Cor ratio expressed with the x against y line: $y = -1.34x + 140$. Error analysis reveals an error of 0.4 in the slope and of 37 in the intercept.

The parotid salivary glands were depicted in all ^{11}C–tyr studies (e.g. fig. 1), and in 3 of these studies, the submandibulary glands were observed as well. In contrast to ^{11}C–tyr, no notable uptake of ^{11}C–me–met into both kinds of salivary glands was observed. Bromocryptine had no effect on the uptake of ^{11}C–tyr into the salivary glands.

DISCUSSION

The uptake of ^{11}C–tyr, ^{11}C–me–met and ^{18}FDG into tumor tissue was investigated with PET in patients with prolactinomas. Furthermore, the effects of a pharmacological intervention with bromocryptine on the amino acid utilization of prolactinoma tissue were measured by the use of ^{11}C–tyr.

A rapid decrease of plasma radioactivity to a low constant level was observed in the four patients after administration of ^{11}C–tyr (see figure 3). A similar profile of the plasma radioactivity curve was observed by Bergström et al (1987b) for ^{11}C–me–met. The PET data were acquired in the period when ^{11}C–plasma activity was constant. Therefore, the T/NT ratio measured in this period is considered to be in a steady state.

When compared, nearly the same imaging–potentials for prolactinomas was found for ^{11}C–tyr and ^{11}C–me–met. Shome and Farlow (1977), who elucidated the entire linear amino acid sequence of human prolactin, found that of the 198 amino acids present, 4 were methionine and 7 were tyrosine. Sequential PET studies with both tracers in the same patient would provide a clearer answer to the question which amino acid is prefered by prolactinomas.

Using ^{18}FDG, prolactinomas could not be visualized because of the lack of contrast in uptake of this tracer between the prolactinoma tissue and the surrounding tissue (cortex, hypothalamus, bone). In patients with a variety of tumors, Minn *et al.* (1988) found a positive correlation between the fraction S–phase cells and the T/NT uptake ratio for ^{18}FDG. Prolactinomas are

slow–growing tumors with very low proliferation rates, which may explain the poor visualization with ^{18}FDG. Consequently, this compound is inappropriate for monitoring therapy of prolactinomas.

Within 18 hours after administration, bromocryptine gave a reduction in ^{11}C–tyr uptake into prolactinomas of about 30%. Bromocryptine exerts a two fold action on the amino acid utilization of prolactin–secreting cells. In cultured pituitary cells exposed to ergocryptine, Maurer (1980) found a rapid reduction of the cellular protein synthesis which could exclusively be ascribed to inhibition to prolactin synthesis. Decreased concentration of prolactin mRNA gave evidence to a dopamine–agonist mediated specific inhibition on gene transcription for prolactin (Maurer 1981). In rat pituitary adenoma cells, reduction of growth and total cellular protein synthesis were observed at higher bromocryptine concentrations than needed for inhibition of prolactin synthesis (Johansen *et al.* 1985). The action of bromocryptine was ascribed to a dose dependent general cytotoxic action on prolactin secreting adenoma cells.

In a 4–patient PET study, Bergström and co–workers (1987a) found a 41% reduction of ^{11}C–me–met uptake into prolactinomas at 2–4 hours after an intramuscular injection with the same amount bromocryptine, as used in this study. Even higher reductions of ^{11}C–me–met uptake up to 60% were reported from a 2–patient study (Bergström *et al.* 1988). Compared to our ^{11}C–tyr studies, these reductions in ^{11}C–me–met uptake were higher and measured at an earlier point of time. A possible explanation might be that bromocryptine also has an inhibitory effect on the transmethylation processes occurring in the prolactinoma tissue. This effect of bromocryptine was indicated by Bergström and co–workers (1987a) as well.

A positive correlation between the decrease of ^{11}C–tyr uptake into tumor and the decrease of prolactin secretion into serum was not found after injection of bromocryptine. Other investigators also show discrepancies between the effects of bromocryptine on protein synthesis and on prolactin release. In immunohistochemical studies in prolactinoma cells, Niwa *et al.* (1987) found that after bromocryptine administration, protein synthesis remained unchanged, while secretion of prolactin was disturbed, associated with a decreased amount of microtubules. Davies *et al.* (1990) found that secretion of prolactin was reduced by bromocryptine while this agent did not affect cytoplasmic levels of prolactin mRNA, suggesting relative autonomy of prolactin synthesis. From these and our studies it is suggested that

bromocryptine has independent mechanisms of action on the synthesis and on the release of prolactin.

The uptake of the different amino acids into prolactinoma tissue was compared with their corresponding uptake into salivary gland tissue. A pronounced preference of ^{11}C–tyr to ^{11}C–me–met was observed for the parotid as well as the submandibulary glands. Analysis of the free amino acid levels of human saliva showed that tyrosine is found in much higher concentrations as compared to methionine (Battistone and Burnett 1961). Furthermore, determinations of the amino acid composition of many proteins in saliva revealed that in general these macromolecules are tyrosine–rich, while for methionine only trace amounts are found (Arglebe 1981). The larger amounts of tyrosine in the secretory products of the salivary glands, as compared to methionine, demonstrate the differences of the biochemistry of the respective amino acids in these glands, which explains the specific high uptake of ^{11}C–tyr as observed by PET. From these results can be concluded that ^{11}C–tyr might be a suitable probe to investigate pathophysiological states of the salivary glands with PET.

In conclusion, ^{11}C–tyr and ^{11}C–me–met are superior to ^{18}FDG for the visualization of prolactinomas. The salivary glands could be visualized with ^{11}C–tyr, but not with ^{11}C–me–met. The utilization of a specific amino acid by tissues for synthesis into molecules which are secreted, such as prolactin and saliva proteins, can be investigated by PET, measuring the uptake of its ^{11}C–labelled counterpart. The bromocryptine–induced reductions in ^{11}C–tyr uptake into prolactinoma tissue did not tally with the decline in prolactin release into serum. Next to MRI and serum prolactin measurements providing information on anatomical structures and hormonal function respectively, PET using ^{11}C–labelled amino acids is a eligible tool to obtain complementary metabolic information on prolactinoma tissue in relation to bromocryptine treatment

ACKNOWLEDGEMENTS

This research was supported by a grant of the Dutch Cancer Society. The cooperation with staff (Prof Dr RH Siemsen) and the cyclotron operators of the Kerfysisch Versneller Instituut is gratefully acknowledged. The authors thank Mrs A. Aalders and Mr B. Barendsen for their assistance with the patients studies.

REFERENCES

Arglebe C (1981) Biochemistry of human saliva. In: Pfaltz CR, Chilla R (Eds) Advances in Oto–Rhino–Laryngology vol. 26, Sialadenosis and Sialadenitis, pathophysiological and diagnostic aspects, Karger, Basel, pp 97–234

Battistone GC, Burnett GW (1961) The free amino acid composition of human saliva. Arch oral Biol 3:161–170

Bergström M, Muhr C, Lundberg PO, Bergström K, Gee AD, Fasth K–J, Långström B (1987a) Rapid decrease in amino acid metabolism in prolactin–secreting pituitary adenomas after bromocryptine treatment: a PET study. J Comput Assist Tomogr 11:815–819

Bergström M, Lundqvist H, Ericson K, Lilja A, Johnström P, Långström B, von Holst H, Eriksson K, Blomqvist G (1987b) Comparison of the accumulation kinetics of L–(methyl–11C)–methionine and D–(methyl–11C)–methionine in brain tumors studied with positron emission tomography. Acta Radiologica 28:389–393

Bergström M, Muhr C, Lundberg PO, Långström B (1988) Bromocryptine treatment reduces protein synthesis in prolactinomas in vitro. 5th International Congress on prolactin, Kyoto, Japan, pp 171, Abstr. No. P–120

Bolster JM, Vaalburg W, Paans AMJ, van Dijk ThH, Elsinga PhH, Zijlstra JB, Piers DA, Mulder NH, Woldring MG, Wynberg H (1986) Carbon–11 labelled tyrosine to study tumor metabolism by positron emission tomography (PET). Eur J Nucl Med 12:321–324

Comar D, Cartron JC, Maziere M, Marazano C (1976) Labelling and metabolism of methionine–methyl–11C. Eur J Nucl Med 1:11–14

Daemen BJG, Paans AMJ, Elsinga PhH, Wieringa RA, Konings AWT, Vaalburg W (1989a) Hyperthermia induced suppression of protein synthesis in tumors as measured by PET. In: Schmidt HAE, Buraggi GL (eds) Nuclear Medicine, Trends and possibilities in Nuclear Medicine, Schattauer Verlag, Stuttgart, New York, pp 77–80

Daemen BJG, Elsinga PhH, Paans AMJ, Wieringa RA, Konings AWT, Vaalburg W (1989b) The effect of radiotherapy on L–[1–11C]tyrosine and 18FDG metabolism of tumors as measured by PET. J Nucl Med 30:789

Daemen BJG, Elsinga PhH, Ishiwata K, Paans AMJ, Vaalburg W (1991) A comparative PET study using different 11C–labelled amino acids in Walker 256 carcinosarcoma–bearing rats J Nucl Med Biol 18: 197–204

Davies JR, Sheppard MC, Heath DA (1990) Giant invasive prolactinoma: a case report and review of nine further cases. Quart J Med 275:227–238

Derlon J–M, Bourdet C, Bustany P, Chatel M, Therlon J, Darcel F, Syrota A (1989) [11C]L–methionine uptake in gliomas. Neurosurgery 25:720–728

Dollar JR, Blackwell RE (1986) Diagnosis and management of prolactinomas. Cancer and Metastasis Reviews 5:125–138

Di Chiro G (1986) Positron emission tomography using [18F]Fluorodeoxyglucose in brain tumors: a powerful diagnostic and prognostic tool. Invest Radiol 22:360–371

Grossman A, Besser GM (1985) Prolactinomas. Br Med J 290:182–184

Hamacher K, Coenen HH, Stöcklin G (1986) Efficient stereospecific synthesis of no-carrier added 2-[18F]-fluoro-2-deoxy-D-glucose using aminopolyether supported nucleophilic substitution. J Nucl Med 27:235-238

Ishiwata K, Vaalburg W, Elsinga PH, Paans AMJ, Woldring MG (1988) Metabolic studies with L-[1-14C]tyrosine for the investigation of a kinetic model to measure protein synthesis rates with PET. J Nucl Med 29:524-529

Johansen PW, Haug E, Gautvick KM (1985) Effect of bromocryptine on hormone production and cell growth in cultured rat pituitary cells. Acta Endocrinologica 110:200-206

Keen RE, Barrio JR, Huang S-C, Hawkins RA, Phelps ME (1989) In vivo cerebral protein synthesis rates with leucyl-transfer RNA used as a precursor pool: determination of biochemical to structure tracer kinetic models for positron emission tomography J Cereb Blood Flow Metab 9:429-445

Lilja A, Lundqvist H, Olsson Y, Spännare B, Gullberg P, Långström B (1989) Positron emission tomography and computed tomography in differential diagnosis between recurrent or residual glioma and treatment-induced brain lesions. Acta Radiologica 30:121-128

Maurer RA (1980) Dopaminergic inhibition of prolactin synthesis and prolactin messenger RNA accumulation in cultured pituitary cells. J Biol Chem 255:8092-8097

Maurer RA (1981) Transcriptional regulation of the prolactin gene by ergocryptine and cyclic AMP. Nature 294:94-97

Minn H, Joensuu H, Ahonen H, Klemi P (1988) Fluorodeoxyglucose imaging: a method to assess the proliferative activity of human cancer in vivo. Comparison with DNA flow cytometry in head and neck tumors. Cancer 61:1776-1781

Muhr C, Bergström M, Lundberg PO, Bergström K, Hartvig P, Lundqvist H, Antoni G, Långström B (1986) Dopamine receptors in pituitary adenomas: PET visualization with 11C-N-methylspiperone. J Comput Assist Tomogr 10:175-180

Niwa J, Minase T, Mori M, Hashi K (1987) Immunohistochemical, electron microscopic, and morphometric studies of human prolactinomas after short-term bromocryptine treatment. Surg Neurol 28:339-344

Paans AMJ, Vaalburg W, Woldring MG (1985) A rotating double-headed positron camera. J Nucl Med 26:1466-1471

Patronas NJ, Di Chiro G, Brooks RA, DeLaPaz RL, Kornblith PL, Smith BH, Rizzoli HV, Kessler RM, Manning RG, Channing M, Wolf AP, O'Connor CM (1983) Work in Progress:[18F]Fluorodeoxyglucose and positron tomography in the evaluation of radiation necrosis of the brain. Radiology 144:885-889

Schober O, Meyer G-J, Duden C, Lauenstein L, Niggemann J, Müller J-A, Gaab MR, Becker H, Dietz H, Hundeshagen H (1987) Uptake of amino acids in brain tumors using positron emission tomography as an indicator for assessing metabolic activity and malignancy. Fortschr Röntgenstr 147:503-509

Shome B, Farlow AF (1977) Human pituitary prolactin (hPRL): the entire linear amino acid sequence. J Clin Endocrinol Metab 45:1112-1115

CHAPTER 7

GENERAL DISCUSSION

7.1 Amino acids

In combination with PET, amino acids labelled with positron-emitting radionuclides have possibilities for the evaluation of a variety of physiological and biochemical functions in tumors, such as protein synthesis, amino acid transport mechanisms or enzyme activities. For the current study, protein synthesis was chosen as subject, because it is an important biochemical process of the tumor tissue that can be influenced by a variety of treatments, such as hyperthermia, chemotherapy and radiotherapy.

For the in vivo investigation of protein synthesis rates by PET, it is important to find a suitable radiolabelled amino acid. As described in chapter 2, uptakes of L-[methyl-^{11}C]methionine, L-[1-^{11}C]methionine, D-[1-^{11}C]methionine and L-[1-^{11}C]tyrosine were compared by PET in tumor and other tissues of Walker 256 carcinosarcoma-bearing rats. From these studies it was concluded that, due to the transmethylation processes, which have a large variation in the respective tissues, the L-methionines were less suitable for measuring protein synthesis. D-methionine, although readily taken up by all tissues, does not incorporate into proteins, and is also not adequate for monitoring this process. L-[1-^{11}C]tyrosine, an amino acid which incorporates rapidly into proteins and which has low amounts of non-protein metabolites, appears to be eligible for measuring protein synthesis with PET.

In PET literature, L-[1-^{11}C]leucine, L-[2-^{18}F]fluorotyrosine and L-[1-^{11}C]tyrosine are presented as amino acids of choice for measuring protein synthesis rates. Since the feasibility of each of these three amino acids for measuring protein synthesis rates has been validated under non-comparable conditions, a judgment on which one is most suitable is not possible. Therefore, a thorough comparative investigation of these three amino acids is still desired in a variety of tumors and other tissues of animals and man. Such a future study must include data on the incorporation rates into proteins and the amounts of non-protein metabolites in tissue and plasma.

7.2 Experimental animal models

To obtain answers to clinical questions concerning the use of PET during tumor therapy, PET data from experiments with tumor–bearing animals are a prerequisite. For this purpose, an animal model was needed suitable for experimental PET. Important criteria for such an animal model were derived:

- sufficient metabolic activity of the tumor
- adequate visualization of the tumor using a PET imaging system with a resolution of 5.5 mm
- growth characteristics which serve the purpose of therapy studies
- homogeneity of the tumor tissue.

Five experimental animal models were compared for experimental PET: the Lewis lung tumor, fibrosarcomateous FIO26 tumor and the lymphosarcomateous LY tumor in mice, and the Walker 256 carcinosarcoma and rhabdomyosarcoma in rats. These models were evaluated with L–[1–^{11}C]tyrosine and, for reason of comparison, with ^{18}FDG, an indicator for glycolytic activity in tissue.

Using L–[1–^{14}C]tyrosine and ^{18}FDG, too low metabolic activities were observed for the Lewis lung and the FIO26 tumors. Due to an insufficient signal–to–background ratio, the metabolic active LY tumor appeared to be inappropriate as well. Necrosis of the Walker 256 tumor resulted in difficulties in defining regions of interest of the areas of metabolic active tumor tissue for PET. In this tumor, the L–[1–^{11}C]tyrosine uptake values as measured by PET were lower than the L–[1–^{14}C]tyrosine uptake values as obtained after dissection of the tumor. Therefore, the Walker 256 tumor is now considered inappropriate for experimental PET. The rhabdomyosarcoma tumor, growing the Wag/Rij rat, showed adequate uptake values for L–[1–^{11}C]tyrosine and ^{18}FDG, a clear visualization with PET and a homogeneous histology. The rhabdomyosarcoma tumor is relatively slow–growing and has a volume doubling time which leaves possibilities for follow–up of tumor volume and PET studies after a therapeutic treatment.

When comparing the growth rates of the respective tumors with the uptake values of L–[1–^{14}C]tyrosine and ^{18}FDG, it could be observed that the L–[1–^{14}C]tyrosine uptake values correlated better with the growth rates than the ^{18}FDG uptake values. This finding tallies with the many unfruitful attempts to assess the grade of malignancy in a variety of tumors in patients by PET using ^{18}FDG. Tracers that incorporate in macromolecules such as proteins or DNA (L–[1–^{11}C]tyrosine, ^{11}C–thymidine) might have a better

potential for diagnosis of the grade of malignancy of tumors.

7.3 Hyperthermia

In clinical practice, early insight into the response of tumors to treatments with heat is a necessity. A rapid indication of thermal damage to tumor tissue provides possibilities for adjustment of treatment protocols.

Hyperthermia leaves many temporary "fingerprints" in the biochemistry of tumors. Especially, inhibition and recovery of protein synthesis after hyperthermia might be an underlying mechanism for a potential prognosis of the thermal sensitivity of a tumor to a dose of heat. Since, PET is able to monitor quantitatively protein synthesis in tumors in vivo, this technique has potential for early prognosis of the later hyperthermia response on tumor growth.

In experimental PET studies with rhabdomyosarcoma-bearing rats (chapter 4), a dose-dependent inhibition and recovery of protein synthesis was observed after application of different doses of heat. This inhibition and recovery correlated with the corresponding inhibition of tumor growth. In this tumor, the PET data on the inhibition of protein synthesis were not mediated by alterations of tumor blood flow.

From these studies we conclude that PET using L-[1-^{11}C]tyrosine is a sensitive method to discriminate between the effects of different thermal doses on protein synthesis in tumors. It is a rapid method which provides early answers on the efficacy of hyperthermia on tumor growth within a few hours after treatment.

7.4 Radiotherapy and its combination with hyperthermia

In cancer patients, hyperthermia is primarily used as an adjuvant therapy in combination with radiotherapy and/or chemotherapy. Therefore, further PET studies are needed to give insight in the metabolic events after combined treatment. Ionizing radiation is known to cause an early inhibition of DNA synthesis, but not an inhibition of protein synthesis and glycolysis. The latter two processes are only acutely suppressed at relatively high radiation doses (>100Gy). However, acute low-dose irradiation effects on amino acid uptake have been reported in literature as well. It is therefore eligible to measure acute and long-term effects on protein synthesis and glycolysis by PET

in tumors in order to evaluate the effects of radiotherapy and its combination with hyperthermia.

In rhabdomyosarcoma–bearing rats, dose–dependent reductions of L–[1–^{11}C]tyrosine and ^{18}FDG uptake were registered by PET as long–term effects of different doses ionizing radiation (chapter 5). The effects on tracer uptake could be correlated with changes of the tumor volume, indicating that PET is an eligible tool to investigate kinetics of tumor growth after radiotherapy. Acute effects of radiotherapy on tracer uptake were not observed, indicating that early predictions of the response of cancer to radiotherapy, as was the case with hyperthermia, were not possible with PET using L–[1–^{11}C]tyrosine. After radiotherapy in combination with hyperthermia, the inhibition of tumor growth was enhanced. Unexpectedly, after the combined treatment, the uptake of tracer remained at the pretreatment level.

As noticed before, ionizing radiation suppresses DNA synthesis already at low doses. Recently, for use in PET, ^{11}C–thymidine has been prepared. This radiopharmaceutical is suited for the investigation of DNA synthesis in tissue. Future studies are needed to evaluate the potential use of ^{11}C–thymidine for early prediction of the outcome of radiotherapy.

7.5 Bromocryptine treatment of prolactinomas.

PET using ^{11}C–labelled amino acids or ^{18}FDG is an elegant tool for monitoring tumor metabolism in cancer patients during a course of treatment. Prolactin–producing pituitary adenomas, prolactinomas, are treated with dopamine agonists which cause a shrinkage of the tumor volume, accompanied by a reduction of the serum prolactin level of the patient. In contrast to experimental tumors in animals, in patients it is difficult to measure volumes of tumors. In prolactinomas, the effect of bromocryptine treatment on tracer uptake, as measured by PET, can conveniently be compared to the changes in the serum prolactin levels.

In prolactinoma patients, administration of bromocryptine resulted in an inhibition of the uptake of L–[1–^{11}C]tyrosine into the prolactinoma tissue, accompanied with a lowering of the serum prolactin level. Because a correlation with a negative coefficient of was observed between the reductions the L–[1–^{11}C]tyrosine uptake and the serum prolactin levels it can be concluded that the respective actions of bromocryptine on prolactinoma protein synthesis and on prolactin release are not coupled. Next to MRI and serum

prolactin levels, PET using ^{11}C-labelled amino acids provides complementary information on the beneficial action of dopamine agonist treatment on prolactinomas.

PET studies with L-[1-^{11}C]tyrosine, L-[methyl-^{11}C]methionine and ^{18}FDG of drug-naive prolactinoma patients demonstrated an excellent nearly equivalent tumor-imaging potential for both amino acids. The tumors could not be visualized with ^{18}FDG.

The salivary glands, showed a preference for L-[1-^{11}C]tyrosine, as compared to L-[methyl-^{11}C]methionine, which could be explained from the amino acid composition of the proteins excreted into saliva. PET using L-[1-^{11}C]tyrosine might be useful for the investigation of pathophysiological states, e.g. radiation damage or Sjögren's disease of the salivary glands.

7.6 Future PET studies in oncology

PET studies of tumors, performed at the pretreatment phase, are of great importance for the selection of cancer therapy.

Multi-tracer PET studies with e.g. radiolabelled amino acids, nucleotides and glucose analogs may characterize the untreated tumors and might be useful for the selection of the most successful treatment protocol.

Complementary magnetic resonance spectroscopy studies, monitoring lactate formation and depletion of high-energy phosphate stores may be used, e.g. to predict radiosensitivity. Non-dividing tumors (e.g. because of hypoxia) are relatively resistant to ionizing radiation and often have high concentrations of lactate. Disadvantages of MRS, as compared to PET, are the relatively poor spatial resolution and low sensitivity.

Oxygenation of a tumor is of importance for the outcome of a radiotherapeutic treatment. Misonidazole is a compound which sensitizes hypoxic cells for irradiation. ^{18}F-fluoromisonidazole, is therefore a suitable tracer for the assessment of hypoxia in tumors. Hence, PET studies with ^{18}F-fluoromisonidazole in untreated tumors have possibilities to direct tumor treatment planning, including fractionation of radiotherapy, neutron therapy or administration of misonidazole to sensitize radiotherapy.

SUMMARY

Aspects of metabolic activities of tumors, such as glycolysis and synthesis of macromolecules, can be discriminated from activities of the tissues they originated from. These altered metabolic states may conveniently be investigated and quantified with positron emission tomography (PET) by the use of radiopharmaceuticals labelled with short-lived positron-emitting radionuclides, such as glucose analogs and amino acids. PET offers ample possibilities to measure the effect of treatment on tumors in terms of induced changes of metabolic activities. These changes can possibly be used as indicators of the therapeutic effects on tumors. The aim of this thesis is to contribute to the knowledge on the applicability of PET for the clinical evaluation of tumor treatment. Before PET can be applied in patients for monitoring therapy-induced changes on tumor growth, studies with tumor-bearing animals are necessary. A general introduction is given in chapter 1.

For the investigation of glycolysis, 2-[^{18}F]fluoro-deoxy-D-glucose (^{18}FDG) was used. In order to select an appropriate labelled amino acid, the dynamic distribution of L-[1-^{11}C]tyrosine, L-[methyl-^{11}C]methionine, L-[1-^{11}C]methionine and D-[1-^{11}C]methionine were comparatively evaluated in tissues of Walker 256 carcinosarcoma-bearing rats (chapter 2). It was found that the position of the ^{11}C-label in the methionine molecule had a marked effect on the distribution of the ^{11}C-activity into several tissues. Tumors accumulated significantly more ^{11}C-activity from L-[1-^{11}C]methionine than from L-[methyl-^{11}C]methionine, whereas in the liver the opposite was found. Furthermore, as expected, in brain a stereospecific uptake preference was observed for L-methionine as compared to D-methionine. With respect to the criteria for the amino acid most suitable for use in PET, such as absolute uptake value, protein incorporation and amount of metabolites, from ^{14}C-experiments it was concluded that L-[1-^{14}C]tyrosine is a better amino acid for measuring protein synthesis than the other amino acids. The L-[1-^{11}C]tyrosine data are in agreement with this conclusion.

For experimental PET, an animal tumor model must be available which meets important criteria such as sufficient metabolic activity, visualization of tumor the PET imaging system and tissue homogeneity. In chapter three, the feasibility of five animal tumor models for experimental PET was assessed by the use of ^{18}FDG and L-[1-^{11}C]tyrosine. The three mice models tested appeared

to be unsuitable for experimentation with PET. The Lewis lung tumor and the fibrosacoma FIO26 showed too low a tyrosine uptake, while the lymphosarcoma LY demonstrated an insufficient tumor to background ratio for visualization with PET. Both the Walker 256 carcinosarcoma and the rhabdomyosarcoma tumor in rat were clearly visualized using ^{18}FDG and L-[1-^{11}C]tyrosine. On account of a more appropriate growth rate and tissue homogeneity, the rhabdomyosarcoma tumor was chosen for further experimentation involving hyperthermia and radiotherapy.

The effects of hyperthermia on L-[1-^{11}C]tyrosine utilization and tumor growth are reported in chapter four. The uptake of L-[1-^{11}C]tyrosine into the rhabdomyosarcoma tumor was dose dependently reduced as measured by PET after hyperthermia at 42, 45 or 47 °C. These reductions in tracer uptake were not related to tumor blood flow. The blood flow was measured with PET using $^{13}NH_3$, and appeared to be unchanged. The heat-induced reductions of L-[1-^{11}C]tyrosine uptake were in agreement with reductions of L-[1-^{14}C]tyrosine uptake into tumor tissue and with the reduced incorporation into tumor proteins, as obtained in corresponding dissection experiments. Also the hyperthermia-induced inhibition of amino acid uptake correlated well with regression of tumor growth. Therefore, PET using L-[1-^{11}C]tyrosine is an appropriate tool for monitoring the effect of hyperthermia on tumor growth.

The potential use of PET to monitor radiotherapeutic effects on tumors is reported in chapter five. Rhabdomyosarcoma tumors were irradiated with single X-ray doses of 10, 30 and 50 Gy, and subsequently investigated by PET using L-[1-^{11}C]tyrosine and ^{18}FDG at different points of time. Dose-dependent reductions of tracer uptake were measured 4 and 12 days after radiotherapy which correlated with changes in tumor volume. Acute effects (within 8 hours) on tracer uptake were not established. After application of a combined treatment of radiotherapy and hyperthermia the uptake of tracers remained at the pretreatment level. This might possibly due to invasion of host cells. From these results it can be concluded that PET using L-[1-^{11}C]tyrosine and ^{18}FDG is apposite to monitor the kinetics of tumor growth and tumor regression, and that PET data obtained during a combined treatment have to be interpreted with caution.

The possibility of PET to evaluate bromocryptine treatment of prolactinoma patients is described in chapter 6. The efficacy of prolactinoma treatment is usually determined by measurement of the serum prolactin level. In this study, the uptake of L-[1-^{11}C]tyrosine into prolactinoma tissue and

the serum prolactin levels were monitored prior to and 18 hours after administration of bromocryptine. Both serum prolactin level and L–[1–^{11}C]tyrosine uptake were decreased after bromocryptine administration. At the point of time studied, the reduction of the L–[1–^{11}C]tyrosine uptake appeared not to be related to the reduction of the serum prolactin level. When compared, the tumor–imaging potential of L–[methyl–^{11}C]methionine and L–[1–^{11}C]tyrosine appeared to be nearly equal. Prolactinomas could not be visualized with ^{18}FDG. Next to MRI and serum prolactin, PET can provide complementary information on metabolism and treatment of prolactinomas.

From these experiments, it is concluded that PET in combination with ^{11}C–labelled amino acids or ^{18}FDG has clinical potential for the non–invasive investigation of the effects of tumor treatment.

SAMENVATTING

In vergelijking tot in normale weefsels, wordt in tumoren vaak een afwijkende activiteit van de basale stofwisselingsprocessen (bijv. glycolyse en eiwitsynthese) aangetroffen. Met behulp van positronemissie tomografie (PET) kunnen deze veranderde stofwisselingsprocessen onderzocht en gekwantificeerd worden. Hiervoor wordt gebruik gemaakt van metabole substraten, zoals aminozuren en glucoseanaloga, die gemerkt zijn met kortlevende positronemiterende radionucliden. PET biedt daardoor ook mogelijkheden om de behandeling van een tumor te beschrijven als een verandering in de metabole activiteit, welke een een indicatie zou kunnen zijn voor de effectiviteit van die behandeling. Het doel van dit proefschrift is daarom een bijdrage te leveren aan het kennisveld over de klinische toepasbaarheid van PET voor de evaluatie van de behandeling van kanker. Hierover wordt een algemene inleiding gegeven in hoofdstuk 1. Alvorens PET in de therapie van kankerpatiënten kan worden toegepast zijn eerst dierexperimentele studies nodig.

In de studies beschreven in dit proefschrift werd voor het onderzoek van het glycolyseproces 2-[^{18}F]fluor-desoxy-D-glucose gebruikt. Met het doel een geschikt gemerkt aminozuur te selecteren werd in diverse weefsels van ratten met Walker 256 carcinosarcomen de opname van L-[1-^{11}C]tyrosine, L-[methyl-^{11}C]methionine, L-[1-^{11}C]methionine en D-[1-^{11}C]methionine geëvalueerd (hoofdstuk 2). De plaats van het radionuclide in het methionine molecuul had een duidelijke invloed op de verdeling van de radioactiviteit in de verschillende weefsels. Het tumorweefsel nam meer van L-[1-^{11}C]methionine afkomstige radioactiviteit op dan van L-[methyl-^{11}C]methionine, terwijl in het leverweefsel het omgekeerde werd gevonden. Verder, zoals verwacht, vertoonde het hersenweefsel een stereospecifieke voorkeur voor L-[1-^{11}C]methionine, dit in vergelijking tot het D-enantiomeer. Gezien de eisen, gesteld voor het meest geschikte aminozuur voor gebruik in PET, zoals absolute opname, inbouw in eiwit en de hoeveelheid niet-eiwit metabolieten, bleek reeds uit ^{14}C-experimenten dat tyrosine meer geschikt was voor het meten van de eiwitsynthesesnelheid dan methionine. De metingen met L-[1-^{11}C]tyrosine, in de bovenstaande vergelijkingen, zijn in overeenstemming met deze conclusie.

Voor dierexperimenteel werk met PET is een tumormodel nodig welke voldoet aan een aantal belangrijke kriteria zoals: voldoende metabole activiteit van

het tumorweefsel, adequate visualizatie van de tumor met een positroncamera en homogeniteit van het tumorweefsel. In hoofdstuk 3 wordt, met behulp van ^{18}FDG en L-[1-^{11}C]tyrosine, de toepasbaarheid van 5 verschillende tumormodellen voor PET geëvalueerd. Geen van de drie onderzochte muizenmodellen bleek geschikt; de Lewis lung tumor en het FIO26 fibrosarcoom vertoonden een te lage tyrosine-opname, terwijl het LY lymfosarcoom een inadequate tumor-tot-achtergrond ratio had om met een positroncamera gedetecteerd te kunnen worden. In de rat werden zowel het Walker 256 carcinosarcoom als het rhabdomyosarcoom door PET, met behulp van L-[1-^{11}C]tyrosine en ^{18}FDG, visualizeerd. Vanwege een geschiktere groeisnelheid en weefselhomogeniteit werd het rhabdomyosarcoom uitgekozen voor verdere hyperthermie en radiotherapie experimenten.

De effecten van hyperthermie op tumorgroei en L-[1-^{11}C]tyrosineopname zijn beschreven in hoofdstuk 4. In het rhabdomyosarcoom bleek de opname van L-[1-^{11}C]tyrosine, zoals gemeten met PET, dosisafhankelijk afgenomen te zijn na een hypertherme behandeling op 42, 45 of 47 °C. Deze reducties bleken niet gerelateerd te zijn aan de doorbloeding van de tumor. De doorbloeding, welke gemeten was met $^{13}NH_3$ en PET, bleek na hyperthermie onveranderd. In analoge dissectie-experimenten met L-[1-^{14}C]tyrosine bleek dat de reducties in opname en in inbouw in eiwit van L-[1-^{14}C]tyrosine gerelateerd waren aan de reducties van L-[1-^{11}C]tyrosineopname in de PET-experimenten. De remming van de tyrosineopname, veroorzaakt door hyperthermie, correleerde met de latere afname van de tumorgroei. Daarom is PET, in combinatie L-[1-^{11}C]tyrosine, een potentiële methodiek om vroegtijdig het effect van hyperthermie op de tumorgroei te prognostiseren.

De mogelijkheid om met PET radiotherapeutische behandelingen te evalueren is beschreven in hoofdstuk 5. Hiervoor werden rhabdomyosarcomen bestraald met enkelvoudige doses Röntgenstralen van 10, 30 of 50 Gy en daarna met PET, gebruik makend van L-[1-^{11}C]tyrosine en ^{18}FDG, in de tijd gevolgd. Tussen 4 en 12 dagen na bestraling werden dosisafhankelijke reducties in traceropname gemeten, welke overeen kwamen met de gelijktijdig optredende veranderingen in het tumorvolume. Direkt na bestraling (binnen 8 uur) werd geen direct effect op de traceropname gevonden. Na een gecombineerde behandeling van radiotherapie met hyperthermie bleef de traceropname op het niveau van de onbehandelde situatie. Dit zou verklaard kunnen worden door oedeemvorming van de tumor, in combinatie met een invasie van macrofagen. Uit deze resultaten kan geconcludeerd worden dat PET, in combinatie met ^{18}FDG of ^{11}C-tyrosine, geschikt is voor het volgen van de kinetiek van tumorgroei of regressie na een

radiotherapeutische behandeling. Voorzichtigheid dient geboden te worden bij het interpreteren van PET-data verkregen na een gecombineerde behandeling.

De optie om met PET de behandeling van prolactinoompatiënten met dopamineagonisten te volgen is gedocumenteerd in hoofdstuk 6. Gewoonlijk wordt het effect van de behandeling van prolactinomen gerelateerd aan de serum prolactinespiegel. In deze studie werden de opname van L-[1-^{11}C]tyrosine in prolactinoomweefsel en het serum prolactine voor en 18 uur na toediening van bromocryptine gemeten. Na toediening van bromocryptine bleken zowel de serum prolactinespiegel als de L-[1-^{11}C]tyrosineopname afgenomen te zijn. De relatieve afname van het L-[1-^{11}C]tyrosine bleek niet direkt gerelateerd te zijn aan de afname van serum prolactine. L-[1-^{11}C]tyrosine en L-[methyl-^{11}C]methionine bieden een ongeveer gelijkwaardige optie om prolactinomen met PET af te beelden, terwijl het niet mogelijk bleek om prolactinomen met ^{18}FDG te visualiseren. Naast MRI en serum prolactine, bied PET complementaire mogelijkheden om het metabolisme en de behandeling van prolactinomen te evalueren.

Uit het werk beschreven in dit proefschrift kan samenvattend gesteld worden, dat PET, in combinatie met ^{11}C-gemerkte aminozuren en ^{18}FDG, een potentiële methodiek is voor de klinische evaluatie van de behandeling van tumoren.

NAWOORD

Adam, alleen wandelend in het paradijs, gaf namen aan al het levende. Als wetenschapper was hij dus zijn tijd al ver vooruit. Voor zijn nakomelingen, in modernere tijden, is het in zijn voetsporen lopen vaak geen solitaire zaak meer. Veel mensen hebben mij dan ook vergezeld bij het tot stand brengen van dit proefschrift.

Graag wil ik de medewerkers van de vakgroep Nucleaire Geneeskunde bedanken, in het bijzonder: Prof. Dr. W. Vaalburg als protagonist voor PET in Groningen, Dr. A.M.J. Paans voor de hulp bij camera's en computers, Philip Elsinga voor de betrouwbaarheid waarmee hij een gestage stroom van radiofarmaca genereerde, en Alco Rijskamp voor de verzorging van de figuren in dit proefschrift.

De gastvrijheid van de vakgroep Radiobiologie heb ik zeer op prijs gesteld. Prof. Dr. A.W.T. Konings ben ik zeer erkentelijk voor zijn creatieve wetenschappelijke inzet en de opbouwende wijze waarop hij mijn werk bekritiseerde. Andre Wieringa en Willy Lemstra wil ik graag bedanken voor hun onmisbare hulp bij het proefdierenwerk.

De samenwerking met de vakgroep Endocrinologie, onder leiding van Prof. Dr. H. Doorenbos, heb ik zeer gewaardeerd. Rolf Zwertbroek wil ik graag bedanken voor de gesprekken over prolactinomen en aanverwante zaken.

Gedurende mijn onderzoeksperiode is het Kernfysisch Versneller Instituut, onder leiding van Prof. Dr. R.H. Siemssen, een voortreffelijk onderdak voor mij geweest. Graag wil ik de cyclotronoperateurs bedanken die hun best deden om zoveel mogelijk bundelstroom te maken.

Hoe goed is het om vrienden te zijn. Jos van Dijken, Gert van Herk, Wouter Meiring en Peter Wortel wil ik bedanken voor hun werk achter de schermen.

Tenslotte zou ik mijn ouders willen bedanken die mij de stimulans en de mogelijkheden gaven om te studeren. Reeds van jongs af aan hebben zij mij op het spoor gezet om deze wereld te ontdekken en te begrijpen.